

Tactile Discrimination with Whiskers

Ph.D DISSERTATION

submitted for the degree of

Doctor of Philosophy

by

Mathew H. EVANS

UNIVERSITY OF SHEFFIELD

Submitted September, 2011



For Merryn.

Acknowledgements

This work could not have been done without the help, input and support of some amazing people.

Thanks to my supervisors Tony Prescott and Charles Fox, for providing help and insights when most needed and giving me more freedom than I knew what to do with. To Martin Pearson, Jason Welsby, Charlie Sullivan and Tony Pipe, thanks for letting me break your whiskers. Nathan Lepora for support when there was none, and for reading manuscripts that no one else would brave. Stuart Wilson, for making me want to be a better scientist. Alex Cope, for his coding wizardry and patience. Robyn Grant for brightening countless grey Sheffield days. Ben Hutchinson, for helping with my coding questions, and for not making me feel like a fool when he did so. Anyone I've shared an office with for putting up with my distracting Guardian football browsing. The BIOTACT consortium for humouring me when I talk at meetings. Especially Brian Quist for some detailed whisker based conversations. Members of Atl@s and the ABRG for the currys and the beers. To caffeine, sugar and yeast. You make it all a bit easier.

Dafydd, Siôn ag Elan am bod y brodyr a chwaer gorau yn y byd. Anti Rhian, a gweddill y teulu am gofyn cwestiynau da ag weithiau gwrandio ar yr atebion. Nain a Taid, Nain a Taid. Oedd chi ddim yne yn y diwedd, ond oedd chi yne i creu y cychwyn.

Mam a Dad, diolch o galon. Am bob peth.

COFIO TRYWERYN

dsr

Abstract

Rodents are excellent at tactile discrimination. They use their whiskers to extract tactile information about the world. Though a huge amount of research has looked at the rodent whisker system in great detail, it remains unclear what kinds of tactile information can be encoded through a whisker in principle, and how such processing can be performed in practice.

The goal of this thesis is to determine what sort of tactile information can be sensed with a whisker, and to evaluate different methodologies for processing this tactile information. Tactile data is generated using a biomimetic artificial whisker and an XY positioning robot, providing a comprehensive test bed for numerous classifiers of different tactile features. A new framework for whisker based tactile sensing is described, to organise and simplify the task of gathering information. Each part of the framework is then addressed to build a complete system for determining the nature of a surface encountered during exploration.

Previously proposed model-based methods, and new data-driven model-free approaches are compared rigorously on a common data set to establish a benchmark for whisker based tactile sensing. These methods are compared in the task of determining the radial distance to contact of an object, and the texture of a surface under different whisker movement conditions. Classifier robustness is evaluated by testing performance in conditions where different contact parameters are changed simultaneously. The best classifiers in each instance are demonstrated on a series of whiskered robots, generating tactile ‘reports’ that could be used for object identification, localisation and navigation.

Contents

1	Introduction	1
1.1	Tactile discrimination	1
1.2	Inspiration from biology; solutions from re-engineering	3
1.3	Structure of the thesis	5
1.4	Contributions of this thesis	7
1.5	List of contributions of this thesis	8
1.6	A note on collaborative work in this thesis	9
1.7	List of publications	11
2	Review of whisker based tactile discrimination	15
2.1	Introduction	15
2.2	Biological whisker systems	16
2.2.1	Whisker array morphology	17
2.2.2	Whisker movement control	18
2.2.3	Neural systems underlying whisker sensing in rats	20
2.2.4	Summary of biological whisker systems	23
2.3	Artificial whisker systems	24
2.3.1	Early whisker-like sensors	25
2.3.2	Actuated artificial whiskers	27

2.3.3	Biomimetic systems for whisker sensing	29
2.3.4	Summary of artificial whisker systems	33
2.4	Whisker based tactile discrimination	34
2.4.1	Whisker contact geometry	35
2.4.2	Radial distance to contact	36
2.4.3	Model-based methods for radial distance estimation	37
2.4.3.1	Static beam equation based classification	38
2.4.3.2	Oscillation frequency based classification for radial distance estimation	41
2.4.4	Model-free methods for radial distance estimation.	42
2.4.4.1	Template based classification	43
2.4.4.2	Feature based classification	43
2.4.4.3	Stationary Naïve Bayesian Classification	44
2.4.5	Texture discrimination	45
2.4.5.1	Resonance hypothesis	45
2.4.5.2	Kinetic signature hypothesis	47
2.4.6	Model-free methods for texture discrimination	47
2.4.6.1	Spectro-temporal feature extraction	48
2.4.6.2	Modulation energy	49
2.4.7	Summary of whisker based tactile discrimination	51
2.5	A framework for whisker based tactile discrimination	53
2.5.1	Separating ‘what’ from ‘where’	54
2.5.2	Filling in the framework	56
2.6	Plan of work in this thesis	58
3	Whiskered robots used in this thesis	61
3.1	Introduction	61

3.2	SCRATCHbot (Spatial Cognition and Representation through Active TouCH)	63
3.2.1	Hall effect sensor based artificial whisker	63
3.2.2	Whisker materials	65
3.2.3	SCRATCHbot whisker design	67
3.2.4	Whisker movement control	69
3.3	XY positioning robot	71
3.3.1	Data Collection on the XY positioning robot	73
3.3.2	Robot control	74
3.4	BIOTACT G1 robot	75
3.4.1	Sensor design	75
3.4.2	Whisker control	76
3.5	CrunchBot: a mobile whiskered robot platform	79
3.5.1	Robot platform	80
3.5.2	Whiskers	81
3.6	Concluding remarks	81
4	Classification of radial distance estimation under varying contact speeds	83
4.1	Introduction	83
4.2	Data collection for radial distance estimation	85
4.3	Classifier specification	86
4.3.1	Static beam equation based classification	87
4.3.2	Oscillation frequency based classification	88
4.3.3	Template based classification	89
4.3.4	Feature based classification	90
4.3.5	Stationary naïve Bayes classification	93
4.3.6	A comparison of all five classifiers	94
4.4	Results	95

4.4.1	Static beam equation based classification	95
4.4.2	Oscillation frequency based classification	97
4.4.3	Template based classification	99
4.4.4	Feature based classification	100
4.4.5	Stationary naïve Bayes classification	102
4.4.6	A comparison of all five classifiers	103
4.5	Discussion of radial distance estimation methods	105
5	Classification of surface angle and texture estimation under varying contact speeds	111
5.1	Introduction	111
5.2	Data collection for angle, speed and texture estimation	114
5.3	Classifier specification	116
5.3.1	Time–domain template based classification	116
5.3.2	Spectral template based classification	119
5.3.3	Feature based classification	119
5.3.4	Stationary naïve Bayes classification	121
5.3.5	Combination of classifiers for full contact parameter estimation	121
5.3.6	A note on the analysis	122
5.4	Results	123
5.4.1	Template based classification	125
5.4.1.1	Raw signal template classification	125
5.4.1.2	Low pass filtered template classification	126
5.4.1.3	High pass filtered template classification	127
5.4.1.4	First derivative template classification	128
5.4.1.5	Second derivative template classification	129
5.4.1.6	Spectral template based classification	130
5.4.2	Feature based classification	131

5.4.2.1	Combining features with multinomial regression	133
5.4.3	Stationary naïve Bayes based classification	134
5.4.3.1	Naïve Bayes based classification using velocity signals . . .	135
5.4.3.2	Naïve Bayes based classification using acceleration signals .	136
5.4.4	Comparing the classifiers	136
5.4.5	Combining the classifiers	137
5.5	Discussion	139
6	Classification with embedded models on whiskered robots	147
6.1	Introduction	147
6.2	Floor texture discrimination on a Roomba: (Evans, M. H. et al., 2009a) . . .	149
6.2.1	Analysis	149
6.2.2	Results	151
6.2.3	Discussion	153
6.3	Radial distance estimation on SCRATCHbot: (Evans, M. H. et al., 2010a) . .	154
6.4	Texture discrimination on the BIOTACT G1 robot: (Sullivan, Mitchinson, Pearson, Evans, M. H. , Lepora, Fox, Melhuish, and Prescott, 2011)	156
6.4.1	Texture classification experiments	157
6.4.2	Stationary naïve Bayes classification	158
6.4.3	Template-based classification	159
6.4.4	Classification results	159
6.4.4.1	Overall classification performance (unmodulated whisking dataset)	159
6.4.4.2	Comparative performance of unmodulated whisking, RCP7 and RCP9 datasets	160
6.4.4.3	Classification performance for just textures or distances (un- modulated whisking dataset)	160

6.4.4.4	Comparative performance for just textures or distances of un-modulated whisking, RCP7 and RCP9 datasets	161
6.4.5	Discussion	161
6.5	CrunchBot: a mobile whiskered robot platform	163
6.5.1	Exploratory behaviour	165
6.5.2	Floor texture discrimination	166
6.5.3	Finite state machine for tactile SLAM	167
6.5.4	Radial distance to contact	169
6.5.5	Surface orientation	169
6.5.5.1	Blob-based mapping	170
6.5.5.2	Angle-based maps with multi-whisker contact geometry . .	170
6.5.5.3	Angle-based mapping with multi-whisker templates	172
6.5.6	CrunchBot Results	173
6.5.6.1	Floor texture discrimination	173
6.5.6.2	Radial distance estimation	174
6.5.6.3	Orientation of a surface	176
6.5.7	CrunchBot Discussion	177
6.6	General discussion	180
7	Conclusion	185
7.1	Limitations of the current approach	188
7.1.1	Whisker design	188
7.1.2	Single whisker contacts	189
7.2	Future work	191
7.3	General conclusions, principles and predictions	193

xi

Chapter 1

Introduction

“To see is not yet to believe: hence Christ offered himself to be touched by the doubting apostle.”

Tuan (1974) in Topophilia: A study of environmental perception, attitudes, and values.

1.1 Tactile discrimination

Touch is an immediate and reliable way of gathering information from the world. We seem to rely on touch as a sense of last resort when other senses are impaired, such when navigating a room in the dark. As Tuan (1974) remarked “the fundamental nature of the sense of touch is brought home to us when we reflect that, without sight a person can still operate with a high degree of efficiency in the world, but without the tactual sense it is doubtful that he can survive”. Without tactile sensing simple tasks such as walking or handling objects would become incredibly difficult. In this thesis we aim to develop an understanding of tactile sensing, sufficient for an agent to navigate by touch sensing alone. In the process we hope to shed light on the nature of tactile sensing, and the kinds of information that can be extracted from the world using touch. Some terms are used throughout this thesis that need to be defined. These definitions specify how each term is used in the thesis.

- Tactile sensing: The act of moving a mechanical sensory apparatus about the world and making physical contact with surfaces with the sensory apparatus to gather touch information.
- Touch information: Information that can be extracted from the deflections of a mechanical sensory device upon contact with an object, that can be used to infer the identity of that object. For example the texture of an object, or the location of an object in space.
- Tactile discrimination: Reporting the touch information acquired during tactile sensing. The accuracy of these reports can be compared for different tactile discrimination methods.

Within the touch domain we focus on whisker based sensing. Whiskers are discrete, mechanically simple elements which are more amenable to investigation than skin based (haptic) touch systems. Unlike distal sensors, whiskers make direct contact with the world and may thus leave less scope for ambiguity in their interpretation. There are also environments where distal sensors are inappropriate, for example in loud, smoke-filled search and rescue operations, or underwater where particles could impede vision. There are properties of objects than can only be sensed by direct inter-active contact such as elasticity and friction, and others – in particular texture – which are considerably easier to sense directly than to infer from distal sensors such as vision.

As important as touch seems to be, it remains unclear what kinds of tactile information can be encoded through a whisker in principle, and how this processing can be performed in practice. Our goal is to determine what kinds of tactile information can be reliably extracted from a whisker deflection during or immediately following a contact.

Determining the nature of a surface with a whisker is a difficult task. Touch is an exemplar of an active sensory modality. A stationary touch sensor, such as a fingertip or whisker, in a static world produces little or no information – the sensor must be moved around regions of interest

to obtain information. Touch sensing is also very sparse. At any moment in time a fingertip obtains information only from a few square millimetres of contact. More extremely, a whisker making contact with an object has an almost vanishingly small area of contact. Touch is a very proximal sense – there are no equivalents to distant visual landmarks in touch – any information gathered from a contact is only available in that location. Gathering information about objects in the environment requires an integration of sensory information with odometry across contacts over time. To accurately infer the properties of objects both the location in space of a contact and the identity of a surface must be determined, all while taking the movement of the whiskers through space into account. A further complication is that though whiskers make direct contact with objects in the world, deflections must be interpreted from recordings at the base, leaving room for uncertainty.

1.2 Inspiration from biology; solutions from re-engineering

Our approach is to look to biology for inspiration for how acute tactile sensing can be, and what kinds of tactile discriminations can be made with whiskers. As difficult as this task seems to be, we do know it can be solved as many mammals have exquisite tactile sensing capabilities. We then re-engineer or model candidate systems that can match or out-perform biological systems in these tactile discriminations. In this way we hope to increase our understanding of the problem of whisker based tactile sensing, and biological whisker systems side by side.

There are many reasons why modelling a system is an important step towards understanding, and why synthetic models (models built in software or hardware) in particular are so useful (Rosenblueth and Wiener, 1945; Mitchinson et al., 2010). Models provide a level of abstraction. Abstraction is important for understanding complex systems like the ones we find in biology. When we observe behaviours or functions in intact biological systems it can be difficult to understand how these observations emerged from the substrate. Within the biological sciences,

certain animals are often used as models for less amenable animals. For example there are many rodent models of human diseases such as Parkinson’s disease (Betarbet et al., 2002) and depression (Willner, 1984). Abstraction can also be gained by isolating certain components from a larger system; for example when studying neural responses in anaesthetised rats to remove the neural activity associated with whisker movement generation, as in Szwed et al. (2006). Abstraction from the complex biology, by isolating certain portions of the whole system, has the unfortunate consequence of potentially changing the function of the system of interest, when compared to the intact animal. It can also be difficult to match up the assumptions one has about the effect of an intervention, and the realities of that intervention. For example lesioning the brain is a useful way of isolating different structures and functions, but it is very difficult to ensure that other regions have not been affected by damaging fibres of passage. Subsequently we can never be sure that the biological models we develop are true reflections of the intact system we hope to understand. Synthetic models have some unique advantages in this regard.

Building synthetic models, in software and hardware simulation, provides the means to study complex *intact* systems interacting with rich environments, while preserving the necessary level of abstraction required for understanding the system. When we build synthetic models we can develop systems that, at some level, we understand completely; any function or performance that emerges can more easily be traced back to this understanding than in biological systems. Any assumptions in our hypotheses are made explicit in a synthetic model, and each can be tested. The level of abstraction can be set by the experimenter, and the necessary and sufficient requirements can be determined for a given goal, to isolate that which is important and that which may be an artefact of a particular biological implementation.

Any models of whisker system processing need whisker deflection data as input to drive them. Whisker physics is difficult to simulate accurately in software (as is discussed in Section 2.3.1 of Chapter 2). Artificial whiskers can be built that have similar mechanical properties to biological whiskers, ensuring that any processing or modelling that relies on data from these whiskers

is comparable to the biological system. Any computational model is only as accurate as the environment it operates in, and by embedding models on mobile robots we can test them on real-world data from rich environments.

There are limitations to simulations of course. Even the best model is exactly that, a model, a fabrication. There will always be assumptions in their design which can skew results. Abstractions from complete systems by their nature will never be able to capture every aspect of the intact system. However, we feel the importance of modelling in software and hardware for hypothesis development and testing is clear. As long as caution is taken in the model's design, and when drawing general conclusions for biological systems from the results.

1.3 Structure of the thesis

Rats are the tactile whisker specialists that we turn to for inspiration. For almost a hundred years researchers have remarked on the importance of whisker based tactile sensing for rats (Vincent, 1912); they become error-prone and slow at maze navigation when whiskers are removed. Rats spend a great deal of their time operating in the dark or underground, using their whiskers to gather tactile information from the world. A great deal of electrophysiological, behavioural and anatomical research has focused on the rodent whisker system, describing the physical apparatus rats use for whisker sensing, the control of this system, and the acuity of tactile discriminations rats can perform. This research is reviewed in Section 2.2 of Chapter 2, and can be used to guide our understanding of whisker based tactile sensing.

Exploring the biology poses certain questions. How can the task performance of rats be achieved in principle? What are the mechanisms or algorithms being implemented by the rat, to achieve the tactile discriminations necessary for navigating the world by the sense of touch alone? How can the act of gathering tactile information with whiskers be organised to provide the animal with sufficient tactile information for identifying objects and surfaces in the environment simply

and efficiently?

In Section 2.5 of Chapter 2 we propose a novel framework for organising the development of a system for achieving our goal: tactile discrimination sufficient for navigating an environment by touch alone. The framework outlines a tactile sensing strategy i.e. how to move the whiskers through the world; and a series of discriminations that allow the agent to determine the nature and identity of any surface in the environment. This information about the identity of a surface can then be used to build up a map of the environment and localise the agent within that map, for example through a system for simultaneous localisation and mapping (SLAM Leonard and Durrant-Whyte, 1991; Dissanayake et al., 2001).

A key component of developing a system for tactile sensing is to build classifiers that can perform the necessary tactile discriminations. Some methods for whisker based tactile discrimination have been proposed in the past, and these are reviewed in Section 2.4 of Chapter 2. The interactive, active nature of whisker based tactile sensing requires that the whiskers be moved to make contact with objects and surfaces in the environment. To this end a number of whiskered robots have been developed for gathering tactile information, and for training classifiers for tactile discriminations. These robots are reviewed in Section 2.3 of Chapter 2.

To compare established methods for tactile discrimination fairly, and to test new methods, we developed a novel system for generating whisker deflection data using an XY positioning robot and a biomimetic artificial whisker. The XY positioning robot allows the collection of large amounts of whisker deflection data, providing the opportunity for a better understanding of the nature of whisker-object contacts. This robot, and others used in the experimental Chapters of this thesis, is described in Chapter 3.

This data is used to systematically test a number of classifiers under a range of conditions to determine which tactile discriminations can be made reliably with a whisker, and which methods are best suited for implementation on more unrestricted mobile robots. Specifically classifiers are built to discriminate the radial distance to contact of an object (Chapter 4), and the texture

and angle of a surface (Chapter 5).

Finally in Chapter 6 the most successful classifiers developed on data collected from the XY positioning robot are tested on a series of other robots, each designed to ask specific questions about tactile sensing. Specifically these are the effects of whisker movement, and performing tactile discriminations in real-time onboard a mobile robot for navigation.

1.4 Contributions of this thesis

Broadly, the contribution of this thesis is to comprehensively address the problem of whisker based tactile discrimination in artificial systems, in a manner that allows the implementation of tactile discrimination algorithms for real-time classification and mapping on board a mobile robot. More specifically a framework for whisker movement in gathering information is established, providing a means to interact with an environment in a principled manner. This framework is necessary as whisker contact geometry and speed has been shown to affect the subsequent whisker deflection signals and make discriminations more difficult. Restricting contacts in this way makes contact signals more consistent, and reduces the combinatorial explosion of contact parameters by separating the classification of object position and surface identity.

An XY positioning robot is developed to allow, for the first time, the systematic collection of large sets of whisker deflection data. This is important as simulation of whisker physics is complex and careful whisker movement control can be difficult to achieve. This means whisker deflection data is scarce and the effect of changing whisker-object contact parameters is poorly understood. The XY positioning robot alleviates these problems by allowing carefully controlled, repeatable, contact to occur over a broad range of whisker-object contact parameters. In the past classifiers and whiskered robots have been developed side by side to solve certain tasks or answer specific questions. The XY positioning robot provides a single robot platform that allows the fair comparison of classification methods. In this way classifiers can be trained,

and data can be imaged in a manner that increases our understanding of tactile discrimination with artificial whiskers, and may in turn aid our understanding of whisker sensing in biological systems.

The XY positioning robot is used to develop and test a range of classifiers, establishing benchmarks for classifying a number of contact parameters simultaneously for the first time. Classifiers have typically been developed to classify single contact parameters such as surface texture or radial distance to contact. On board a mobile robot, and in the rodent, a whisker may make contact with an object that is at an unknown location with respect to the agent, moving at a certain speed and have varying surface properties such as texture or orientation. Discriminations of surface texture or object location will need to be invariant of these other contact parameters, or the classifier must be able to classify these parameters simultaneously. In this thesis classifiers are developed for simultaneous classification of radial distance to contact and contact speed, and separately for simultaneous classification of surface texture, angle to the agent, and contact speed.

Finally, a comparative robotics approach is used to test the applicability of classifiers developed in the thesis to data collected from other robotic platforms. The effects of biomimetic whisker movement is explored, as well as the effect of robot movement. This series of work results in the implementation of real-time tactile discriminations on board a mobile robot, allowing simultaneous localisation and mapping (SLAM) algorithm based navigation to be performed using only tactile and odometry information.

1.5 List of contributions of this thesis

- Development of an XY positioning robot system for the systematic collection of whisker deflection data.
- A novel framework for whisker based tactile discrimination.

- Simultaneous classification of radial distance to contact and contact speed.
- Simultaneous classification of surface texture and angle, and contact speed.
- Exploration of the effect of whisker movement control strategies on texture discrimination.
- Implementation of classifiers for tactile discrimination on a mobile robot for real-time simultaneous localisation and mapping (SLAM).

1.6 A note on collaborative work in this thesis

The work presented in this thesis was completed in collaboration with other members of the Active Touch Laboratory at Sheffield (ATL@S) and the Bristol Robotics Laboratory as part of the FP7 BIOTACT project (Biomimetic Technology for Vibrissal Action Touch Grant ICT-215910), and this is reflected in the collaborative papers listed below. Specifically, many of the robots described in this thesis were developed at BRL, with some input from us at ATL@S. I developed the XY positioning robot software and hardware, and all the classifiers covered in Chapters 4, 5 and 6. Some classifiers that had been proposed in the literature were adapted for our paradigms and coded up from scratch. The naïve Bayes classifier was adapted from work previously published in collaboration with Nathan Lepora of ATL@S.

ScratchBot, the BIOTACT G1 robot and all the artificial whiskers described in Chapter 3 were designed and built by members of BRL, namely Martin Pearson, Charlie Sullivan and Jason Welsby, though certain design decisions such as whisker material, size and whisk speeds were taken with input from ATL@S. G1 whisker control strategies were developed by Ben Mitchinson. Data collection paradigms on each robot, for the classifications presented in this thesis, were specified by me, and experimental designs were then developed in collaboration with the appropriate members of BRL. CrunchBot’s software was developed in collaboration with Charles Fox of ATL@S, I developed the classifiers, Charles developed the SLAM code, other control soft-

ware such as the FSM were developed in collaboration. CrunchBot's hardware was built with the help of members of BRL, and Andy Ham at the University of Sheffield.

1.7 List of publications

PDFs available at <http://matevans.postgrad.shef.ac.uk/>

Journal papers

Sullivan, C., Mitchinson, B., Pearson, M., Evans, M., Lepora, N., Fox, C., Melhuish, C., and Prescott, T. (2011). Tactile Discrimination using Active Whisker Sensors, IEEE Sensors journal.

Peer-reviewed conference papers

Fox, C., Evans, M., Lepora, N., Pearson, M., Ham, A. and Prescott, T. (2011). CrunchBot: a mobile whiskered robot platform. Proceedings of Towards Autonomous Robots, Springer.

Lepora, N., Fox, C., Evans, M., Mitchinson, B., Motiwala, A., Sullivan, C., Pearson, M., Welsby, J., Pipe, T., Gurney, K. and Prescott, T. (2011). A General Classifier of Whisker Data using Stationary Naive Bayes: Application to BIOTACT Robots. Proceedings of Towards Autonomous Robots, Springer.

Evans, M., Fox, C.W., Pearson, M.J., Lepora, N.F., Prescott, T.J. (2010). Whisker-object contact speed affects radial distance estimation. 2010 IEEE International Conference on Robotics and

Biomimetics (ROBIO).

Lepora, N.F., Evans, M., Fox, C.W., Pearson, M.J., and Prescott, T.J. (2010). Naive Bayes texture estimation. IEEE International Conference on Robotics and Biomimetics (ROBIO)

Evans, M., Fox, C.W., and Prescott, T.J. (2010). Tactile discrimination using template classifiers: Towards a model of feature extraction in mammalian vibrissal systems. Proceedings of From Animals to Animats 11, 11th International Conference on Simulation of Adaptive Behaviour, (SAB), p178-187.

Lepora, N.F., Evans, M., Fox, C.W., Diamond, M., Prescott, T. and Gurney, K. (2010). Naive Bayes texture classification applied to whisker data from a moving robot. IEEE Proceedings of the International Joint Conference on Neural Networks (IJCNN)

Prescott, T., Pearson, M., Fox, C., Evans, M., Mitchinson, B., Anderson, S. and Pipe, T. (2010). Towards biomimetic vibrissal tactile sensing for robot exploration, navigation and object recognition in hazardous environments. Proc. Robotics for Risky Interventions and Environmental Surveillance (RISE).

Evans, M., Fox, C.W., Pearson, M.J., Prescott, T.J. (2009). Spectral template based classification of robotic whisker sensor signals in a floor texture discrimination task. Proceedings of Towards Autonomous Robotic Systems (TAROS), p19-24.

Fox, C., Evans, M., Stone, J. and Prescott, T. (2008). Towards Temporal Inference for Shape Recognition from Whiskers. Proceedings of Towards Autonomous Robotic Systems (TAROS)

Posters

Evans, M., Fox, C.W., Pearson, M.J., Prescott, T.J. (2009). Object location, orientation, and velocity extraction from artificial vibrissal signals. In Society for Neuroscience Abstracts. Society for Neuroscience (Program No. 174.8/ Z12)

Evans, M., Fox, C.W., Pearson, M.J., Prescott, T.J. (2008). Radial distance to contact estimation from dynamic robot whisker information. In Barrels XXI (SfN Satellite Meeting), 2008.

Fox, C.W., Evans, M., Prescott, T.J. (2008). Template-based classification of whisker contact edge orientation and radial distance in a simulated mobile robot. In Barrels XXI (SfN Satellite Meeting), 2008.

Chapter 2

Review of whisker based tactile discrimination

2.1 Introduction

In light of our approach described in Chapter 1 which takes inspiration from biological systems to understand complex problems, in this Chapter (Section 2.2 we review the structure and control of the rat whisker system. We go on to review the artificial whisker systems that have been built to model some of the tactile sensing capabilities of rats in Section 2.3. A functional review of whisker sensing is given in Section 2.4, looking at the tactile discriminations that rats can accomplish, and potential mechanism by which these discriminations could be performed. While it is still unclear precisely what information in the environment the rat is encoding, or how this encoding is taking place, we draw conclusions about the current state of knowledge on whisker based tactile discrimination. Finally a novel framework and a series of experiments to develop a system for tactile discrimination sufficient for navigation is proposed.



Figure 2.1: Whiskers are found in many mammals, such as the Brazilian porcupine (*Coendou prehensilis*) (a), and so called ‘whisker–specialists’ such as the Etruscan shrew (b), the world’s smallest terrestrial mammal.

2.2 Biological whisker systems

Whiskers (also known as vibrissae) are found in almost all terrestrial mammals, *Homo Sapiens* excepted, and some marine mammals (Ahl, 1986). Monotremes (mammals that lay eggs, evolutionary precursors to placental mammals) do not have whiskers, so whiskers are thought to have evolved in the marsupials \approx 120 million years ago (Brecht et al., 1997). Whiskers are usually used for touch sensing, though rats also use them for social interaction (Prescott et al., 2011) and harbour seals have been shown to use their whiskers for hydrodynamic trail-following to capture aquatic prey (Dehnhardt and Ducker, 1996; Dehnhardt et al., 2001). Although whiskers are hairs, their structure is highly specialised for tactile sensing, with regards to their surface structure and stiffness (Sarko et al., 2011; Chernova and Kulikov, 2011). Whiskers vary in length, thickness, shape and stiffness between animals (Chernova and Kulikov, 2011).



Figure 2.2: (a) A close up of the rat whisker array. Rats' whiskers are conical, tapered and slightly curved.(b) A blindfolded seal trained to follow hydrodynamic trails using its whiskers.

2.2.1 Whisker array morphology

Whisker touch has long been known to be of critical importance to rats (Vincent, 1912; Hutson and Masterton, 1986). Rats typically have around thirty prominent whiskers on each cheek (or mystacial pad), arranged in a regular grid of rows and columns (see Figure 2.2 (a) and Figure 2.4 (b)), which is identical in all rats (Diamond et al., 2008 (a)). These large *macro*-vibrissae vary in length and width across the whisker pad, from the largest (2–40mm in length (Diamond et al., 2008 (a))) in the most caudal column down to the smallest in the rostral column. A dense array of 40–70 smaller *micro*-vibrissae (a few mm in length (Diamond et al., 2008 (a))) are located around the lips (Brecht et al., 1997). Physical differences between the whiskers affect their mechanical properties, such as their bending and damping characteristics (Hartmann et al., 2003), which could have repercussions for sensing, which are discussed in detail in Section 2.4 of this Chapter.

2.2.2 Whisker movement control

Though a distinction is made between *macro* and *micro*-vibrissae, the whisker array is actually a physically continuous system with an important functional distinction. While the *micro*-vibrissal array is static the *macro*-vibrissae are actuated. Initially characterised by Welker (1964), this back and forth movement of the whiskers has been called ‘whisking’ and has been the subject of a great deal of research.

By definition whiskers can only encode information about objects when they make contact with them. To gather information about the world rodents sweep their whiskers through the air, and bring them on to surfaces in the environment. A single ‘whisk’ is defined as one cycle of whisker protraction (forward movement) and retraction (backward movement), and without perturbation rats typically whisk in short bouts of ≈ 10 cycles, at around 5–8Hz (Carvell and Simons, 1990).

Though initially thought to be very regular (Semba and Komisaruk, 1984), recent studies using optoelectronic monitoring techniques (Bermejo et al., 2002) and high speed videography (Sachdev et al., 2002; Towal and Hartmann, 2006) has revealed that rat whisking can be highly irregular and complex: full of asynchronies, where different whiskers are protracted by different amounts (Sachdev et al., 2002); and asymmetries, where the whiskers on either side of the head are moved out of phase with one another (Towal and Hartmann, 2006). These irregular movements are thought to be the result of active sensing strategies (Hartmann, 2001; Berg and Kleinfeld, 2003; Mitchinson et al., 2007).

Whisking is anticipatory, whiskers move asymmetrically to precede a head movement (Towal and Hartmann, 2006); and regulatory, whisker movement velocity is controlled to reduce variability in average whisking velocity (Towal and Hartmann, 2008). Specifically rats seem to use particular strategies for sensing, such as the rapid cessation of protraction (RCP) upon initial contact with a surface, and contact induced asymmetry (CIA) in the whisker movements, where

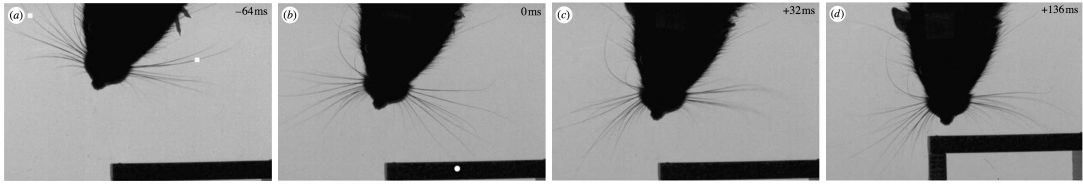


Figure 2.3: High speed video frames demonstrating rapid cessation of protraction and contact induced asymmetry following a unilateral whisker contact at time $t = 0$. (a) ($t = -64\text{ms}$) The rat approaches an object while ‘free whisking’ in air. (b) ($t = 0\text{ms}$) a whisker on the left side of the rat makes contact with an object. The point of contact is indicated by the white circle. (c) ($t = +32\text{ms}$) Whiskers on the right side of the animal reach maximum protraction, though the whiskers ipsilateral to contact are already partially retracted as protraction on that side stopped shortly after contact. (d) ($t = +136\text{ms}$) A pronounced asymmetry in the maximum protraction of the whiskers on the subsequent whisk cycle. Protraction has increased on the side contralateral to contact, and has decreased on the side ipsilateral to contact. This allows the rat to explore more of the environment while ensuring a gentle surface contact. Images used with permission from Mitchinson et al. (2007)

a whisker contact on one side of the rat’s head causes an increase in the protraction of whiskers on the side contra-lateral to contact (Grant et al., 2009). Rats also control the spread and contact force of whiskers to ensure even, light contacts across the whisker array, a strategy described as minimal impingement, maximal contact (MIMC, Mitchinson et al. (2007)). Figure 2.3 shows freeze frames from high speed video showing an example of contact induced asymmetry. The effect of some of these control strategies on whisker based tactile discrimination is assessed in Section 6.4 of Chapter 6.

Whisker movement is actuated by a series of muscles that surround each whisker. The arrangement of these muscles constrains the possible whisker movement patterns, for example: each whisker is to some extent mechanically coupled to the adjacent whisker in the same row (Dörfl, 1982; Hill et al., 2008; Haidarliu et al., 2010), muscle tension during protraction causes whiskers to rotate torsionally as they sweep through the air (Knutsen et al., 2008); whisker protraction and retraction is controlled by different groups of muscles (Dörfl, 1982; Szwed et al., 2006), so the velocity of whisker movement, and the variance in this velocity, is different in each phase of whisker movement during a whisk (Berg and Kleinfeld, 2003). In addition, head movement

greatly effects the velocity of whisker contacts (Grant et al., 2009), and whisker movement is controlled to sweep space in anticipation of head movement (Towal and Hartmann, 2006). Though some have been identified (Grant et al., 2009), it remains unclear which components of whisker movement are actively controlled by the rat, which are artefacts arising from limitations of biological systems, and which if any are important for sensing. Section 6.4 of Chapter 6 goes some way to start answering these questions.

2.2.3 Neural systems underlying whisker sensing in rats

Individual whisker deflections are encoded by cell responses of around 200 cells in each whisker follicle complex (Dörfel, 1985, see Figure 2.4). Primary afferent neurons in the trigeminal ganglion synapse at the trigeminal nuclei of the brainstem (Torvik, 1956). Signals then follow parallel pathways through the different nuclei of the thalamus (Deschenes et al., 2005). Subsequently signals arrive at the somatosensory ‘barrel’ field (Woolsey, 1970), a distinctive region of cortex with representation for each individual whisker. Neurons in a particular barrel respond with the highest amplitude and shortest latency to deflections of a single ‘principal’ whisker (Woolsey, 1970; Rice and Van Der Loos, 1977), though their receptive fields can extend to several whiskers (Petersen, 2007).

The whole pathway from whisker tip to cortex preserves a clear whisker topology making the system amenable to research; with corresponding barrels in somatosensory cortex, barreloids in the ventral postero-medial thalamic nucleus (Van Der Loos, 1976), and barrellettes in the trigeminal nucleus (Veinante and Deschenes, 1999) for each whisker on the rat’s face.

Neurons in the rat whisker system respond with temporal accuracy to touch events (Szwed et al., 2006), with cells in barrel cortex responding within 10ms of initial contact (Armstrong-James et al., 1992). As whisking muscles do not have spindles, whisker position at the moment of contact cannot be recovered using proprioception (Fundin et al., 1994). However a particular class of cells fire preferentially to the phase of the whisker during protraction (Mehta et al., 2007).

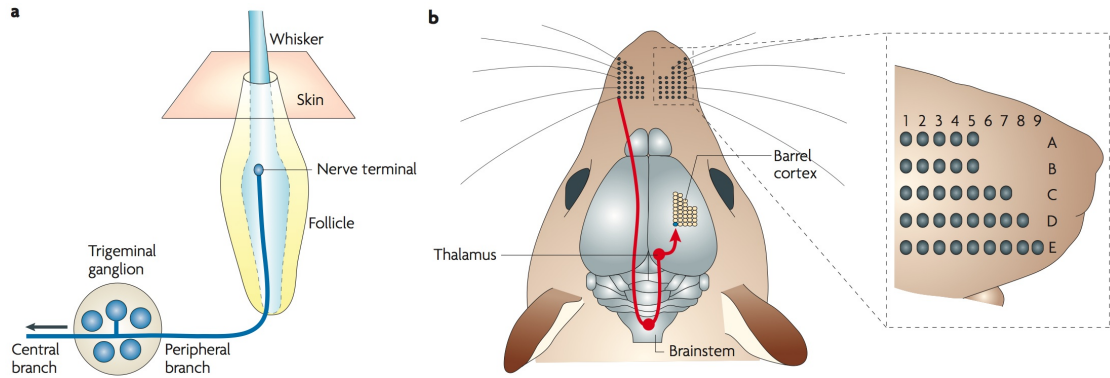


Figure 2.4: (a) A diagram of the rat whisker follicle. Mechanoreceptors (like those found in glabrous skin (Johansson and Vallbo, 1979)) respond to movements of the whisker within the follicle, either by the muscles in the follicle or through contacts with objects in the world. Mechanoreceptors encode the direction, velocity and duration of whisker deflections. (b) Whiskers are arranged in a regular grid of five rows on each side of the face. Primary afferent neurons in the trigeminal nerve carry information from the follicle to the cell bodies close to the brainstem. From here the neurons project across the midline to the trigeminal complex in the thalamus. Thalamic neurons project to the ‘barrels’, an area of somatosensory cortex that responds to and processes whisker deflections and preserves the regular grid arrangement of whiskers on the face. Figures taken with permission from Diamond et al., 2008 (a).

It is thought that whisker-object contacts are controlled through a series of nested loops, with reciprocal connections between somatosensory and motor cortices; a closed positive feedback loop through the brainstem from the trigeminal ganglion, to the trigeminal nuclei, and facial motor nucleus (Nguyen and Kleinfeld, 2005); and connections between the basal ganglia, parallel connections in the thalamic nuclei, cerebellum, superior colliculus, and facial nucleus (see Kleinfeld et al., 1999 and Kleinfeld et al., 2006 for a detailed review of these loops, and Figure 2.5 for a schematic of these loops). It is thought that the tight temporal coupling of fast sensory reports of contact timing, and efferent copies of motor command signals ultimately allow the rat to monitor the angular position of the whisker (Kleinfeld et al., 2006; Mehta et al., 2007), and carefully control whisker movement for better sensing as was described in Section 2.2.2. This may be analogous to learning the forward model of the system (Wolpert et al., 1995; Dearden and Demiris, 2005).

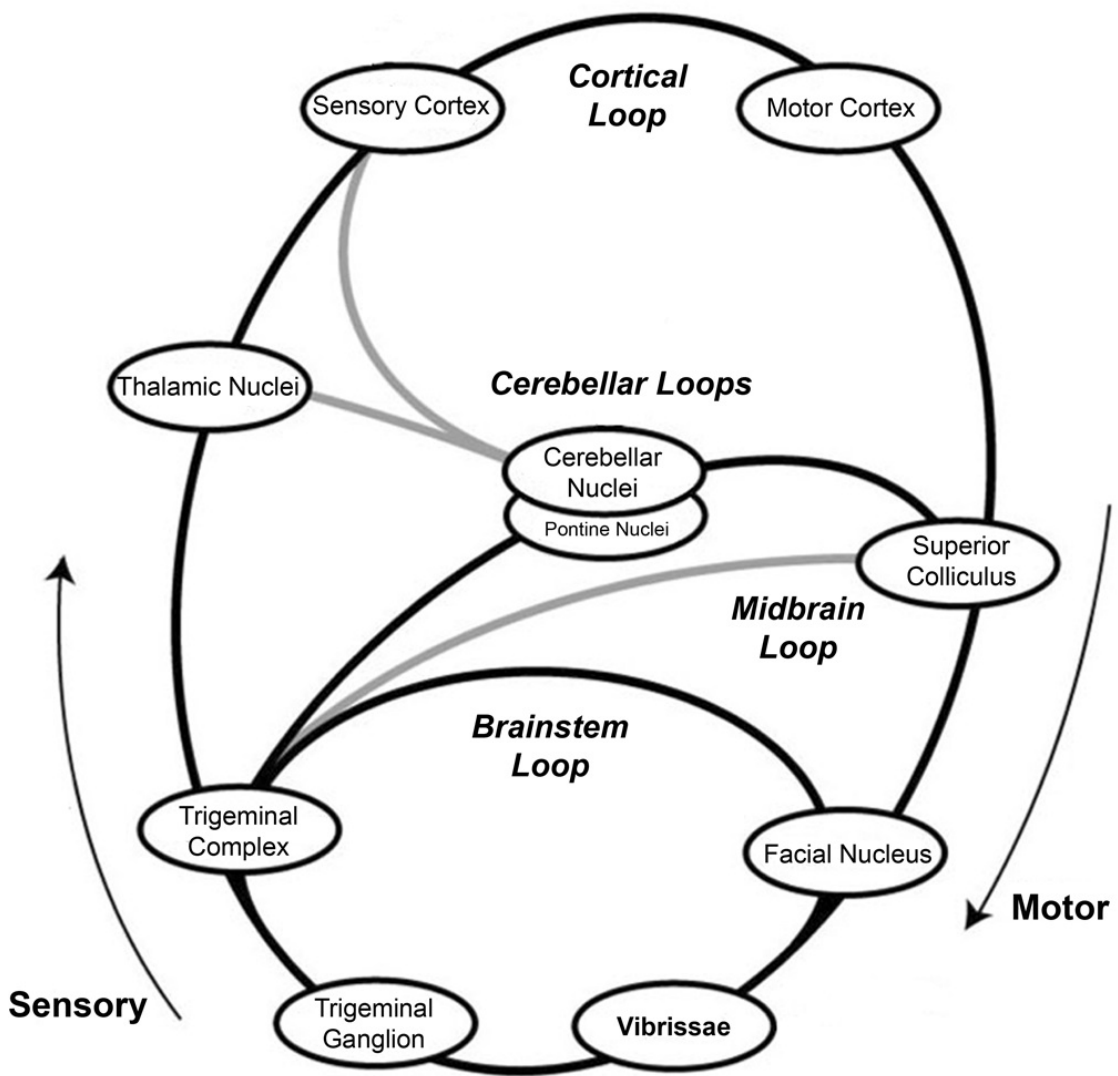


Figure 2.5: A simplified schematic of the neuroanatomical loops found in the rat whisker system. Ascending sensory projections carry whisker deflection information from the whisker follicle sinus complex to the trigeminal complex in the brainstem, through thalamus and on to the somatosensory cortex. Descending motor projections carry commands to the muscles in the whisker pad through the superior colliculus and facial nucleus. Also shown are the brainstem and cerebellar loops that are thought to be involved with whisker movement control. Additional parallel thalamic connections to the motor cortex (Yu et al., 2006), and loops through the basal ganglia (Deschenes et al., 1996), are not shown. Figure taken with permission from Mitchinson et al., 2010, modified from Kleinfeld et al., 2006

2.2.4 Summary of biological whisker systems

We have seen that rats have a sophisticated and highly evolved tactile sensory system. Whiskers vary in size and density across the array. Whisker are moved back and forth through the air in a behaviour known as whisking. Whisker movements are under active control, and rats seem to use different strategies to carefully move their whiskers when interacting with the world around them. The precise reasons for this active control is unknown, though it is thought that these strategies improve sensing. Whisker processing is very fast in the rat, which may indicate that useful information is more directly available within the whisker deflection signal than in other modalities where a great deal of pre-processing must take place.

Active whisker control may be similar to eye movement control in active vision (Aloimonos et al., 1988). The field of active vision explores how the sensors may be moved to efficiently search an environment. The difference between active vision and active touch is in the scale of the movements with respect to the environment. In active vision the sensors can be moved to search a whole environment, for tasks such as scene identification or mapping (Davison and Murray, 2002). Active whisker touch can only be used over a very local region of the environment, therefore active whisker control may be thought of as analogous to micro-saccades for gaze stabilisation (Collewijn and Kowler, 2008) or pupil diameter and lens focus, for luminance and depth of field control in the eye (Koss and Wang, 1972), (Takehiko and Haruo, 1991).

What are the implications of these physical properties for artificial whisker systems? It is clear that the tactile information available to rodents, and the sensing strategies utilised, are very rich. Understanding this system could have repercussions for understanding brain systems within the rat whisker system, as well as for developing tactile sensing machines that could be used in a wide number of industrial applications. Robots that have been built to encompass some of the physical attributes of whisker systems are described in the next section. Different methods of sensory transduction are compared, as well as contrasting approaches to whisker actuation. Another question is: what role do whisker control strategies play in sensing? The effects of

whisker control strategies on sensing with artificial whiskers are evaluated in Sections 6.3 and 6.4 of Chapter 6.

2.3 Artificial whisker systems

We have seen in the previous Section that rats have a sophisticated whisker system that they use to gather tactile information from the world around them. Without whiskers of our own it is very difficult to gain insights into the particular difficulties and benefits of this sensory modality. Whisker movement seems to be integral to the sensing process in rats, but in the animal it can be difficult or impossible to evaluate the benefits of different whisking strategies on sensing. One way to understand how complex biological systems, such as the rat whisker system, operate is to develop models of that system.

By developing artificial whiskers, researchers can become familiar with the task of gathering and processing whisker information. The acuity of whisker sensing in a range of settings can be evaluated. The importance of whisker material, shape and size in sensing can be determined, as well as the kind of sensory transducer fixed to the base. The choices roboticists make in the placement and actuation of whiskers give the opportunity to evaluate how whisker movement effects sensing. Building robots also helps us understand the biological system by conducting experiments that would be impossible or very difficult to perform in the animal. For example, as was discussed in Section 2.2.2 the effect that whisker movement has on sensing is poorly understood. With a whiskered robot we can precisely control and change whisker movement, and determine the effects each change has on whisker deflections and subsequent analysis.

This Section reviews the efforts that have been made to build whiskered robots, either as engineering exercises or to understand the sensory capabilities of rodents. Conclusions are drawn about the state of the art in whiskered robots, and where improvement is needed to answer certain pertinent questions from the biology, and develop robots capable of using whisker based

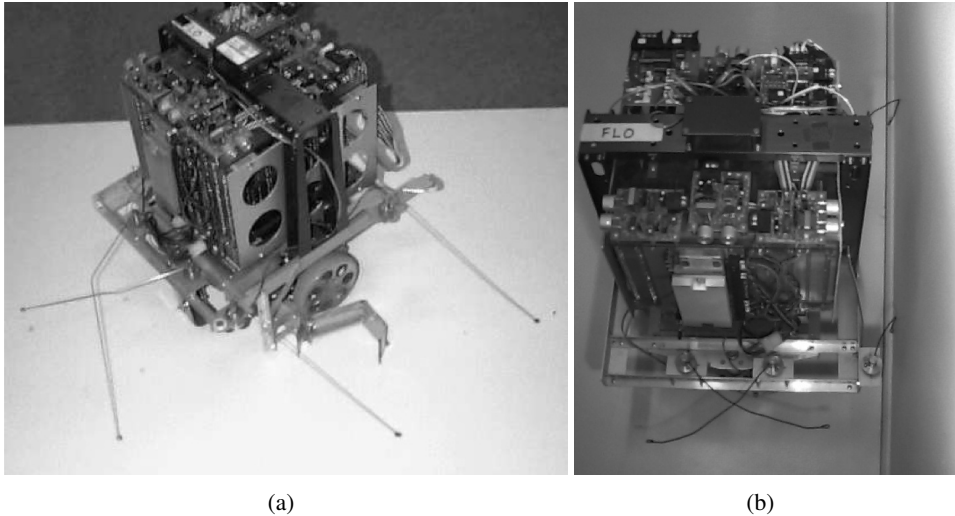


Figure 2.6: (a) The Yamabico Robot with whiskers used by Jung and Zelinsky (1996). (b) The Yamabico robot during a wall following task. Figures reproduced with permission from Alex Zelinsky.

tactile sensing effectively in real-world environments.

2.3.1 Early whisker-like sensors

The first attempts at whisker-like sensing were mathematical models, Salisbury (1984) describing how a group of hinged probes could be used for determining object shape by measuring the angles and forces at the joints. Whiskers are difficult to simulate accurately, an issue which is discussed in more detail in Section 2.4.3 of this review. A more straightforward method of generating appropriate tactile data is by building artificial whiskers and mount them on robots. The first hardware implementation used tactile sensors to provide binary contact/ no contact reports (Schiebel et al., 1986). Taking inspiration from cat whiskers, the first hardware whisker-like models featured a separate contact detector at the tip, to determine whether a contact has taken place, as well as a potentiometer at the whisker base (Russell, 1992). Using curved rods to prevent large axial loads, the potentiometer was used to measure the angle of rotation of the ‘whisker’. Using a combination of measuring the rotation of deflection and a tip contact sensor

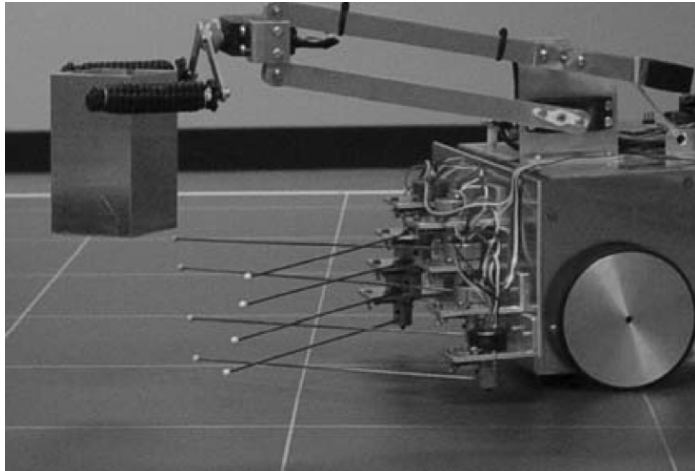


Figure 2.7: The original ‘whiskerBOT’, built by Russell and Wijaya (2005). Figure used with permission

it was possible to recover the curvature of simple objects.

Jung and Zelinsky (1996) demonstrated whisker based navigation as a potential supplement to vision, allowing a robot to efficiently drive around the perimeter of a known environment using information from an array of static whiskers. The authors describe a robot (pictured in Figure 2.6) with four simple whisker sensors that could report a binary contact/no contact for wall following (similar to a subsumption architecture (Brooks, 1986, 1991) based line following robot, such as that of Prescott and Ibbotson, 1997). Rich object ‘features’ were also reported from the whiskers, for example a ringing to signify that the whisker had deflected past a table leg, though the authors do not detail how the features are extracted from whisker deflections, how accurately the objects are sensed, or how this information is used in navigation.

Rigid metal whiskers were used to infer the contours of objects on a mobile robot called WhiskerBOT (Russell and Wijaya, 2003, 2005, shown in Figure 2.7). Here the whiskers themselves were not actuated, the array of eight passive whiskers was moved around an arena and into objects by the motion of a robot platform. By knowing the geometry of the whiskers in space, their size, and the angle of whisker deflection using a potentiometer, it was possible to infer the location

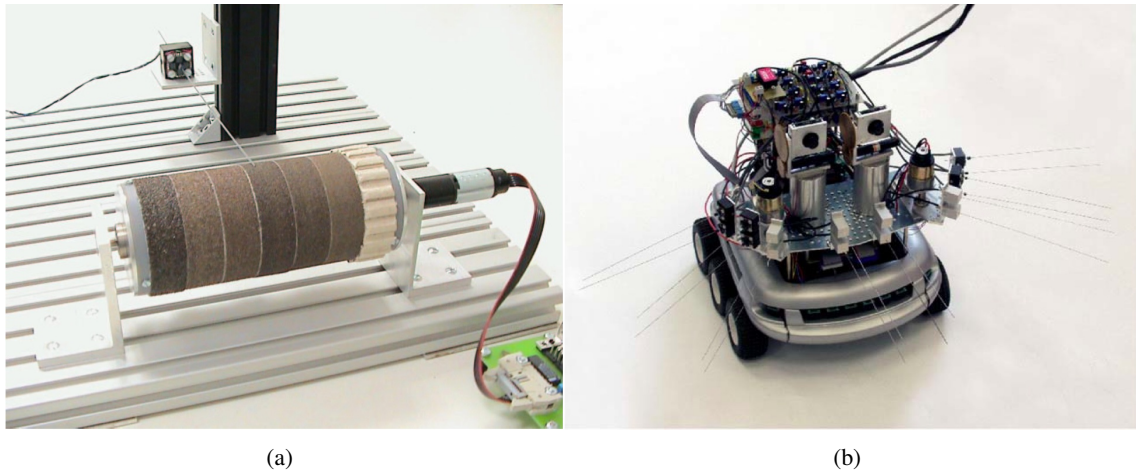


Figure 2.8: (a) Experimental design for gathering data for texture discrimination from Kim and Moller (2004). (b) Koala robot equipped with a range of different artificial whiskers from Kim and Moller (2007). Figures used with permission from D. Kim.

of whisker contact in space using static beam equations (Young et al., 2003, discussed in more depth in Section 2.4.3.1 of this review). By making many such contacts and extrapolating across them it was possible to determine the identity of an object from a group of possibilities, and the objects were subsequently retrieved by the robot.

2.3.2 Actuated artificial whiskers

As we have seen in the review of the biology in Section 2.2.2, whisker actuation is an important feature of biological whisker systems. Actuated whiskers have been developed for a number of robots. In a unique design Wilson and Chen (1995) used a pair of pressurised tubes laid end to end as a whisking mechanism, with a steel wire ‘whisker’ mounted at the end. By using measurements of bending from two strain gauges near the whisker base, and pressure from the tubes in a closed loop control system, it was possible to infer whisker tip contact location in space. Object shape could then be determined, with fits to the contact points accurately recovering the slope and area of a square.

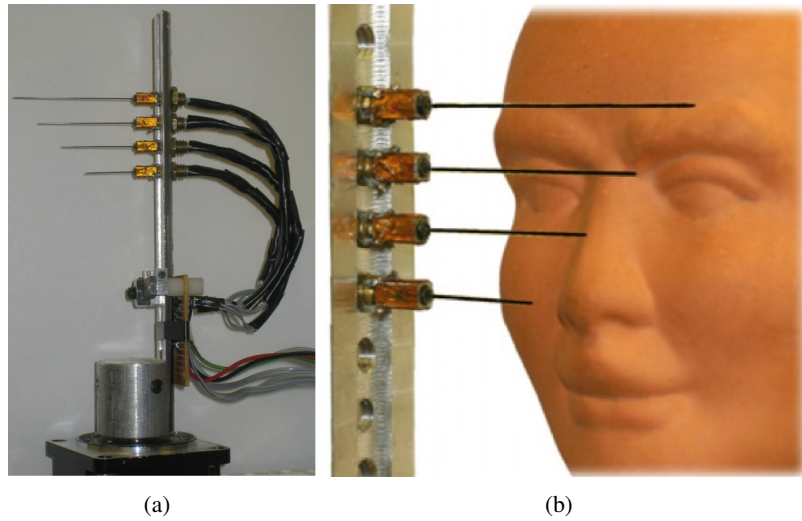


Figure 2.9: (a) The vibrissal Sensobot. (b) Extracting complex object contours. Artificial whiskers are rotated into objects with a given force, and moments are measured at the base. Pictures reproduced with permission from Gopal and Hartmann (2007).

In a series of papers Kim and Moller (2004, 2007) developed a number of whisker sensors and data collection paradigms. Metal wire whiskers 0.5mm in diameter and of differing length (80mm–150mm) were attached to piezo bending sensors to measure whisker oscillations, Hall effect sensors (based on the movement of a magnet in an electric field, described in Section 3.2.1 of Chapter 3) to measure whisker bending (both in Kim and Moller, 2004), or microphones to measure oscillations for texture discrimination (Kim and Moller, 2007). These whiskers could be mounted on rotational DC motors (with 120° range) on a mobile Koala robot (see Figure 2.8 (b)), or statically mounted to make contact with a rotating textured drum (see Figure 2.8 (a)). In the oscillating case, all whiskers on the same side of the robot are moved together as they are fixed to the same metal plate. Sensor signals were amplified and transmitted to an onboard computer. The results of the experiments performed with these robots are discussed in Section 2.4.3.1 of this Chapter.

Figure 2.9 shows the vibrissal sensobot robot developed by Gopal and Hartmann (2007) to quantify sensory data acquisition in rats. Specifically the experimenters developed a model based on

classical elasticity theory to determine the radial distance to contact along a whisker as it rotates into an object. Four nitinol whiskers of different lengths were fixed to a set screw, with two orthogonal pairs of strain gauges to measure bending moments at the base. The results of this paper are discussed in comparison to other methods in Section 2.4.3.1 of this Chapter.

2.3.3 Biomimetic systems for whisker sensing

Moving beyond tactile sensors for specific tasks, a number of projects have aimed to model more than one aspect of biological whisker systems on integrated robotic platforms. These robots differ from those in the preceding Sections in that they have whiskers in addition to other biomimetic (literally to mimic biology, taking ideas from biological systems to technology Vincent et al., 2006) features.

The Darwin IX robot (Seth et al., 2004, pictured in Figure 2.10 (a)), the latest in a series of mobile ‘brain-based devices’ used tactile discrimination as part of a wall following and avoidance task. Using a simulated nervous system running on a remote cluster it was possible to discriminate textured surfaces comprising a series of pegs similar to braille characters (Loomis, 1942). A column of whiskers (Figure 2.10 (b)), with polyamide strain sensors along their length, would strike the pegs in a specific temporal pattern. This pattern was learnt by the simulated neural system of the robot through a series of ‘lag cells’. The robot would eventually learn to appropriately avoid a given surface in 96.6% of trials.

A great deal of work on whisker based tactile sensing was done as part of the AMouse project (Fend et al., 2005, see Figure 2.11). To begin with the authors looked at the effect different whisker materials had in sensory transduction (Lungarella et al., 2002). They found that rat’s whiskers responded more diversely on different surfaces – changes in surface roughness resulted in large changes in whisker deflection patterns – than did other materials such as broom bristles or human hairs. Natural whiskers also had a narrower band of frequencies in their deflections. They went on to suggest that actively controlling the whisker was critical to sensing, and show

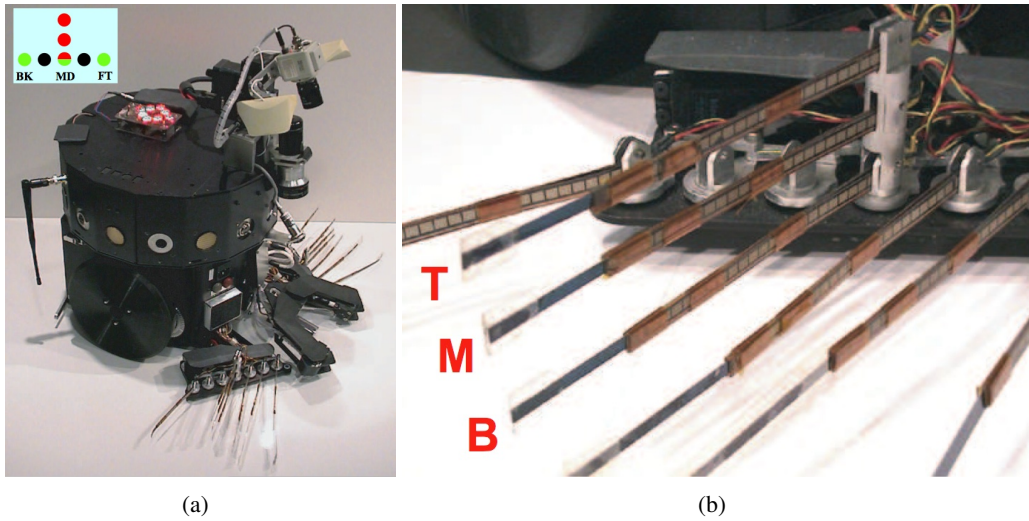


Figure 2.10: (a) The Darwin IX robot. The inset diagram shows whisker array arrangement. Wall following whiskers are marked in green (FT,MD,BK). Whiskers used for texture discrimination are marked in red. Whiskers marked in black were not used here.(b) Close up of the whiskers used for tactile discrimination, labelled T, M, B for top, middle and bottom respectively. Figures reproduced with permission from Anil Seth.

that combining information from different whiskers improves the sensitivity of the system in a texture discrimination task (Fend et al., 2003).

In another study Fend et al. (2006) showed that whisker array morphology was important for sensing, both on a mobile robot and in simulation using artificial evolution. In a wall following and object avoidance task the most successful whisker morphology is one that most closely resembles that of a rat, specifically with the longest whiskers most caudal on the array and whisker length progressively becoming shorter towards the rostral end. In a simulated evolution experiment flexible whiskers were shown to be ‘fitter’ than rigid whiskers. The experimenters propose that this fitness could be due to the robustness flexible whiskers would have to small changes caused by the evolutionary algorithm. In the rigid case, a small change in whisker morphology could have a large impact on sensory transduction. Flexible whiskers deform, which can eliminate the effect small changes will have on sensory transduction between trials. Different results may be found if the behaviour of the evolutionary algorithm were modified.

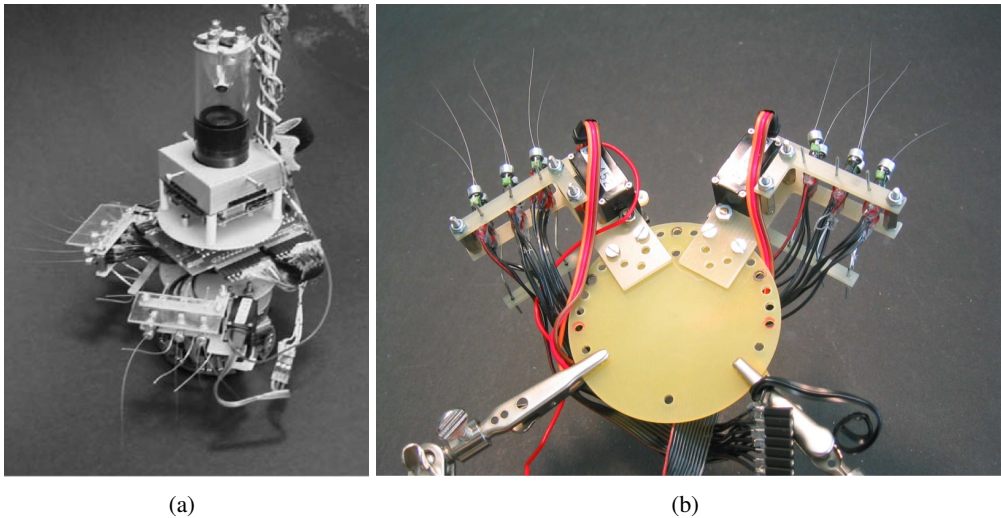


Figure 2.11: (a) AMouse (b) A close up of AMouse’s whisker array. The configuration of the whiskers can be changed to investigate the influence array morphology has on sensing. Figures used with permission from V.V. Hafner and Rolf Pfeifer.

Psikharpax (Meyer et al., 2005, see Figure 2.12 (a)) is an artificial rat developed to integrate a number of biomimetic neural architectures on a mobile robot. Particular effort was made in the development of Psikharpax to have a whisker array arranged to physically match the system in rats (N’Guyen et al., 2009). Two thin sheets of carbon–charged silicon conductive elastomer was used to mimic a sort of artificial skin. The conductivity of the sheet varies when it is deformed. By fixing a conductive carbon fiber vibrissa (0.5mm in diameter) between four conductive probes, the changes in resistance can be measured as the whisker is moved in two axes. Two arrays of thirty three whiskers were arranged in grids on either side of the robot ‘head’ (see Figure 2.12 (b)). An additional advantage of this system is that it could be deformed to investigate the effect whisker pad morphology can have on sensing.

Utilising this dense whisker array as a complement to vision the researchers hoped to demonstrate action selection and navigation on a biomimetic mobile robot. Texture discrimination on Psikharpax is described in Section 2.4.5.2 of this Chapter.

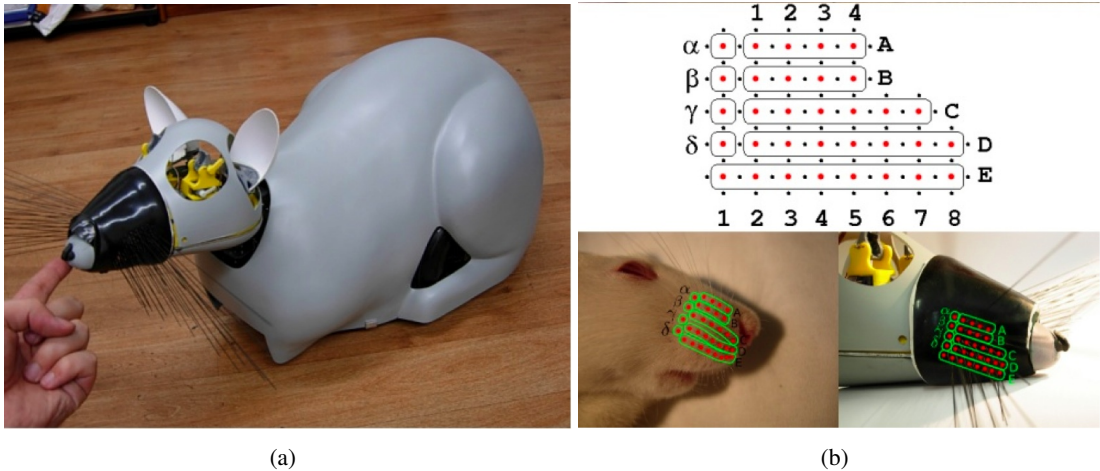


Figure 2.12: (a) The Psikharpx robot. (b) The Psikharpx whisker array. The relative size and arrangement of whiskers on the robot were based closely on the rodent system. Figures used with permission from N'Guyen et al. (2009)

The second robot to bear the name Whiskerbot was developed at Bristol Robotics Laboratory as part of a collaborative project between engineers, computational neuroscientists and ethologists to re-engineer the rat whisker system. Whiskerbot was a mobile whisking robot, using six 200mm conical glass-fiber composite whiskers arranged in two rows of three, and measuring base deflections at 10kHz using strain gauges.

Whiskerbot was developed using biologically plausible mechanisms rather than pure engineering solutions. Models of neural structures for sensing and architectures for motor control were developed and integrated on to the robot. These models were implemented on the robot both to test these models more thoroughly than can be done in simulation, and to aid the development of hypotheses about the biological system.

A model of the whisker follicle sinus complex developed by Mitchinson et al. (2004) was implemented on a FPGA (field-programmable gate array, a form of programmable logic board ideal for mobile robots, that can perform computations independent of a computer) hardware onboard the robot to generate spike trains in real time in response to whisker deflections. Whisker movement was controlled using a pattern generator model operating on the principle of minimal

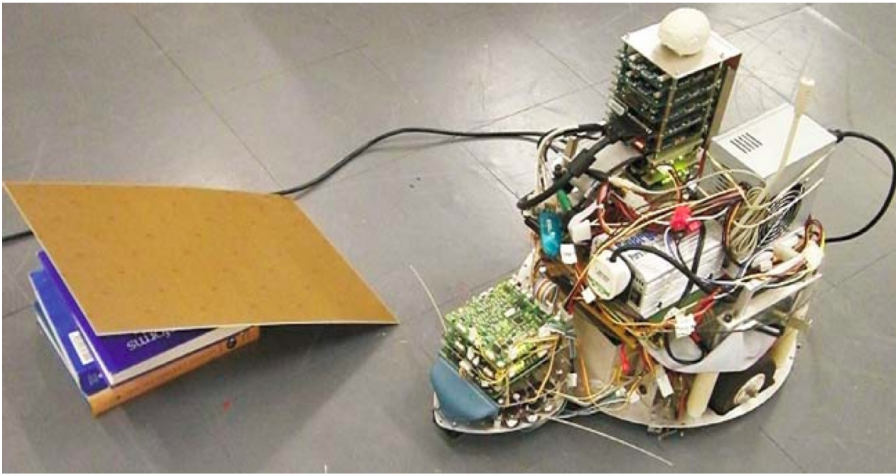


Figure 2.13: The second Whiskerbot, developed at the Bristol Robotics Laboratory in collaboration with the University of Sheffield.

impingement, maximal contact (MIMC Mitchinson et al., 2007, described in Section 2.2.2 of this review). Models of the basal ganglia (Prescott et al., 2006) and superior colliculus were used to control exploratory and orienting behaviours. Whiskerbot was later used in a texture discrimination experiment, evaluating a number of methods under conditions of varying whisker motion (Fox et al., 2009a). These results are discussed in comparison with other methods in Section 2.4.3 of this review.

2.3.4 Summary of artificial whisker systems

We have seen that a number of sophisticated and innovative robots have been built recently to answer a range of questions about whisker sensing. Each approach has been successful in its own right, and some have generated results and approaches that may be taken forward for future robots. However there are a number of limitations for each of the platforms described in this Chapter. The robots presented here show a progression towards modelling a wide range of biological whisker system properties simultaneously; such as whisker morphology, whisker materials, whisker actuation, sensory transduction and closed loop motor modulation based on

sensor input.

A question that remains is: do the robots here control and constrain whisker–object collisions enough to develop a good understanding of whisker sensing? For a given experiment there are a number of possible degrees of freedom that need to be controlled. Are the robots controlled well enough to reveal which aspects of whisker movement are important for or aid sensing? On the other hand, when a robot is carefully constrained, as in the case of Sensobot 2.3.2, the movement may be too restricted to explore things such as the effect of whisker movement control strategies described in Section 2.2.2 of this Chapter. At the same time none of these robots is sophisticated enough to interact with a rich real–world environment. In Chapter 3 we review the robots that are used to generate data in this thesis, to address some of the limitations of previous robotic platforms.

2.4 Whisker based tactile discrimination

We have now reviewed the structure and control of the rat whisker system (Section 2.2), and the robots that have been built to model these physical characteristics (Section 2.3). This Section reviews tactile discrimination with whiskers. The tactile sensing capabilities of rats are reviewed. A logical first step is to determine how well a rat can localise a contact in space. Firstly we will review how well rats can recover whisker contact geometry (Sections 2.4.1 and 2.4.2). Secondly we will review a rat’s ability to discriminate surface textures (Section 2.4.5). Methods for extracting this tactile information from whisker data are described. Many of the algorithms and strategies described were developed on the robot hardware described in the preceding Section 2.3.

Conclusions are drawn about the limitations of the work published in the literature, and what steps are required to address these problems.

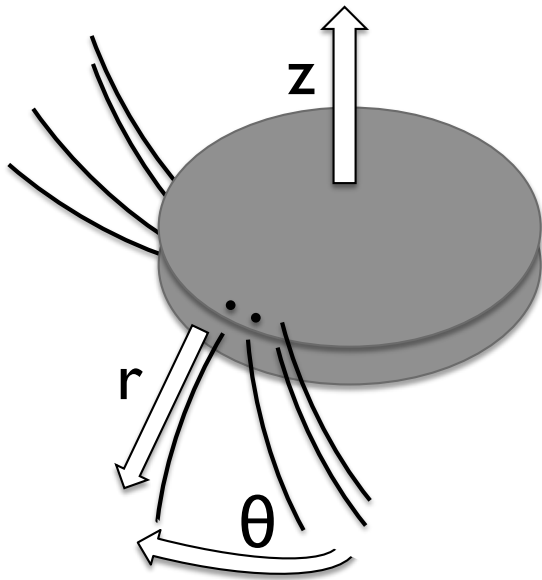


Figure 2.14: Whisker array geometry.

2.4.1 Whisker contact geometry

A great deal of research has focused on the responses of neurons in the whisker system, in a wide range of situations, (see Ahissar and Arieli, 2001; Kleinfeld et al., 2006; Szwed et al., 2006; Diamond et al., 2008 (a) for in depth reviews, and Section 2.2.3 for additional descriptions of these loops). Of particular relevance to the task of tactile discrimination sufficient for navigation is the ability of a rat to monitor its own whisker movement, and therefore the location of contacts in head centred space. Head centred whisker geometry is shown in Figure 2.14.

As discussed in Section 2.2, rat whisking muscles do not have spindles, so whisker position at the moment of contact cannot be recovered using proprioception. However rats can still reliably infer the angular position of contacts in space. Rats can discriminate the angular position θ of vertical poles to within 6° (Knutsen et al., 2006). Individual rats reached acuity thresholds as low as 1° . Performance was best in rats who were initially trained with all their whiskers intact, but then had the whiskers trimmed to one column. It is speculated that contact timing is critical to determining this object position parameter, and head and whisker movement is critical for

good task performance (Knutsen and Ahissar, 2009; Mehta et al., 2007). Lesioning the facial motor nerves reduced performance to chance level, showing how important whisker movement is to accurate sensing.

2.4.2 Radial distance to contact

If the angle θ and elevation z of contact have been determined, the deflection signal needs to be analysed to discriminate the radial distance to contact r and recover the 3-D location of contact in space. Radial distance is important as it allows the agent to determine whether the object has been contacted at the tip or the shaft of the whisker, and potentially allow the recovery of surface contours. Decisions about how best to move the whiskers in subsequent whisks may also be dependent on accurate measures of object location.

In the rat an identity code for whiskers has been proposed as a method of determining the location of a contact in space (Brecht et al., 1997). Given the geometry of the whisker tips – assuming whisker shape, length and position is known – the identity of whiskers that have made contact with an object is enough to determine not only the elevation Z and angle θ , but also radial distance r of an object. This is due to the particular morphology of the rat whisker array. As described in Section 2.2.1, whiskers increase in length across the grid-like whisker pad, from short micro-vibrissae around the lips to long macro-vibrissae in the most caudal columns. If a vertical pole is placed in the path of a whisker pad protraction the shorter whiskers will whisk past the pole and not make contact. Longer whiskers strike the pole, and the rat can determine that the pole is located somewhere between the tips of the first whisker to make contact and its most adjacent, rostral neighbour.

However it has been shown that the sensitivity of the whisker system to radial distance is too acute to rely on an identity code alone. Rats trained to determine the width of an aperture could discriminate differences as small as 3mm (Krupa et al., 2004), and asymmetries between the distance of two edges of an aperture of 10.8 mm (Shuler et al., 2002). These differences are

small enough that the same group of whiskers make contact with the stimulus on different trials, indicating that the rat is not using the number or identity of contacted whiskers to determine the radial distance of objects. An additional metric must be being used. Cells in the trigeminal ganglion have been shown to respond more strongly to contacts closer to the base than contacts at the tip (Szwed et al. (2006), addressed further in 2.4.3.1). Information theory analysis of the responses showed discrimination acuity of 30% of whisker length in some single cells. It's possible a coarse coding of radial distance across a number of neurons and whiskers could increase acuity (Eurich and Schwegler, 1997).

2.4.3 Model-based methods for radial distance estimation

Numerous models have been produced to understand and replicate the radial distance detection abilities of rats, falling into two broad categories: model-based and model-free. Model-based methods make generative physical assumptions about the whisker; model-free methods are based on the data alone. The ideal model-based method would be a probabilistic inverse model of the whole physical system. Forward models of whiskers are relatively simple to build using finite-element simulators (though are non-trivial due to the presence of large contact forces on small masses causing numerical instabilities; and are time-consuming to run), however it is difficult to determine the accuracy of such models as whisker physics is still poorly understood. We previously found that to simulate contacts between a surface and a 10-element mass-on-spring model in real-time requires an unacceptable relaxation of the whisker stiffness to avoid numerical errors (Fox, Evans, M. H., Pearson, and Prescott, 2008). An image from this simulation is shown in Figure 2.15. In theory, given a set of strain data recorded at the whisker base, we could run all possible FEM simulations then choose the one which produces the most similar results to the observations. On current hardware this is difficult due to the large number of states that a flexible whisker can exist in. An approximation would be to draw Monte Carlo samples from the set of possible generative processes (Hammersley and Handscomb, 1975; Doucet et al.,

2001), but again this set is large and each FEM simulation requires a long time to run accurately.

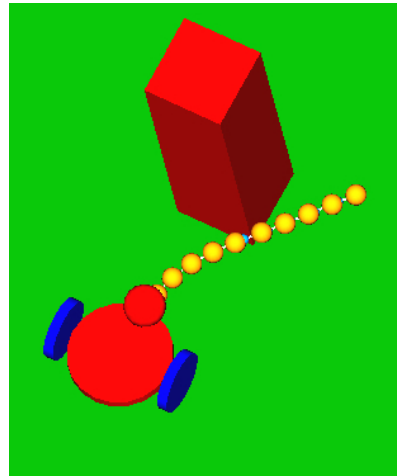


Figure 2.15: A screen grab of the Freebots whisker simulation used in Fox, Evans, M. H., Pearson, and Prescott (2008).

Simplified model-based methods can be built from stronger assumptions about the dynamics and about the environment.

2.4.3.1 Static beam equation based classification

It has been proposed that the increased activity of trigeminal ganglion cells for contacts at progressively shorter radial distances (Szwed et al., 2006) may be because the cells are responding to increases in bending moments at the base of the whisker (Solomon and Hartmann, 2006). Beam theory states that the radial distance r to deflection along a cantilever beam determines the radius of curvature of the beam κ (Young et al., 2003)(Megson and Megson, 2005). Curvature is proportional to the bending moment M at each point along the beam x following

$$\kappa(x) = \frac{M(x)}{EI}, \quad (2.1)$$

where E is the elastic modulus, and I is the area moment of inertia of the whisker.

The relationship between r , M at the base, and whisker deflection angle θ can be expressed (Gopal and Hartmann, 2007) as;

$$r = 3EI_{\text{base}} \frac{\theta}{M}. \quad (2.2)$$

Taking inspiration from insect antenna static beam equations were applied to measurements taken from the base of cylindrical beams to determine the radial distance to contact on a robot by Kaneko et al. (1998). These measurements were used over iterative contacts to recover the contours of a surface. Data collected from metal wire whiskers and Hall effect sensors on Kim and Moller (2007)'s Koala robot (described in Section 2.3.2 of this Chapter) could be used with the static beam equations described above to recover the curvatures of cylinders of different widths, and discriminate square from round objects. They go on to show that a single whisker is useful for measuring contact properties in a plane, but vertical shape properties require multiple whiskers. In the last few years work has focused on applying static beam equations specifically to rodent whiskers, by modifying the equations to account for whisker taper, and using time derivatives for biological plausibility (Birdwell et al., 2007). If it is assumed that the whisker is in static equilibrium at all times static beam theory can be used to examine a series of contact locations over time, and under highly controlled and replicated conditions it is possible to reconstruct 3D face models from a metal whisker (mounted on Sensobot, described in Section 2.3.2 of this Chapter) using this method (Gopal and Hartmann, 2007).

The experimenters built an array of 4 whiskers, with 4 strain gauges on each (opposing pairs in 2 axes). These four whiskers were attached to a vertical rod which rotated into a small sculpted head. Radial distance to contact was determined for each whisker, and a spline was fitted to match these points and reconstruct the contours of the surface. The array was repositioned after each trial and whisked again until the whole of one side of the face had been covered by contact

points. The information from one side was then mirrored to reconstruct the other side of the face. A total of 1036 contact points were made, with a large proportion of which (42%) occurring at or near the tip.

These results are interesting because their original paper Birdwell et al. (2007) highlighted that the static beam model was only really accurate for contacts near the base (< 10% accuracy within the first 70% of total whisker length), but here a large proportion occurred at or near the tip. How can this wealth of information be used effectively by the rat if it is inaccurate? Gopal and Hartmann (2007) go on to propose that when the model reads out a value for r that is the same as or longer than the known whisker length, they assigned it a value of being the whisker length. In this way, even if the accuracy is a little off, it will be clear if the output implies a tip contact or not. This method allows the rat to know whether the whisker contacted with the tip or the shaft of the whisker. This result arose only as a consequence of building a hardware implementation of the model.

However these static equations rely on static measurements of whisker bending during contact, and real whiskers are not in static equilibrium at all times. In particular when they encounter an obstacle there are large oscillations, and they often build up force ‘sticking’ against it, then eventually ‘slip’ away from it and perform ‘ringing’ oscillations based on their natural frequencies.

In addition, static beam equations, and analyses relying on instantaneous measures of moments only account for the dynamic properties of objects if additional observations are made. As stated in 2.2, one way is to measure θ , the angle of whisker rotation during contact. It is proposed that a rat would be able to keep track of this angle when it is moving the whiskers around. A robot would also be able to keep track of whisker movement for the most part. Problems emerge when θ is not known precisely, or if the object itself is moving. These equations would need to be modified to account for situations where contact speed is a variable, and would not be usable when contact speed is unknown.

2.4.3.2 Oscillation frequency based classification for radial distance estimation

Another model based approach has used Elastic beam theory (Rao, 2004) to determine the radial distance to contact, by measuring changes in natural frequencies during and immediately after contact (Kim and Moller, 2004). A beam fixed at one end will oscillate at a specific frequency when struck, depending upon the physical properties of the beam, such as its shape, size and the material it is made of (Rao, 2004; Kim and Moller, 2004). The frequency of these vibrations will differ depending on whether the beam collides with an object and is then released into air, or if the beam remains in contact with the object after initial collision.

In the second ‘pinned’ case the frequency of oscillation will change depending upon the radial distance of the pinned point along the beam. By monitoring the natural frequencies of the beam during contact it is possible to determine the radial distance to contact along the beam. Attaching a ‘payload’ mass at the end of a piece of wire to accentuate vibrations during contact, it was shown that such a system could work in practice (Ueno et al., Dec 1998). It was subsequently shown that a vibration based approach was possible without a payload mass (Kim and Moller, 2004). However the beam used was cylindrical and made of metal, which would increase the duration of oscillations compared to a tapered, highly damped biomimetic whisker.

Implementing this approach on biomimetic whiskers poses certain problems. Specifically, the mechanical properties of rodent or biomimetic whiskers are not ideally suited to maintaining vibrations during static contacts, or in air immediately following a contact. A thorough examination of whisker vibration mechanics are beyond the scope of this paper, though we can elaborate on a few points.

Whiskers are highly damped, with a low modulus of elasticity and low damping ratio and Q value. The Q factor is approximately the number of oscillations required for a freely oscillating system’s energy to fall off to $1/e^{2\pi}$, or about 1/535, of its original energy (Crowell, 2000). Informally, Q is the number of times a struck beam will oscillate before coming to rest. Systems

designed to have a strong resonance or high stability of oscillation have a high Q . A tuning fork for example has a Q of 1000. Rat's whiskers are highly damped, with a Q of around 2.5–5 (Hartmann et al., 2003). Whiskers are tapered, which can additionally dampen oscillations (Williams and Kramer, 2010). Contacts are typically very short (<100ms), which makes accurate measurement of vibration difficult. Peaks in the resonance curve for a whisker are quite broad. Figure 2.16 shows the resonance curve of a metal wire and a rat whisker. This broadness makes any small changes in the frequency of these peaks ambiguous.

Whisker vibration, and resonance frequencies in particular have been implicated in texture discrimination (covered in depth in Section 2.4.5). It may be that the vibration properties of whiskers are tuned to texture discrimination. It follows therefore that this vibration based approach may not be applicable to radial distance estimation on biological or biomimetic whiskers.

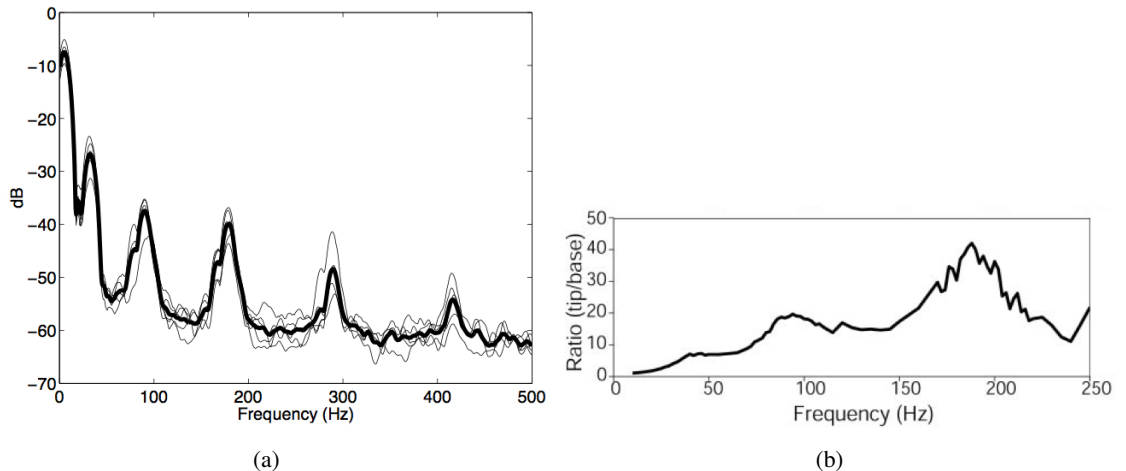


Figure 2.16: Resonance curves of 2 whiskers. (a) Resonant curve of a metal wire (Taken with permission from Kim and Moller (2004)). (b) Resonant curve of a rat C1 whisker (Taken with permission from Hartmann et al. (2003)).

2.4.4 Model-free methods for radial distance estimation.

The alternative to model-based, assumption-laden approaches are model-free heuristics derived from the data alone, either by hand or by automated search. The advantage of this approach is

that less prior knowledge is required in the design of the classifier. Model parameters are instead derived from the data. Resultant classifiers can be simpler to implement, and faster to run, as there are fewer parameters underlying the model. A disadvantage is that you must collect sufficient data to train the classifier before it can be tested or implemented in a trial.

2.4.4.1 Template based classification

Inspired by results from audio time series analysis (Downie et al., 2005), a simple approach is to hand-set or learn a set of exemplar data points, then make classification based on the nearest neighbour. Or, instead of matching the raw data, we might compute statistics from it (for example by using principle components analysis) and compare those to find the best match.

In the very simplest case, template based classification (Brunelli, 2009) involves recording example sensory data as templates during a training phase, and comparing the stored templates to novel data during the test phase. By systematically comparing the novel data to signals encountered previously, a classification can be made by declaring which of the stored templates the novel signal is most similar to.

Vision in jumping spiders works on a template matching principle (Land, 1969a,b), and template matching has been used in tasks such as heart beat electrocardiogram QRS detection (Afonso, 1993). Template classifiers work well in conditions with a small number of classes. Though when the data is sampled from a continuous distribution, or with numerous variables, it is difficult to know before hand how many templates are required for accurate classification.

2.4.4.2 Feature based classification

Feature based classification involves finding invariant features in the data that correspond to parameters in the real world. For example using scale invariant feature transformation (SIFT) algorithms in vision (Ke and Sukthankar, 2004; Juan and Gwun, 2010). Frog prey capture

is based on the principle of feature detection, with responses elicited for any object matching the size and angular velocity of a fly (Lettvin et al., 1959). In the rat whisker system some researchers have reported cells that respond to ‘kinetic features’ in whisker deflections (Petersen et al., 2008) (this work is described in more detail in Section 2.4.3 when discussing texture discrimination).

The downside of this kind of approach is that it may be difficult to find appropriate features, or it may take a long time to extract them. Alternative approaches are to use methods such as using principal component analysis (PCA) to find the ‘features’ in the data, as has been done for texture discrimination (work by Hafner et al. (2004), reviewed in Section 2.3.1).

2.4.4.3 Stationary Naïve Bayesian Classification

Decision making in monkeys is thought to utilise a neural mechanism of evidence accumulation for competing percepts according to Bayesian sequential analysis (Gold and Shadlen, 2001).

A neural–inspired Bayesian classifier has been used in our own lab to discriminate whisker data in texture estimation tasks (Lepora, **Evans, M. H.**, Fox, Diamond, Gurney, and Prescott, 2010b; Lepora, Pearson, Mitchinson, **Evans, M. H.**, Fox, Pipe, Gurney, and Prescott, 2010a). Bayesian classification involves modelling the likelihood of measurements from example sensory data. Given new test data these likelihoods are used, assuming flat priors in the simplest case, with Bayes rule to calculate the posterior probability of the test data being drawn. A naïve Bayes classifier is formally described in Section 4.3.5 of Chapter 4.

A stationary naïve Bayes classifier (Lewis, 1998) is the simplest implementation: assuming the measurements to be statistically independent, along with an assumption of identical likelihoods over time, to calculate the posterior probability for each class of training data. The utility of the stationary naïve Bayes rule is that it greatly simplifies the process of calculating the poste-

riors to an algorithm that is linear sum over log-likelihoods. Then the classification is similar in algorithmic complexity to a linear perceptron.

2.4.5 Texture discrimination

Texture discrimination in rodents has received a great deal of attention, and some controversy, ever since it was shown more than twenty years ago that rats could perform well in texture discrimination tasks using information from their whiskers (Guic-Robles et al., 1989), and were able to discriminate a smooth surface from a rough surface containing shallow ($30\ \mu\text{m}$) grooves that are spaced at $90\ \mu\text{m}$ intervals (Carvell and Simons, 1990). Rats can be said to excel at texture discrimination. Though no direct comparison has been made (Diamond et al. (2008 (a)), it is thought that rodent discrimination compares favourably with that humans, who are capable of discriminating texture roughness differences of 5% in 75% of trials (Morley et al., 1983). It has been shown that rats can discriminate smooth from rough surfaces with 1–3 whisker contacts within 98–330 ms of initial contact (von Heimendahl et al., 2007), indicating that this system is both reliable, and extremely fast compared to other sensory modalities.

With the exception of tactile prey capture in shrews (Anjum et al., 2006; Munz et al., 2010) texture discrimination is the only demonstrated instance of a rodent determining ‘what’ something is using the large macro-vibrissae (though gross shape discrimination has been shown in rats using the micro-vibrissa around the mouth and lips (Brecht et al., 1997)), so it is an important field of research to consider with our aim of developing a system for tactile sensing.

2.4.5.1 Resonance hypothesis

It has been proposed that the whisker array could function like a collection of band pass filters, or a cochlea, and provide a spatial code for texture discrimination (Neimark et al., 2003; Ritt et al., 2008). Whiskers vary in shape, size and stiffness across the array (Hartmann et al., 2003).

These differences ensure that the resonant frequency of each whisker is different. If a surface has the correct spatial frequency, and the whisker moved at a certain speed, the vibrations elicited by the surface on the whisker would be at that whisker's resonance frequency. Such a vibration would cause large oscillations at the base, and in turn a robust response in the whisker primary afferent neurons. As a result each whisker in the array would act as a sensor for a narrow band of textures, and monitoring the activity of cells from the whole array would provide a system for discriminating many different textures.

Though appealing, this theory has been widely criticised (Wolfe et al., 2008; Diamond et al., 2008 (c)). If the theory were true the whole whisker array would need to be brought into contact with a surface before a discrimination can be made. For comparison, in audition the entire cochlea is always exposed to incoming sounds. Rats are capable of discriminating textures with brief touches from only a few whiskers (Simons et al., 1995; von Heimendahl et al., 2007). Also rats can discriminate, and cells respond to, surfaces that elicit vibrations over a wide range of frequencies, and not only at the resonant frequency of the whisker (Lottem. and Azouz., 2008).

This resonance hypothesis has been shown to work in software simulation (Bernard et al., 2010), but not in hardware. A hardware implementation would require an array of differently sized whiskers, and information would be pooled across them. N'Guyen et al. (2010) has shown that an array of differently sized whiskers can result in improved texture discrimination, though not by explicitly utilising each whisker's resonant frequency (this work is described in more detail in Section 2.4.6.2). Testing this theory is beyond the scope of this thesis as we are concentrating on the efficacy of single whiskers for tactile discrimination. We may return to this kind of multi-whisker methodology for texture discrimination in the future.

2.4.5.2 Kinetic signature hypothesis

The theory of rat texture discrimination which has reached closest to consensus is the kinetic signature or ‘stick-slip’ hypothesis (Wolfe et al., 2008). Cells in the rat whisker system have been shown to respond strongly and accurately to high velocity whisker deflections (Arabzadeh et al., 2005), with spike alignment within 0.2 ms in the primary afferent neurons and a few ms in the barrel cortex. When a whisker is moving across a textured surface, the tip of the whiskers shifts from bump to bump in a ‘stick-slip’ pattern (Ritt et al., 2008).

It is thought that recording the timing, magnitude, frequency or pattern of these high-velocity ‘stick-slip’ events would allow the rat to encode a surface efficiently (Arabzadeh et al., 2006), as different textures elicit a unique ‘kinetic signature’ in the temporal profile of deflection velocity. In support of this hypothesis Panzeri et al. (2001) and Foffani et al. (2009) found that patterns of spike timing in somatosensory cortex is a better predictor of surface texture than spike number alone.

This strategy would be of particular use when discriminating natural surfaces which may not have predominant spatial frequencies, different grades of sandpaper for example. To date no one has implemented a texture discrimination system based on the kinetic signature hypothesis.

2.4.6 Model-free methods for texture discrimination

Texture discrimination is an obvious application for artificial whiskers, and many of the robots described in Section 2.3 were used for texture discrimination, and the results of those experiments are presented in the next few sections. Many of the whisker based texture discrimination systems developed from an engineering perspective have used a data–driven model–free approach, attempting to extract features from the whisker deflection time series to perform texture discrimination.

2.4.6.1 Spectro-temporal feature extraction

As part of the AMouse project (Fend (2005), described in Section 2.3.3 of this Chapter) used a standard back-propagation neural network classifier using features extracted from the spectrum to discriminate four textures on data collected under unconstrained ‘real-world’ conditions. The ‘features’ used here were a fast Fourier transform (FFT), spectro-temporal analysis (principle components analysis of a time windowed FFT), and the amplitudes of the raw signal.

Classification based on the FFT was as good as for the raw signal ($\approx 75\%$), but spectro-temporal analysis was poor. In addition it was found that under active exploration the robot would often only make contact with the surface with one or two whiskers. Movement had to be modulated to ensure at least four whiskers made contact as this was a requirement for good classification when robot movement was unconstrained. The authors remark that texture discrimination is much more difficult when the angle and distance of the surface with respect to the robot is unconstrained, a critical point that is returned to later when we develop a framework for tactile sensing in Section 2.5.

The authors later showed that whiskers could be used as simple binary touch sensors as a supplement to vision in a navigation task (Fend et al., 2005), and went on to detail how whiskers could be used for additional information when building place cells (Hafner, 2005). Though it is important to stress that these methods are not strictly ‘whisker-based’ navigation as vision was so heavily used.

Using the same AMouse robot, data was collected in an attempt to predict the responses of cells in the whisker system by generating receptive fields in artificial neurons (Hafner et al., 2003, 2004). Spectrograms were generated from the whisker deflections, these were then compressed using principle components analysis. Simulated neurons were trained to sparsely code for the principle component of each surface. The resulting neurons had spectro-temporal receptive fields. The emergence of receptive field properties of this kind is analogous to simple cells in

vision (Olshausen et al., 1996). The authors suggested that cells responding to spectro-temporal features in the signal may be found in the rat.

2.4.6.2 Modulation energy

Cells of this kind have indeed been found: recordings in rat barrel cortex found cells that respond differently when the whisker contacts surfaces of different roughness (Arabzadeh et al., 2005). To find out what features in the signal these cells could be responding to a complementary robotic study was carried out (Hipp et al., 2006). Magnetic field sensors were mounted on metal wire whiskers, and actuated to sweep across different sandpapers. They found that good classification performance was possible by extracting two features from the power spectrum of the whisker deflection time series. These features were the total power spectral density (PSD), called modulation power in the paper, and the frequency peak of a normalised PSD, which is referred to as the modulation centroid.

Modulation power increased with surface coarseness, while the modulation centroid decreased by the same measure. The experimenters go on to show that the deflections of rat whiskers during artificial whisking against surfaces can also be processed with these two features. The authors go on to propose that cell responses in barrel cortex may be responding to the product of these two features in their mean firing rates.

Other cells responding to ‘kinetic features’ in whisker deflections have been reported by Petersen et al. (2008). Cells in the ventral posterio-medial (VPm) thalamic nucleus responded preferentially to a diverse range of stimulus features, such as the velocity, position and acceleration of the whisker. 25% of the cells only encoded velocity. 19% of the cells encoded two or more features. It may be possible to develop a biologically inspired feature bank for decoding whisker signals, potentially responding to the output of a model of the primary afferent neurons. This sort of computational model could then provide insights into the sorts of decision making algorithms that could be performed subsequently in cortex, though for now this is work for the

future.

Building simple classifiers from the frequency spectrum of the whisker deflection has also been successful elsewhere. A battery of methods were tested to determine precisely how whisker based texture sensing is affected by changes in contact geometry (Fox et al. (2009a), following the remarks in Fend (2005)). On data gathered from ‘Whiskerbot’, a mobile whisking robot described in Section 2.3.3 of this Chapter, using a conical glass–fibre composite whisker and measuring deflections at 10kHz using a strain gauge, it was shown that the angle of the surface and the pattern of whisker movement affected the nature of the data being recorded, and the subsequent success of any analysis.

Classification performance of a Gaussian classifier using the centroid energy features described above was compared to classification based on simpler ‘onset-offset’ features, a simple neural network classifier and the outputs of simulated primary afferent neurons. By inspection of the raw data the experimenters found increased power in 2-3Khz range for rough surfaces which was absent in smooth surfaces during contact onset (defined as a significant deviation in the short-term variance of the signal from the long-term average). In the contact offset a greater variance in signal power was observed for rough versus smooth surfaces, though this difference was not restricted to a particular frequency band as in the onset.

The experimenters went on to test classification based on the output of simulated whisker primary afferent cells (Mitchinson et al., 2004). All three sets of features were capable of simple rough/smooth discrimination, though those based on the ‘onset-offset’ and primary afferent outputs performed better across all the settings tested than the centroid energy methods.

Using a feature extraction method N’Guyen et al. (2010) proposed that the resonance (Section 2.4.5.1) and kinetic signature theories (Section 2.4.5.2) may in fact be complementary. As part of the Psikharpx project (detailed in Section 2.3.3 of this Chapter) the experimenters developed algorithms for whisker based texture discrimination (N’Guyen et al., 2010), potentially as a supplement to vision. A texture discrimination algorithm was applied to data from a grid of

thirty three carbon fibre whiskers, of varying length, fixed to a sheet of conductive elastomer (N'Guyen et al., 2009).

Using two robot movement paradigms, head fixed and mobile, the whiskers were swept across different graded sandpapers. A feature was extracted from the signal called instantaneous mean power (IMP), which is related to the spectral centroid described in Section 2.4.6.2, for each of the thirty three whiskers in the array. This thirty three element vector for each surface was fed as input to a multi-layer perceptron to perform supervised learning. Classification performance in the ‘head fixed’ condition was very good (>90%) in an eight texture discrimination task using all thirty three whiskers. IMF from data collected on a mobile robot was later used in a simplified two-alternative forced-choice experiment to show that this texture discrimination method could be used on a mobile robot, though whisker-object contact geometry was always fairly consistent. However performance is much worse when only a subset of whiskers is used for discrimination, and some whisker columns in the array perform much better on specific textures. This seems to be due to the different lengths of the whiskers in the different columns of the whisker array.

Though this is not an example of each whisker being used as a resonator for a particular surface spatial frequency (as in the resonance hypothesis in Section 2.4.5.1), the mechanical properties of the whiskers were important for texture discrimination; in the way that these properties facilitate the transduction of whisker oscillations. It follows therefore that the magnitude and temporal pattern of whisker oscillations is important for texture discrimination (in line with the kinetic signature hypothesis), and that having an array of whiskers with different mechanical properties can improve classification (as suggested in the resonance hypothesis).

2.4.7 Summary of whisker based tactile discrimination

We have seen that the rat is capable of performing a number of tactile discriminations, such as contact localisation in 3-D (Section 2.4.1), and texture discrimination (Section 2.4.5). Many

hypotheses have been generated to explain the processing that rats need to perform to succeed in these tasks. Insights from cell responses can also guide the search for candidate mechanisms, as in the case of using bending moments for radial distance estimation (Section 2.4.2). However, it is difficult to draw any concrete conclusions about the state of the art in tactile discrimination. From the biological literature we see that whisker sensing can be fast and acute, whisker movement seems to be important, and on the engineering side various methods can be used to successfully discriminate a wide range of contact parameters.

The classifiers detailed in this review have almost all been reported under highly controlled conditions, and it is difficult to intuit how the results may generalise to other paradigms. For example, classification of texture is trivial if all other contact properties are held constant, but the classifier boundaries move around as contact type varies (Fend, 2005; Fox et al., 2009a).

It is possible that a contact object may be moving at unknown velocity (as in the case of shrew prey capture, Anjum et al., 2006), and this velocity may confound certain classifiers. In the case of texture, it suggests that bumps on the surface of an object will seem to have a higher spatial frequency due to increased speed of motion. Both model-based and model-free methods suffer from the problem of interrelationships between contact properties. For example, the model-based methods described in Section 2.4.3.1 assume that the contact object is not moving, and a moving object could introduce ambiguities into their results. Nearest-neighbour template methods suffer because a change in one parameter could completely change the shape of the data, rendering templates trained to detect another parameter useless. A potential solution would be to learn a large number of templates covering all possible combinations of contact parameters, but this can lead to combinatorial explosion.

2.5 A framework for whisker based tactile discrimination

This problem of deciding what and where an object in the world is can be reduced if certain assumptions are made about the nature of whisker-object contacts, and by accumulating information across a number of controlled, sequential contacts. When a contact has taken place, certain geometric properties of the object's location with respect to the agent can be determined. By monitoring contact onset times, whisker geometry and movement it is relatively straightforward to work out where the contacted surface is in the horizontal and vertical plane (as discussed in Section 2.4.1). This is especially true in artificial systems where whisker position can be monitored. Without measuring whisker deflections during contact the radial distance to contact r from the agent is unknown. Surface properties such as orientation, curvature, size, texture and softness are also only available once the whisker deflection has been measured and processed.

In the unrestricted case, where a whisker can collide with any object while moving at an unknown velocity in an ambiguous direction, the combinatorial explosion of contact parameters make deciphering the whisker deflection signal close to impossible.

In order to build a coherent whisker based tactile sensing system, the process of determining object location and identity must initially be simplified. As was outlined in Chapter 1 we define tactile discrimination as reporting the properties of any surface a whisker encounters. These reports could then be sent to another system for integrating information across whiskers and numerous contacts, or for use in tasks such as navigation.

It is possible for a given surface to have innumerable properties, each of which requiring a separate test to distinguish them. In this thesis we will consider a world of reduced complexity, where objects are square cornered, straight sided, vertically aligned and vary only in location and texture. For example, the floor of a house or office where all the furniture either have straight sides, or square legs. Reducing the complexity of the environment in this way removes any

problems that would be associated with object curvature, or the effect on whisker deflections caused by unusual contact angles e.g. whisker slippage (Kaneko et al., 1998; Solomon and Hartmann, 2008).

With these restrictions the task of whisker based tactile discrimination remains unsolved, though these measures leave a tractable problem that we feel is an important first step in developing a comprehensive tactile sensory system, and provides a benchmark for future expansion. In this tactile ‘box world’ a whisker contact presents a ‘where’ and ‘what’ problem for the agent. A framework for organising and solving these problems is shown in Figure 2.17. Using a biomimetic whisking strategy, sensing can be thought of as a series of iterative decisions; with each contact a separate tactile discrimination. In our ‘box world’ each contact will either be with a surface or a corner, at an unknown distance from the whisker base, and the surface will be at a certain angle, and have a specific texture.

2.5.1 Separating ‘what’ from ‘where’

In this framework the discrimination of object location is separate from the discrimination of object identity. Object identity can only be determined from contacts using the whisker tip, assuming straight whiskers, as contacts along the whisker shaft will be with the corners of objects. We know that if contact with a corner is made, it will be at some point along the shaft of the whisker as the tip would flick past the object.

In the horizontal plane the corner of an object does not hold enough information about surface texture to make a discrimination as the contact point is very small. The point contact of a corner does not hold any information about the orientation of a surface with respect to the agent either. By determining the radial distance to contact along the whisker, object location can be identified with respect to the agent. It is then possible to reposition the whisker for the next contact to ensure that the tip makes contact with the surface of the object.

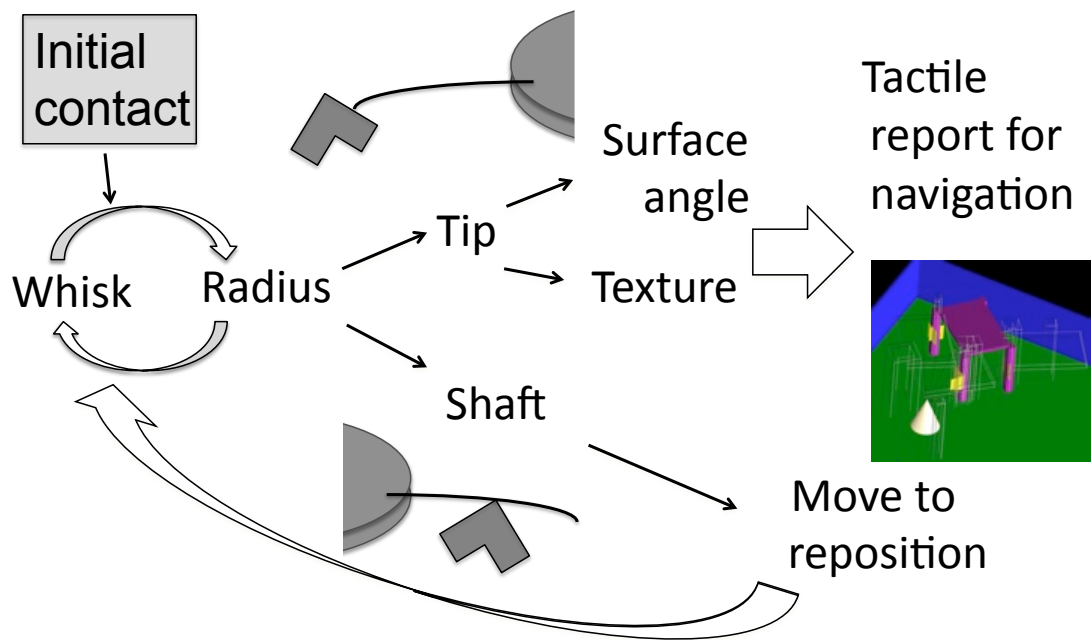


Figure 2.17: A new tactile framework for extracting contact parameters. The framework simplifies the task of whisker based tactile discrimination, and guides the movement of whiskers during exploration. An agent moves the whiskers in an oscillatory fashion. Upon initial contact with a surface a initial ‘tip or shaft’ decision is made based on radial distance estimation (Chapter 4). If a shaft contact is made the whiskers can be accurately repositioned. If contact has been made at the tip a surface angle and texture discrimination is made (Chapter ??). The results of these discriminations can be used for subsequent map building or object recognition.

A tip contact is by definition at a fixed distance from the base of the whisker, so radial distance does not need to be determined. Surface angle and surface texture can now be determined. Whisker movement and sensing is interdependent – texture discrimination is confounded by whisker movement changes (Fend, 2005; Fox et al., 2009a). Therefore each classification in the framework needs to be invariant for contact speed, as whisk rate, body and object movement will effect the whisker signal. This repositioning of whiskers to tip contact may be analogous to making a microsaccade in vision to stabilise a visual target’s location on the fovea of the retina. A larger scale search strategy would be needed to guide whisker movements when searching an environment.

Though rodents are capable of discriminating both ‘what’ and ‘where’ parameters of a contact Diamond et al. (2008 (a), it is unclear whether combining this information is critical for their classification in biological systems. In robots, it has been shown that classification of surface properties is difficult when the contact location and geometry are unknown (Fend, 2005; Fox et al., 2009a). A similar effect in biological systems is difficult to investigate as cellular recordings must be made in awake, exploring rats. An additional avenue of research would be to investigate whisker movements when rats make mistakes in texture discrimination experiments. A prediction from artificial whisker experiments would be that rats would make more sensory mistakes when whisker movement is atypical, for example if whisker velocity is outside of the normal range.

2.5.2 Filling in the framework

The first experimental goal of this thesis is to test candidate methods for tactile discrimination in each of the ‘what’ and ‘where’ problems outlined in the tactile framework. The best methods could then be implemented in a single system on a mobile robot, and the tactile discriminations can be used in a simultaneous localisation and mapping (SLAM) task.

With our goal of developing a system for tactile discrimination, how can we decide which meth-

ods will be most successful? And how can we decide which whisker movement strategies are the most successful? New robotic paradigms need to be developed to comprehensively test and compare classifiers for whisker based tactile discrimination, and for evaluating the effect whisker movement has on sensing. The second goal of the experimental work in this thesis is to develop robot hardware for developing and testing different methods for whisker based tactile discrimination in a fair and comprehensive manner.

A specific goal of the models developed in this thesis is to keep the processing as simple as possible. In the past certain researchers have reported hypotheses or methods for whisker based tactile discrimination that may be more complex than is necessary to explain a given result. For example a machine learning inference machine such as a support vector machine (Cortes, 1995) is likely to out-perform many of the classifiers presented in this thesis, but inferring how this performance was achieved, as in what features in the input signal was the classification based on, would be difficult.

We hope to determine the amount of processing that is sufficient for good task performance in each part of the tactile framework described in Section 2.5 above. To do this we have had to develop a novel XY positioning robot system to generate precise and repeatable whisker data. In this way we aim to still understand how a given discrimination is being performed, even when the task demands become more complex. Once we have established benchmarks for comparison on a precisely controlled robot, we apply the classifiers to data collected on more complex robots to observe and understand how different task demands affects whisker processing.

Tacking the problem in this manner allows us for the first time to determine how each of the classifications that biological whisker systems are capable of could be performed in simulation. These results may guide our understanding of the processing in biological whisker systems, and highlight problems that rodents have found solutions to such as the interaction between motion and sensing.

2.6 Plan of work in this thesis

A specific goal of the models developed in this thesis is to keep the processing as simple as possible. In the past certain researchers have reported hypotheses or methods for whisker based tactile discrimination that may be more complex than is necessary to explain a given result. For example an off the shelf machine learning inference machine may out perform many of the classifiers presented in this thesis, but how this performance was achieved may remain a mystery without a deep understanding of that software. We hope to determine a benchmark for the amount of processing that is sufficient for good task performance in each part of the tactile framework described in Section 2.5 above.

It is difficult to judge which of these methods would perform best under the particular task demands of our tactile framework. In previous studies the data collection paradigm was different in each case. The whiskers are all unique, the sensory transduction methods are various, and whisker movement and contact geometry is different in each experiment. A given classifier's performance could be tuned to a particular experimental design, and may not work as well in other situations. Considerations of generalisability and robustness are also important when comparing methods for embedded robotics.

A fair comparison of these methods requires a new, common dataset collected on a standard whisker sensor. A large dataset is required to test each classifier's performance over a range of conditions in each part of the tactile framework, as the dataset size increases exponentially as more parameters are added i.e. total data (T) = instances of a parameter (n) raised to the power of the number of parameters (P) therefore, $T = n^P$. Though a dimensionality reduction is achieved by separating the ‘what’ and ‘where’ tasks in the tactile framework, a novel approach must be taken to generate sufficient data to properly train and test these classifiers.

In Section 3.3 of Chapter 3 a methodology is outlined to collect such a dataset using an XY positioning robot and a biomimetic artificial whisker. Other robots developed in parallel to the XY

positioning robot are also described in Chapter 3, each with a different role in the development of models and theories of whisker based tactile sensing.

In Chapter 4 the XY positioning robot is used to generate a large data set, and classifier performance on a radial distance estimation task is compared for a range of methods. Namely the methods are; template based classification (**Evans, M. H.** et al., 2010b), feature based classification (**Evans, M. H.** et al., 2010a), static beam equations (Birdwell et al., 2007), frequency analysis (Kim and Moller, 2004) and stationary naïve Bayes (Lepora, **Evans, M. H.**, Fox, Diamond, Gurney, and Prescott, 2010b). Results are compared for these different methods with a range of performance criteria in Section 4.4 of Chapter 4. Each classifier is assessed under ideal conditions, and with reduced training sets with a view to selecting methods that will function robustly at the required point in the framework under less controlled conditions, such as on a mobile robot.

In this Chapter we have seen that contact geometry and whisker movement has a fundamental effect on texture discrimination. In Chapter 5 a second large dataset is collected on the XY positioning robot to build classifiers for simultaneous surface angle and texture discrimination, under conditions of varying contact speed. The methods compared for texture discrimination are raw data template based classification, spectral template based classification (**Evans, M. H.** et al., 2009a), stationary naïve Bayes classification (Lepora, **Evans, M. H.**, Fox, Diamond, Gurney, and Prescott, 2010b), and frequency features based classification (Hipp et al., 2006; Fox et al., 2009a). Results are compared for these different methods with a range of performance criteria in Section 5.4 of Chapter 5.

The most successful classifiers for radial distance, contact speed, surface angle and texture classification are then applied to data on a range of different whiskered robots (described in Chapter 3) in Chapter 6. These robots provide tests of a classifier's applicability to real-world tactile discriminations (Section 6.2), the effect of different whisker control strategies (Sections 6.3 and 6.4), and finally real-time processing onboard a mobile robot performing tactile SLAM (Sec-

tion 6.5). Finally the implications of the work and possible future directions are summarised in Chapter 7.

Chapter 3

Whiskered robots used in this thesis

3.1 Introduction

This Chapter describes a series of robots developed for investigating whisker based tactile sensing.

The classifiers described in Chapters 4, 5, and 6 were developed and tested on these robotic platforms. The reasons behind the development of each robot is outlined, their hardware and software specification is detailed, as well as the contributions made by each research partner – the Active Touch Laboratory at Sheffield University (ATL@S) and Bristol Robotics Laboratory (BRL) – in the development of each robot.

These robots build on previous efforts described in Section 2.3 of Chapter 2 in a number of ways. Care was taken to build whiskers that were as biomimetic as possible (Section 3.2.2), modelling the mechanical properties of rat whiskers at the scale required for a mobile robot. Sensory transduction is achieved with a Hall effect sensor (Section 3.2.1), which is robust to damage and sensitive to both slow and fast whisker deflections. Whisker actuation is a key component of biological whisker sensing (described in Section 2.2.2 of Chapter 2), and all the robots presented

here address the task of careful whisker movement. The robots are also versatile enough to be useful in a range of experiments.

Most importantly the robots presented here are complementary, developed to aid research with a common goal of understanding whisker sensing. The robots are used as experimental apparatus for a whole group of researchers developing parallel models for motor control, sensory processing, navigation, action selection and sensory noise cancellation.

The first robot described here is SCRATCHbot (Section 3.2), an integrated hardware platform similar to the biomimetic systems described in Section 2.3.3 of Chapter 2. Many of the artificial whisker technologies developed for SCRATCHbot were then applied to other robots with very specific research goals in mind. Secondly, the XY positioning robot (Section 3.3) was developed to generate large datasets for developing and testing classifiers for tactile discrimination in this thesis. This is the robot used in most of the work in Chapters 4 and 5. Thirdly, the BIOTACT G1 robot arm (Section 6.4) was developed with industrial applications in mind, building on the technologies and architectures first tested on SCRATCHbot, and implementing classification systems from the XY positioning robot. Finally, CrunchBot is the last robot described in this Chapter (Section 6.5). CrunchBot was necessary to complement and fill a gap in the functionality of the other robots with respect to the goals of this thesis; a simplified mobile robot to prototype candidate systems for real time sensing and navigation.

This Chapter concludes by reviewing how the robots all make important contributions in the task of developing tactile sensing systems, and an understanding of how the whisker system works in rodents.

3.2 SCRATCHbot (Spatial Cognition and Representation through Active TouCH)

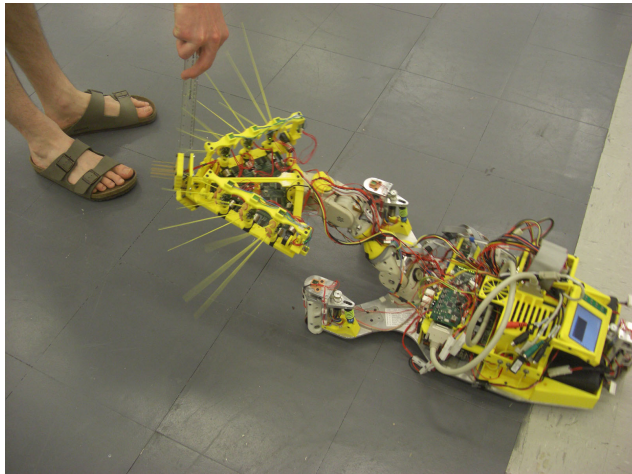


Figure 3.1: The SCRATCHbot biomimetic whiskered robot.

SCRATCHbot is a biomimetic robot based on the rat whisker system developed by Pearson et al. (2010). The goal in developing SCRATCHbot was a single robot platform that could integrate ideas and models from the diverse fields of research involved in understanding the rodent whisker system. Features of the biological system that had been deemed important for sensing in the ethology and neurophysiological literature, such as active whisker control and whisker array morphology, were included in the design of the robot.

3.2.1 Hall effect sensor based artificial whisker

All of the robots detailed in this Chapter share a common element: artificial whiskers with a Hall effect sensor for transduction of whisker deflections. The Hall effect is the production of a voltage difference across an electrical conductor, transverse to an electric current in the conductor and a magnetic field perpendicular to the current (Hall, 1879). Less formally, a Hall effect sensor outputs a voltage, which changes depending on the strength of a nearby magnetic

field.

As described in Popovic (1989), a Hall effect sensor is a plate of semiconductor material fitted with four electrical contacts. If a magnetic field is applied to Hall sensor the Hall voltage V_H , which is the sensor output signal, appears between the two sensor contacts. V_H is roughly proportional to the product of the component of the magnetic induction perpendicular to the plate plane B and the bias current I applied to the two other contacts,

$$V_H = \frac{R_H}{t} GBI, \quad (3.1)$$

where R_H , denotes the Hall coefficient, t the plate thickness and G the geometrical correction factor (the ratio of V_H in an idealised device to that of an actual device). The Hall coefficient R_H characterises the intensity of the Hall effect in a specific material.

In the artificial whiskers built at BRL a magnet is bonded to the base of the whisker, and a Hall effect sensor is placed beneath this magnet. Figure 3.2 is a diagram of the Hall effect sensor used in the artificial whiskers. When the whisker is deflected the movement of the magnet is proportional to whisker bending. Hall effect sensors have some advantages over other sensing methods. The sensor output voltage provides information about the magnitude of whisker deflection whether the whisker is moving or not, therefore the information is useful for static as well as dynamic classification approaches. Hall effect sensors are robust to damage, especially when housed in a rubber filled follicle (see Section 3.2.3), which is an important consideration when measuring whisker deflections as they are constantly striking objects in the environment. Hall effect sensors are also relatively inexpensive, and can be made quite small which makes them ideal for application to large arrays of whiskers.

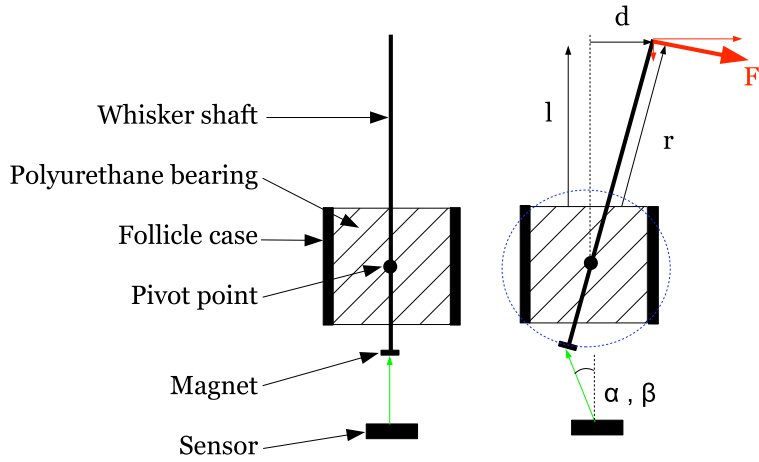


Figure 3.2: Diagram of the artificial whisker Hall effect sensor

3.2.2 Whisker materials

The material a whisker is made from has a critical influence on the way a whisker interacts with a surface, and as a result the nature of the deflections created at the whisker base (Hartmann et al., 2003). Whiskers are specialised tools for tactile sensing, differing in structure from other mammalian hairs to ensure strength and stiffness (Chernova and Kulikov, 2011).

Rat whiskers have evolved to have near perfect mechanical properties for gathering tactile information (Chernova and Kulikov, 2011). Rat whiskers are stiff when moved in air, but bend in contact. Rat whiskers are highly damped, with damping ratios (ζ , related to the quality factor Q discussed in Section 2.4.3.2 of Chapter 2 such that $\zeta = \frac{1}{2Q}$) of ≈ 0.15 (Hartmann et al., 2003). This ensures that the whiskers do not oscillate when whisked in air, which can add noise to the deflection signal and make contacts difficult to detect. This damping also increases when the whisker is in the animal, as observed contact induced oscillations are smaller in whisking rats than isolated whiskers (Hartmann et al., 2003). Whiskers are tapered, which has certain advantages (some are described in detail by Williams and Kramer (2010); taper reduces the total deflection angle at the base for a given contact force, because the tip region absorbs most of the

force by deflecting a great deal. This reduces the required sensing range of the whisker follicle, and therefore allows the sensors (mechanoreceptors in the rat) to be more sensitive. Rotational stiffness changes along the length of the whisker (as in how much the whisker bends for a given force of contact at each point along the whisker), making the bending of the whisker at the base a better measure of radial distance to contact than with a cylindrical beam. Tapered whiskers are more robust to the resonance frequency, as the lower mass of a narrow tip helps to dampen any oscillations. The mechanical properties of a truncated cone, the resonance frequency and bending properties, change less when it is shortened (e.g. 5% is removed from the tip) than in a similar sized cylinder. This makes whisker sensing more robust to sensor damage.

Finally, the tip of a conical whisker can ‘whip’ more across bumps of a surface, allowing a higher number of more regular ‘slips’, ‘sticks’ and ‘rings’ to encode the surface texture, as opposed to a low number of high velocity slips (as in the kinetic signature hypothesis described in Section 2.4.5.2 of Chapter 2).

It is worth mentioning that building artificial whiskers to test models of rat sensory abilities does pose some unique challenges. Due to the size of mechanical motors and sensors there is a minimum size that a whisker can currently be built to. This minimum is typically quite a lot larger than the true size of a rat whisker, and scaling all the properties of a whisker such as stiffness or resonance frequency has proved difficult. For example Bronnikov et al. (1999) showed that as certain polymers reduce in scale, Young’s modulus for the substance decreases, possibly due to the volume of the polymer. These sorts of problems make it very hard to build models of whiskers that behave as real whiskers do in all situations.

A great deal of effort was made to find materials for artificial whiskers in the BIOTACT robots that would match the mechanical properties of real whiskers at different scales. Whisker material and dimension varies across the robot platforms to reflect this process of evolution, though they fall into two broad categories; Acrylonitrile butadiene styrene (ABS) plastic or Nanocure RC25 (Nanocure, 2011). Each whisker is made on either a fused deposition modelling (FDM) or a data

light processing (DLP) Envisiontec Perfactory® rapid prototyping machine (Envisiontec, 2011).

Any differences between the whiskers are described in each robot's accompanying text.

3.2.3 SCRATCHbot whisker design

SCRATCHbot's whisker sensor consisted of a flexible ABS plastic whisker shaft (200mm long, 2mm diameter, Young's modulus $E \approx 2.3\text{GPa}$) mounted at its base into a short, polyurethane rubber filled, inflexible tube called a follicle case (see fig 3.3). ABS plastic was used for the whisker shaft because of its flexibility, appropriate mechanical match to scaled-up biological whiskers, and suitability for rapid prototyping using the FDM approach.

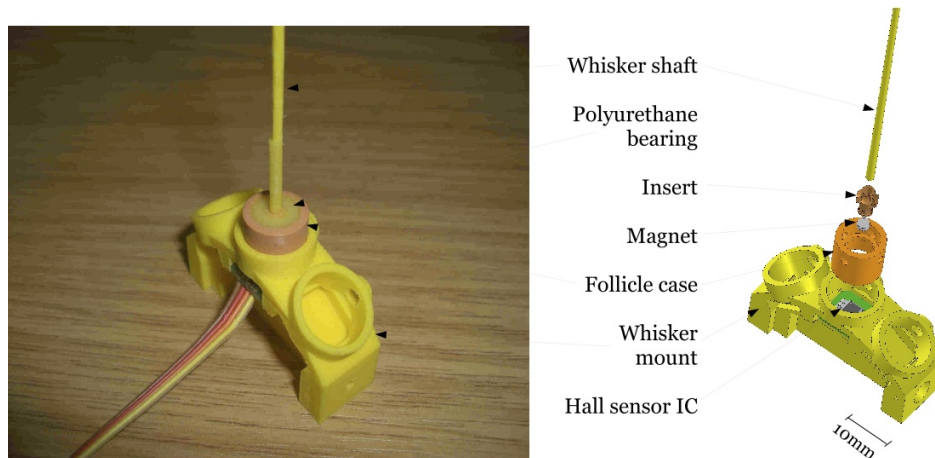


Figure 3.3: Diagram of whisker follicle sensor construction.

A magnet was bonded to the base of the whisker shaft in such a way that when the follicle case/whisker shaft assembly was located into the whisker mount (see fig 3.3), the magnet was positioned directly above a tri-axis Hall effect sensor IC (Melexis MLX90333, Melexis (2008)). The tri-axis Hall effect sensor used here can measure the voltage changes in three orthogonal axes, i.e., x and y across the plane of the sensor, and z upwards towards the whisker. This sensor technology was chosen for its robustness (no physical coupling between sensor and environment), ability to measure displacements in two dimensions, cost (≈ 6 euros), size (S08

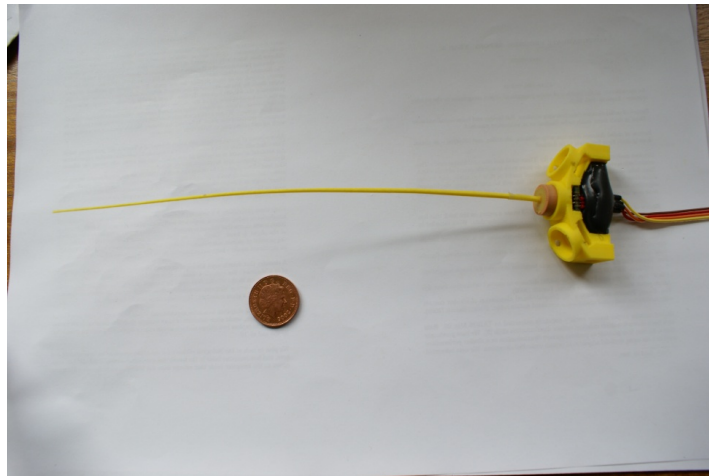


Figure 3.4: A single artificial whisker shaft and follicle, with a British 1p coin for scale

IC package $3 \times 4\text{mm}$) and re-programmability, which allows the sensitivity of the sensor to be adjusted after manufacture to best suit the current experiment or application.

The Hall effect sensor IC was programmed to generate two voltages, the magnitudes of which being proportional to the two orthogonal displacement angles (α, β) of the magnet from its resting position above the sensor (see Figure 3.2). As forces are applied to the whisker shaft, the moment experienced at the base will rotate the magnet around the pivot point, nominally in the centre of the polyurethane bearing. A trigonometric operation in the DSP microchip core of the Hall sensor IC decouples the α and β angles and removes the z -component introduced by the arc of travel of the magnet, as indicated by the blue dotted line in Figure 3.2. This operation ensures that the output voltages from the IC are linearly proportional to the tangent component of the alpha and beta angles, or x and y as they will be referred to hereafter.

To set the operating range of the sensor a calibration stand was constructed to allow a fixed deflection, d , to be applied to the whisker shaft at a known radial distance, r , from the base in the two dimensions (refer to Figure 3.2). The output voltage from the IC was then scaled to $\pm d$ in both dimensions, with $d=0$ set to 50% of the maximum output voltage V_{DD} , i.e., 2.5V. For the whisker sensor used in the experiments reported here, the voltage range was set as 5 - 95% V_{DD} .

through $\pm d = 60\text{mm}$ applied at $r = 150\text{mm}$.

3.2.4 Whisker movement control

SCRATCHbot has nine whiskers on each side of its head (see Figure 3.1), arranged in three columns of three whiskers. Each column is individually actuated to rotate, and a whisking pattern generator (WPG) models the function of a central pattern generator (though no centralised pattern generator has been found in the rat; whisking control seems to be distributed through a number of loops in the rat (Kleinfeld et al., 2006), Section 2.2.2 of Chapter 2). The WPG for each column was coupled to every other column to cause synchronised whisking. To cause a minimal impingement (MI, Mitchinson et al., 2007, Section 2.2.2 of Chapter 2) control strategy the reports of whisker deflections were fed back into the WPG on the side ipsilateral to contact, which suppresses subsequent protractions. The effect of this control strategy on whisker deflections can be seen in Figure 3.5.

SCRATCHbot has great potential as a system for integrating models of processing and control in the whisker system. The robot has also proven useful in hypothesis generation. For example, during an orient to stimuli task, whisker movement itself elicits deflections of the whisker. A threshold based contact detector results in ‘ghost orients’ when self generated motion causes whisker deflections to cross this threshold. This led to an implementation of adaptive filter noise cancellation, suggesting a possible role of the cerebellum in the whisker system (Anderson et al., 2010).

The limitation of a complex system like SCRATCHbot is that there are many degrees of freedom. Careful control of the robot, for example to gather data to train models of sensory processing, is difficult to achieve and time consuming. When developing classification systems for sensing it is important to gather large datasets, testing a wide range of contact parameters, to draw robust conclusions about the nature of whisker object interactions. Actuation of the whiskers is also not precise enough to investigate the effect small differences in whisker movement can have

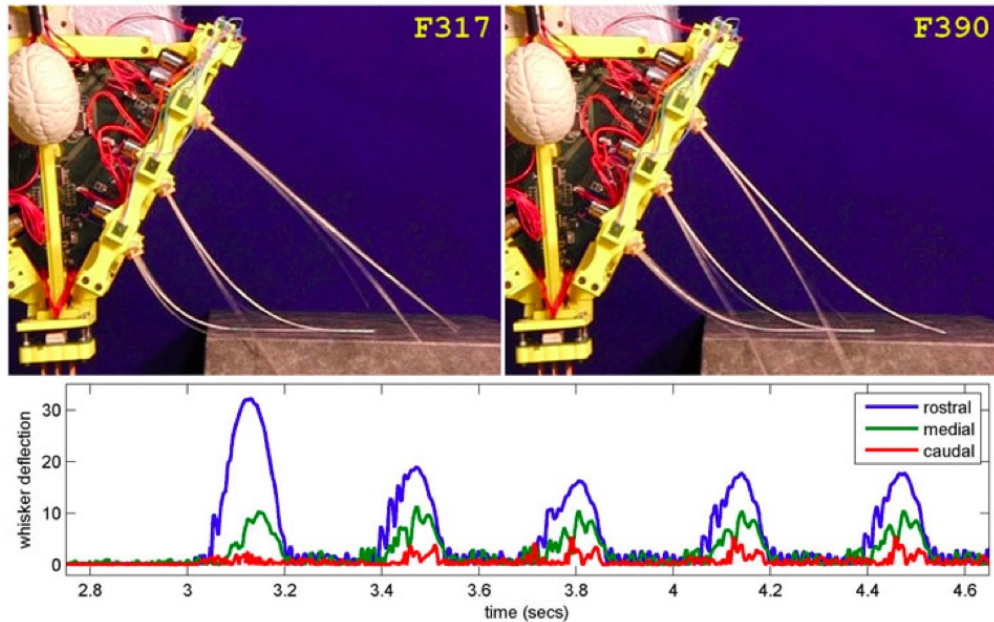


Figure 3.5: A demonstration of MI on SCRATCHbot. Robot head location is fixed as SCRATCHbot whisks into an object. The two photos are of an initial unmodulated whisk (upper left photo), and a second modulated whisk (upper right photo). Whisker deflection signals from one whisker in each column is plotted in the lower panel. During the unmodulated whisk, whiskers in the most rostral column are heavily deflected while the whiskers in the most caudal column barely make contact. During the subsequent modulated whisks, whisker spread is reduced causing a reduced deflection of the rostral whiskers and increased deflection of the caudal whiskers. Whisker deflections are more consistent across the array as a result, which could aid discrimination. Figure taken with permission from Pearson et al. (2010).

on sensing. For these reasons we developed the XY positioning robot described in the next section.

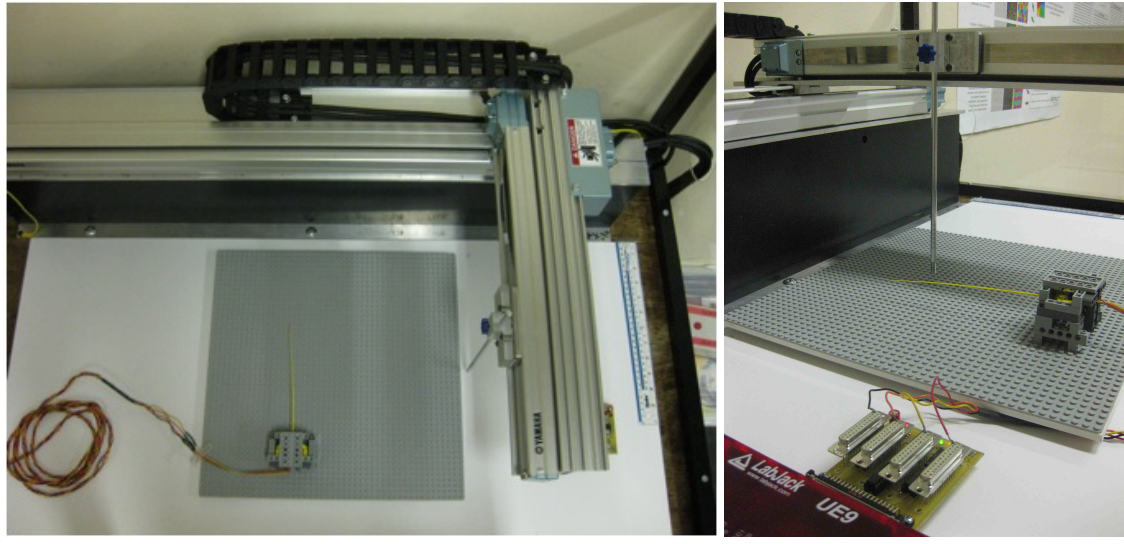


Figure 3.6: The XY positioning robot (a) from above, to show the range of movement available. (b) From the side

3.3 XY positioning robot

Developing models of whisker based perception in the past has been problematic. In passive sensory modalities such as vision and audition it is generally quite easy to present stimuli to a passive sensor on a robot, or images and tones can be simulated and used to train a computational model. There is no obvious analog for tactile stimuli, and the true nature of tactile stimuli is too poorly understood to be simulated accurately. Whiskers are especially difficult to simulate accurately, as they have very low mass but high spring constants when modelled as a series of masses on rotational springs, leading to numerical instabilities (Fox, Evans, M. H., Pearson, and Prescott, 2008). Additionally, when the parameters of a whisker-object contact become more numerous (e.g. speed and radial distance to contact, surface texture, orientation and softness etc) it becomes very difficult to constrain the contact and generate reliable signals in either simulated or physical robots. For these reasons acquiring sufficient examples of carefully controlled whisker contacts with tactile stimuli to train models and classifiers has proved difficult. To fa-

cilitate the study of artificial vibrissal sensing we developed a novel system for generating large sets of whisker deflection signals.

An XY positioning robot was programmed to move objects into a SCRATCHbot artificial whisker sensor in an accurate and highly repeatable manner. A Cartesian robot (see Figure 3.6) was chosen as it is capable of a wide range of movement, is very accurate and can move at speeds which approximate scaled whisk velocities. Deflections for the whisker are streamed to a PC, and can be processed in real time to control subsequent movement of the positioning robot (described in Section 3.3.1 of this Chapter).

We mimic a MI control policy that has been observed in rats and discussed in Section 2.2.2 of Chapter 2. In contrast to the passive case, this policy keeps the amplitude and duration of whisker deflection within a limited range, and also keeps whisker ringing after contact to a minimum. An additional benefit is that the forces acting on the whisker are much smaller, meaning whisker breakage is less likely – an important consideration for biological systems and autonomous robotics.

As a complete tactile-data acquisition system this robot is capable of running indefinitely without interruption. With the correct experimental design it is possible to generate large, rich datasets for developing models of tactile discrimination. Sensory-motor interaction could also be explored more comprehensively in the future, such as assessing the effect different movement trajectories have on deflection signals. Though this has been done to some extent recently on other robots (as in Sullivan, Mitchinson, Pearson, **Evans, M. H.**, Lepora, Fox, Melhuish, and Prescott (2011), Section 3.4 of this Chapter), these experiments are much more difficult to run, requiring a great deal of input from the experimenter as the robot has so many degrees of freedom. Though the work in this thesis describes the first use of an XY positioning robot for generating whisker deflection data, we hope that this apparatus will be used for exploring many other aspects of tactile sensing in the future, such as with artificial fingertips for studying haptic touch.

The robot (Yamaha-PXYX, Yamaha Robotics) has a movement range of 350x650mm, and can

move up to 720mm/s. Repeatability of the robot is ± 0.01 mm, and the maximum load it can carry is 1.5kg. Objects are carried by the robot into an artificial whisker fixed to the table, as this allows us to control the contact as carefully as possible. Moving the whisker into an object would cause the whisker to oscillate unpredictably during movement between contacts, and as a result each contact would be slightly different. Subsequent robots described in this thesis allow for exploring these trial to trial variations and their effect on sensing. A controller (Yamaha RCX 222, 2-axis robot controller) takes instructions from a PC through an RS232 cable, and the controller interprets the instructions, completes path integration, and drives the motors. Instructions for the robot are generated inside a MATLAB (www.mathworks.com) loop, and can be easily updated during robot operation, depending on the whisker input.

3.3.1 Data Collection on the XY positioning robot

Deflections of the whisker were transmitted through the Hall effect sensors to a LabJack UE9 USB data acquisition card (www.labjack.com) at a rate of 1 kHz (though can be sampled up to a total of 50kHz, or 25kHz per whisker channel) for each of the x and y directions. Each trial lasted 4s. This data was sent to a computer through the BRAHMS middleware (brahms.sourceforge.net) for analysis in MATLAB.

BRAHMS is a Modular Execution Framework (MEF) developed at the University of Sheffield for executing integrated systems built from component software processes, allowing the connection of processes together into systems, by linking the outputs of some processes into the inputs of others. BRAHMS is conceptually similar to MATLAB's Simulink or open platform such as YARP <http://eris.liralab.it/yarp/>.

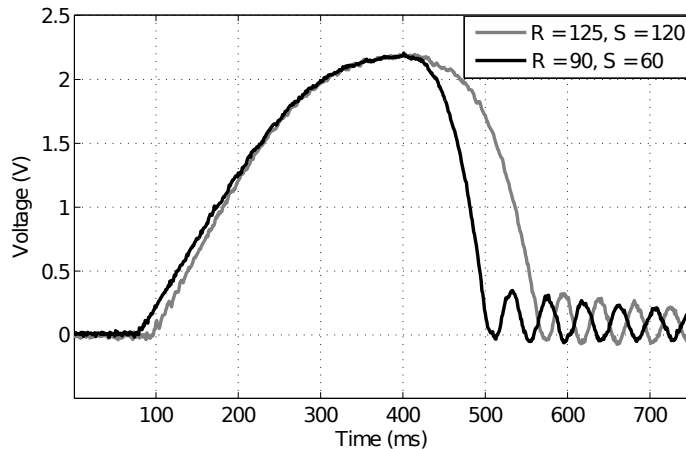


Figure 3.7: Example deflection signals from the artificial whisker. Magnitude of deflection, or force, has been used as a discriminator of radial distance to contact. Here the two traces are at different radial distances, but create the same magnitude of deflection.

3.3.2 Robot control

Minimal impingement was implemented by instructing the robot to move an object into the whisker at a given speed until a deflection threshold is crossed, at which point the robot retracts the object as fast as possible (720mm/s). Temporal latency for the loop is ≈ 300 ms from initial contact due to the controller duty cycle.

Chapter 4 describes the first experiment conducted on the XY positioning robot, evaluating classifiers for radial distance estimation under conditions of varying contact speed. Later in the thesis Chapter 5 describes a second XY positioning robot experiment, where data was collected to train and test classifiers for texture discrimination, and surface orientation estimation under conditions of varying contact speed. Finally the classifiers described in Chapters 4 and 5 are tested on the other robots described in this Chapter to assess their applicability to different robot platforms and whisker control strategies.

3.4 BIOTACT G1 robot

The BIOTACT G1 robot (Sullivan, Mitchinson, Pearson, **Evans, M. H.**, Lepora, Fox, Melhuish, and Prescott, 2011) was developed at BRL to more carefully explore models of whisker movement pattern generation, and whisker sensing for industrial application. The specification for the robot hardware, whisker morphology and range of movement was developed in collaboration with researchers at ATL@S.

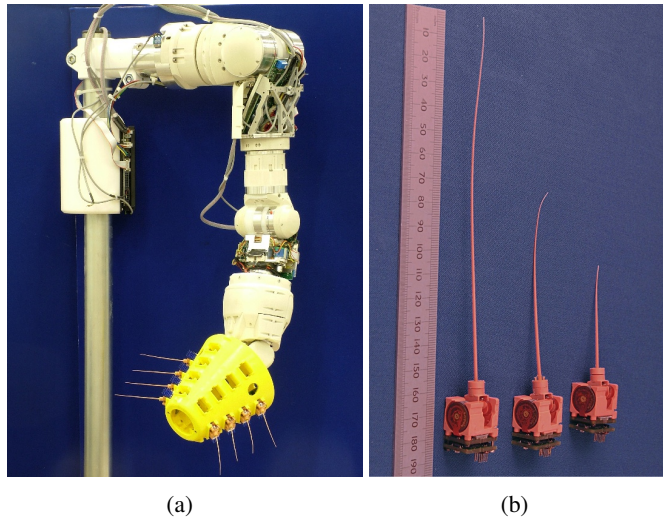


Figure 3.8: (a) The BIOTACT G1 whiskered robot arm. (b) Whisker modules.

3.4.1 Sensor design

The G1 (Generation 1) BIOTACT sensor consists of a truncated conical ‘head’ made from ABS plastic, which holds up to 24 whisker modules. The whisker modules are arranged in six radially symmetric rows of four and are oriented at outwards from the cone surface. For the purposes of our experiments and to enable accurate and repeatable location and movement of the sensor, it is mounted on the end of a seven degree of freedom robot arm (Figure 3.8 (a) shows the G1 sensor fitted with eight whiskers). Also, for the experiments reported in Section 6.4 of Chapter 6, the head was not fully populated with whiskers. Two rows were fitted with three whiskers each to

create a bilaterally symmetric configuration.

The individual whisker sensors are completely modular in design, incorporating their own actuation mechanism and control electronics. The whisker modules are capable of whisking at frequencies of up to 10 Hz which is roughly comparable to the whisking rate of real rat mystacial whiskers (Carvell and Simons, 1990, Section 2.2.2 of Chapter 2).

Software to process the signals from the whisker sensors and to control the whisking patterns is written in C++ and executed under the BRAHMS middleware on a PC which connects to the sensor head via a USB2 connection, enabling data transfer and feedback updates at 2kHz.

The whiskers operated used the same Hall effect sensor as described in Section 3.2.1, and made from Nanocure RC25. Whisker lengths in the test configuration were not all the same: they increased from front to rear in order that all whiskers could touch a plane surface orthogonal to the axis of the cone. This variation in whisker size was motivated by the observation that the whiskers within each row of the mystacial pad of rats and other whisking mammals closely follow an exponential increase in length from the front to the rear (2.2.1 of Chapter 2). In our experiments we used whiskers of length 80mm, 112mm and 158mm.

3.4.2 Whisker control

A biomimetic whisker movement strategy termed rapid cessation of protraction (RCP, described in Section 2.2.2 of Chapter 2) was implemented to assess any effect on whisker deflections and subsequent classification.

Although a number of active sensing strategies have been demonstrated on earlier whiskered robot platforms (described in Section 2.3.3 of Chapter 2), the consequences of this active control for sensory discrimination has not previously been investigated or measured. The first efforts to do this using the BIOTACT sensor are described in Section 6.4.1 of Chapter 6. The following equations were first described in Sullivan, Mitchinson, Pearson, **Evans, M. H.**, Lepora, Fox,

Melhuish, and Prescott (2011), and are included to provide insight to the classifications presented in Section 6.4 of Chapter 6.

A contact signal is derived on each side from the x - deflection of the whiskers on that side (contact usually elicits strong x -deflection since the sensory x -axis is parallel to the actuated axis). A third-order lowpass Butterworth filter with 50Hz cutoff frequency, H_{50} , is first used to smooth the noisy whisker sensory signals and remove whisker resonance vibrations. The maximum absolute value of this signal, across all whiskers w on a side during a given whisk cycle n , forms the contact signal, π_i ,

$$\pi_i(n) = \max_{w \in [1, 12]} |H_{50}(x_{i,w}(n))|. \quad (3.2)$$

This signal was used to suppress protraction ipsilaterally, through the gating variable z_i , without affecting the oscillator dynamics. The gating variable dynamics were given by

$$z_i(n) = \langle \max((1 - T/\tau_z)z_i(n-1), \sigma_z \pi_i(n)) \rangle_0^1, \quad (3.3)$$

where σ_z is a gain associated with the motor modulation, T is the integration step, τ_z a time constant, and $\langle \cdot \rangle_a^b$ is a limit operation (transforming values not in the interval $[a, b]$ onto the nearest value that is in the interval). The max operation sets $z_i(n)$ to a decayed version of $z_i(n-1)$, or a new value proportional to the gain σ_z and contact signal $\pi_i(n)$. Contact on any whisker, thus, suppresses protraction ipsilaterally, an effect which decays with time constant τ_z .

Figure 3.9 shows how the gating variable z_i can be influenced by the gain σ and time constant τ . To generate the plots contact signals from the whisker sensors were simulated in MATLAB.

An obstruction was simulated at a different location on each side by setting the protraction angle

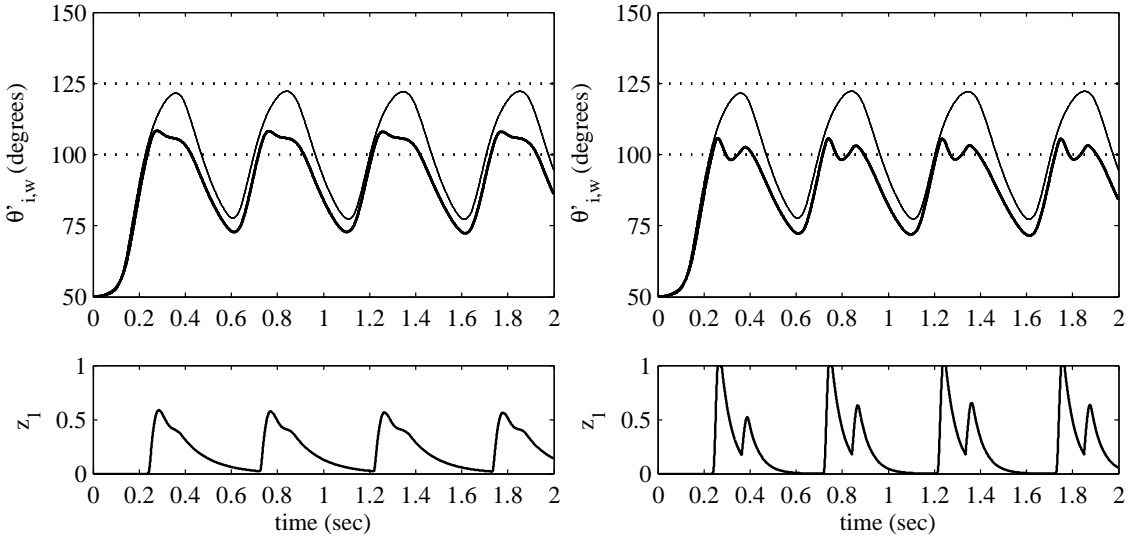


Figure 3.9: (a) Whisking with RCP modulation. When the left whiskers (thick line) were driven past a simulated obstacle (lower dotted line), a resultant contact signal temporarily excited the gating variable z_1 (lower panel) and suppressed protraction ipsilaterally. The right whiskers (thin line) did not reach the obstruction on that side (upper dotted line), and were not modulated (thus, they showed the expected movement of the left whiskers if the modulation had been absent). (b) Whisking with strong and fast RCP modulation. Left whiskers (thick line) quickly detached from the simulated obstacle (lower dotted line), and protraction begins again within a single whisk, leading to a biphasic whisk profile and two distinct contacts with the obstacle. The movement of the right whiskers (thin line) showed the expected movement of the left whiskers if the modulation had been absent.

for contact θ' of whisker 1 to 100° and whisker 2 to 125° . Setting $\sigma_z = 0.7$ and $\tau_z = T_W/4$ generated the results graphed in Figure 3.9 (a). Protraction on the contacting (left) side was suppressed during contact, such that the depth of contact is controlled. The oscillator dynamics were unaffected, so the phase behaviour was unchanged. Furthermore, the gating variable z_1 was all but recovered by the time of the next contact, so there was no inter-whisk modulation; that is, this aspect of control was entirely *reactive*.

Stronger and faster RCP control could be simulated by setting $\sigma_z = 2$ and $\tau_z = T_W/10$; the results are shown in Figure 3.9 (b). In this case, protraction was more strongly suppressed such that the protraction angle θ_1 quickly fell below the threshold for suppression, and the contact signal

π_i became zero. Thus, the gating variable z_1 quickly recovered (lower panel), and protraction began again within the same whisk period, resulting in a biphasic whisk profile. It was hypothesised that this control loop may be the origin of the biphasic whisks that have been observed in whisking animals (Towal and Hartmann, 2008).

Note that in the experiments presented in Section 6.4.1 of Chapter 6 τ_z was set to $T_W/4$ throughout and the maximum value of σ_z was 0.9 so that this biphasic whisking was not encountered.

An additional contact induced asymmetry (CIA, described in Section 2.2.2 of Chapter 2) whisker control strategy observed in rodents was also implemented in Sullivan, Mitchinson, Pearson, **Evans, M. H.**, Lepora, Fox, Melhuish, and Prescott (2011). The effect of this control strategy on tactile discrimination is not assessed in this thesis.

3.5 CrunchBot: a mobile whiskered robot platform

CrunchBot (Fox, **Evans, M. H.**, Lepora, Pearson, Ham, and Prescott, 2011) allows the integration of a complete tactile sensory system on a mobile robot while keeping the degrees of freedom to a minimum. The need for a robot like CrunchBot became apparent as more complex artefacts such as SCRATCHbot (Section 3.2) and the BIOTACT G1 (Section 3.4) were difficult to control, had high degrees of freedom and most importantly were located at the Bristol Robotics Laboratory. CrunchBot was developed within the ATL@S Laboratory, in collaboration with BRL, to be a simpler whiskered robot platform that could be located in our own lab. CrunchBot could then be used as a testbed for classifiers that have been developed on the XY positioning robot, or for integration of disparate systems for sensing and navigation.

This section describes the hardware and software architecture of CrunchBot, as well as some details of the localisation and mapping systems that utilise tactile reports generated by classifiers discussed in Section 6.5 of Chapter 6.

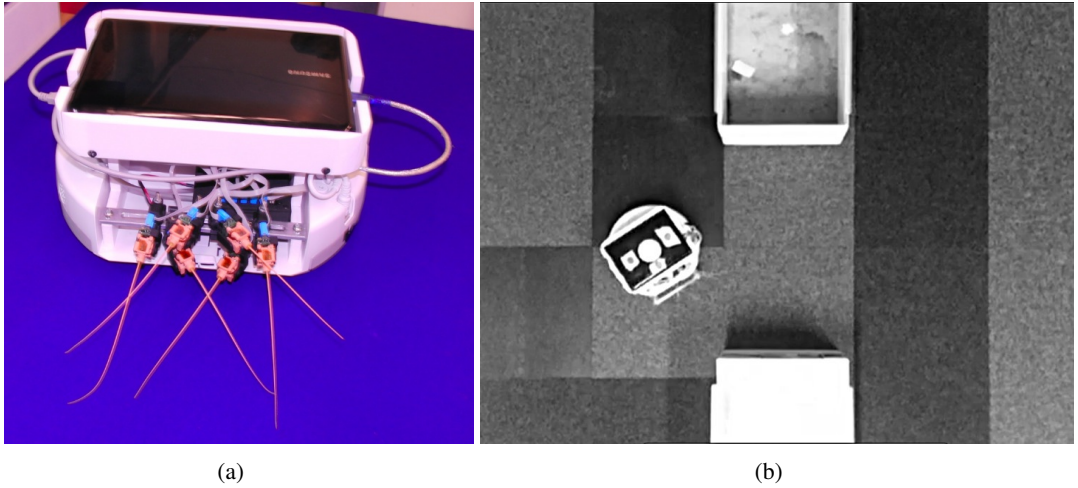


Figure 3.10: (a) CrunchBot. (b) Overhead view of CrunchBot in the arena environment. Different carpet tile textures can be seen on the floor along with square obstacles.

3.5.1 Robot platform

The whiskers are mounted in the cargo bay of an iRobot Create base (www.irobot.com), being positioned on an adjustable metal bar and rapid prototyped ball joint mountings. These mountings allow adjustment of the whiskers, which is particularly important for obtaining good floor contacts. We have also extended the cargo bay mounting to accommodate a netbook PC, which is used for local control of the robot. The netbook runs Ubuntu 10.10 on a single-core Intel Atom processor. A circular buffer in shared memory is used to make data from the Cesys driver available to other processes. The netbook hosts a Player server (playerstage.sourceforge.net) providing high-level, networked API interfacing to the Create's serial port commands. Low-level processes such as texture and shape recognition and basic motor control can run on the netbook, reading the raw data from the circular buffer. These processes send their results to a desktop machine which handles mapping. Communication is via the C++ Thrift RPC (remote procedure call) protocol <http://thrift.apache.org/>. Differential and absolute odometry data from the Create is also sent to the mapping server. Preliminary experiments showed that the odometry

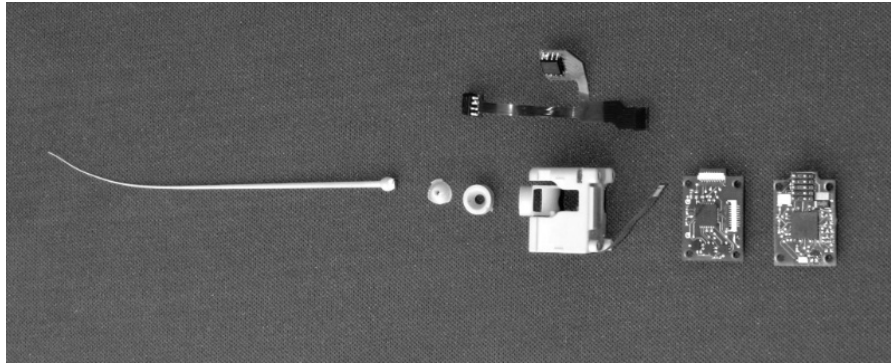


Figure 3.11: A single Crunchbot whisker unit

of the Create, once loaded with the sensing and control hardware, is accurate to $< 5\%$ of any straight line or turn on the spot movements. It was useful to cache commonly used trigonometric quantities describing the whisker geometry to enable fast lookup during navigation.

3.5.2 Whiskers

CrunchBot's six Nanocure RC25 whiskers (pictured in Figure 3.11) measure 160mm in length, 1.45mm diameter at the base tapering linearly to 0.3mm at the tip.

Data from the whiskers was collected using an FPGA configured as a bridge to a USB 2.0 interface. Up to 28 whiskers can be connected to this FPGA bridge at one time. Using the vendor provided software driver and API (Cesys GmbH <http://www.cesys.com/en/home.html>), a user can request the data from all whiskers at minimum intervals of $500\mu\text{s}$ (a maximum sample rate of 2kHz).

3.6 Concluding remarks

We have reviewed the group of robots developed during the BIOTACT project to understand whisker based tactile sensing. A description of each robot's role within the project was given,

and detailed methodologies specifications for the robots have been described. Each robot complements the others; The XY positioning robot serves as a powerful data acquisition tool, generating data that can be used to answer questions, and test algorithms in ways that are not possible on other, less controlled, whiskered robots; The BIOTACT G1 robot provides the opportunity to investigate the effects that different whisker control strategies have on sensing, with a view to optimising sensing for industrial applications; CrunchBot facilitates fast prototyping of sophisticated systems for sensory integration and tactile SLAM; SCRATCHbot, with its BRAHMS-based control architecture allows the combination of all these methods on a biomimetic mobile robot with high degrees of freedom. In the next two Chapters the XY positioning robot is used to generate large data sets for the development and evaluation of classification methods introduced in Section 2.4 of Chapter 2, for the tactile ‘where’ and ‘what’ problems outlined in the tactile framework (Section 2.5 of Chapter 2), namely radial distance estimation (Chapter 4), and angle and texture discrimination (Chapter 5), all under variable contact speeds. Successful methods for radial distance, angle and texture estimation are then applied to data collected on the different robots described in this Chapter. Data collection paradigms and results of classification on whisker data from each robot is given in Chapter 6.

Chapter 4

Classification of radial distance estimation under varying contact speeds

4.1 Introduction

Determining the location of contact in space is an important first step for whisker based tactile discrimination. The location of a contact can be used to build up a map of the environment. Object contours can be recovered by extrapolating over a number of contact locations (discussed in Section 2.4.3.1 of Chapter 2). Subsequent whisker and agent movements may be planned more effectively if the location of an object in space is known. As was discussed in Section 2.4.1 of Chapter 2 the location of contact in space in the horizontal and vertical plane can be recovered by monitoring whisker movement and the physical dimensions of a whisker. We also saw in the same Section that rats can perform this discrimination. The radial distance from the face to the object cannot be directly measured with a whisker. As well as refining the reports of

contact location, determining the radial distance to contact can improve texture discriminations (Fox et al., 2009a, reviewed in Section 2.4.5 of Chapter 2). Rats appear to move their whiskers to ensure contacts with the whisker tips (as discussed in Section 2.2.2 of Chapter 2), indicating that the rat may be using an initial measure of surface location to control subsequent whisker movements. An object contact along the shaft of the whisker provides information about the concavity of a surface (Solomon and Hartmann, 2009), which can be determined with a measure of radial distance.

In the tactile framework proposed in Section 2.5 of Chapter 2, radial distance estimation is the first discrimination that needs to be made. This measure allows the agent to reposition the whiskers for the next contact to ensure a surface–tip contact, and determine the orientation and texture of the surface (addressed in Chapter 5). Radial distance classification, as is the case in each discrimination in the tactile framework, needs to be invariant for contact speed as the agent, whiskers and object may be moving at an unspecified speed.

This Chapter compares candidate methods for radial distance estimation, under conditions that are relevant to our goal of implementation on a mobile robot, specifically different contact speeds and conditions with reduced training data.

Section 4.2 describes a data collection paradigm on the XY positioning robot (Section 3.3 of Chapter 3) to generate data for developing, training and testing five methods for estimating the radial distance to contact of an object along a whisker. These five methods, in order of presentation, are; static beam equation based classification (Sections 4.3.1 and 4.4.1, reviewed in Section 2.4.3.1 of Chapter 2), oscillation frequency based classification (Sections 4.3.2 and 4.4.2, reviewed in Section 2.4.3.2 of Chapter 2), template based classification (Sections 4.3.3 and 4.4.3, reviewed in Section 2.4.4.1 of Chapter 2), feature based classification (Sections 4.3.2 and 4.4.4, reviewed in Section 2.4.4.2 of Chapter 2) and stationary naïve Bayes classification (Sections 4.3.5 and 4.4.5, reviewed in Section 2.4.4.3 of Chapter 2). The specification for each classifier is detailed, as well as the criteria for comparison between the methods. The classifiers

are compared on a number of criteria, and conclusions are drawn about the results in relation to application of each method to the tactile framework (Section 2.5 of Chapter 2), and on other less restricted robots.

4.2 Data collection for radial distance estimation

Preliminary investigations highlighted that the closest contact that could be made by the whisker at any reasonable speed without saturating the Hall effect sensor was $\approx 80\text{mm}$ from the base. Contacts at less than 5mm from the tip did not deflect the base of the whisker for long enough before slipping past to allow an MI type contact. Therefore, the 185mm length whiskers provide a 100mm range of radial distances. Contact speeds above 216mm/s either cause the whisker to slip past the object before a retraction, or saturates the sensors. 36mm/s was the lower bound on the speed here. Contacts were sampled at radial distance intervals of 1mm, and speed intervals of $\approx 7\text{mm/s}$ over the previously described ranges. In total 101 radial distances and 26 speeds were sampled, giving 2626 different radial distance and speed combinations. Contact combinations were randomly interleaved to limit any affects of changing whisker properties. For each contact combination the whisker was deflected by the robot in both a clockwise and anticlockwise directions (-ve and +ve in x), ensuring that the whisker did not bend over time through repeated unilateral deflections. The experiment was performed twice (two runs of clockwise and anti-clockwise, generating four separate sets in total) to generate sufficient data for classification. Data from each trial was stored separately. Deflections from the clockwise robot movement trials (-ve in x) were converted so all data samples were equivalent. Trials were ordered into arrays by speed and radial distance to contact. Each trial was aligned to peak deflection, and shortened to only the 325ms either side of the peak deflection.

4.3 Classifier specification

We compare the performance of five methods that have been used in the past. Namely they are static beam equation based classification (Birdwell et al., 2007), oscillation frequency based classification (Kim and Moller, 2004), template based classification (**Evans, M. H.**, Fox, Pearson, and Prescott, 2010b), feature based classification (**Evans, M. H.**, Fox, Lepora, Pearson, and Prescott, 2010a) and stationary naïve Bayes classification (Lepora, **Evans, M. H.**, Fox, Diamond, Gurney, and Prescott, 2010b). They are assessed under ideal conditions, and with reduced training sets to assess the ability of the classifier to generalise, and to determine how applicable each method would be to situations where large sets of carefully collected training data are unavailable, for example on a mobile robot. The data were separated into training and test sets that were each complete data sets of 26 speeds and 101 radial distances. A reduced set was generated by randomly sampling a subset of this training set as follows;

N is the total number of files (2626). The index of each file is taken, and their order is randomised(using the MATLAB (www.mathworks.com) `randperm` function, which utilises a Mersenne Twister). For a given subset size e.g. 80%, take the first $0.8 \times N$ files and use them for training the classifier. Performance was tested with subsets of 80%, 60%, 40%, 20%, 10% and 5% of the total. This process was repeated five times using a different random number seed to account for any sampling biases. For the static beam equation based method, the size of the training set is irrelevant as it is a generative method. Instead, performance across different speeds is assessed, and the effect of fitting the model parameters to the data is compared to setting the parameters with measured values.

Signals were placed in the training or test sets at random from the original data. In each case classifiers were developed on the training sets, and performance was determined on the test set.

4.3.1 Static beam equation based classification

It has been shown that the radial distance to contact of an object along a whisker can be determined by recording the forces and moments at the base of the whisker and applying them to static beam equations from classical elasticity theory (Birdwell et al., 2007, Section 2.4.3.1 of Chapter 2). We aimed to determine how well this approach would work on biomimetic whiskers, under conditions of variable contact speed.

Certain variables about the deflection must be determined to be used as input to the equations. Protraction angle can be determined as we know the time delay of the robot – each robot protraction will be of a given duration. We control the speed of the robot, so for a given speed we can work out the distance travelled by the stimulus, and therefore the angle of the deflection (θ in Figure 2.14 of Chapter 2). We can use this protraction angle θ in the following equation to find r , the radial distance to contact (Birdwell et al., 2007),

$$r = \frac{C\theta L}{C\theta + ML} \quad (4.1)$$

where L is the whisker length, M is the bending moment measured at the whisker base. C is a constant based on the whisker's material properties, elastic modulus E and area moment of inertia $I_{base} = \pi r_{base}^4$, with r_{base} being the radius of the whisker at the base. These values are combined to give

$$C = \frac{3EI_{base}}{4}. \quad (4.2)$$

The output voltage of the Hall effect sensor is linearly proportional to the bending moment, although it must be calibrated to be used in the equations by applying a scaling factor S_f . The equation was tested on the data set with values from each parameter taken from measurements of the whisker. The scaling factor S_f was adjusted to find the value that reduced the classification error between the data and the whisker.

Analysis of each contact began by finding the amplitude of deflection at peak protraction, this was achieved by finding the maximum amplitude of deflection during contact, the same operation as in Equation 4.5. This value is then used as input to Equation 4.1. After the radial distance of a test data file is estimated it is rounded to the nearest integer (using the MATLAB `round` function) to more directly compare performance to the other classification methods.

The output is recorded and later compared to the correct radial distance.

In addition a brute force search was used to find values for each of the parameters that provided the lowest classification error. The analysis was repeated with a range of values about the preset value. The ranges and increments used were: E (0.5–3, in increments of 0.1), r_{base} (0.5–1.5, in increments of 0.1), L (170–240, in increments of 5) and S_f (0.0005–0.005, in increments of 0.0005).

4.3.2 Oscillation frequency based classification

It has been shown in the past that it is possible to determine the radial distance to contact of an object along a whisker by monitoring changes in the natural frequencies of the whisker during and immediately post contact (Kim and Moller, 2004).

In previous work it has been shown that a spectral template classifier can be used to discriminate textures with an artificial whisker in a real world texture discrimination task (**Evans, M. H.** et al., 2009a, described in Section 6.2 of Chapter 6). The methodology is the same as that for the template classifier described in Section 4.3.3, but with an additional preprocessing step. Here a fast Fourier transform (FFT) was performed on the filtered data in MATLAB, with a library called FFTW (FFTW, 1998; Frigo and Johnson, 1998), which uses the Cooley-Tukey algorithm (Cooley and Tukey, 1965). The MATLAB FFT function returns the discrete Fourier transform (DFT) of the input signal (x) of length N , computed with a fast Fourier transform (FFT) algorithm,

$$X(k) = \sum_{j=1}^N x(j) \omega_N^{(j-1)(k-1)}, \quad (4.3)$$

where $\omega_N = e^{(-2\pi i)/N}$ is the N th root of unity.

The absolute value of the DFT ($|X|$) is then stored as a template for comparison with DFTs of incoming test data.

4.3.3 Template based classification

Template based classification (Brunelli, 2009, discussed in Section 2.4.4.1 of Chapter 2) involves recording example sensory data as templates during a training phase, and comparing the stored templates to novel data during the test phase. By systematically comparing the novel data to signals encountered previously, a classification can be made by declaring which of the stored templates the novel signal is most similar to.

It has been shown in our own lab that templates can be used for discriminating groups of tactile features simultaneously in simulation (Fox, **Evans, M. H.**, Pearson, and Prescott, 2008; Fox, **Evans, M. H.**, and Prescott, 2009b) and hardware (**Evans, M. H.** et al., 2008), even in conditions where the templates are learnt over time (**Evans, M. H.** et al., 2010b), and that spectral templates can be used to discriminate whisker deflection signals from floor surface textures in a real world environment (**Evans, M. H.** et al., 2009a, work described in Section 6.2 of Chapter 6).

In the present study each template corresponds to a speed-radial distance pair. Classification based on these templates is therefore simultaneous classification of both speed and radial distance. Preliminary investigations comparing different preprocessing methods found that low pass filtering the raw signal provided the best results.

From the training data set a subset of trials – representative of the larger set – were stored in an array as templates. The number of templates chosen were dependent on the experimental

condition. During the test phase, trials were taken at random from the test set as inputs to the classifier. An element-wise sum of squared errors calculation was made between the input I and each template T_i ,

$$e(T_i) = \sum_{t=1}^n (I(t) - T_i(t))^2. \quad (4.4)$$

where n is the length of the template, in samples. The template with the lowest sum of squared error was determined the winner, and a recording was made in an output array of the estimated speed and radial distance to contact of the input trial.

4.3.4 Feature based classification

Feature based classification (discussed in Section 2.4.4.2 of Chapter 2) involves finding invariant features in the data that correspond to parameters in the real world. For example using scale invariant feature transformation (SIFT) algorithms in vision (Ke and Sukthankar, 2004; Juan and Gwun, 2010). Frog prey capture is based on the principle of feature detection, with responses elicited for any object matching the size and angular velocity of a fly (Lettvin et al., 1959). In the rat whisker system some researchers have reported cells that respond to ‘kinetic features’ in whisker deflections (Petersen et al., 2008).

To successfully implement a feature based classifier, appropriate features must first be found. Inspection of the whisker data showed that peak deflection magnitude could be used as a feature for radial distance discrimination at a given speed. Deflection magnitude was taken as the Hall effect sensor output voltage at peak deflection, which is proportional to the bending moment M . Feature f_1 can be defined as,

$$f_1 = \max_t M(t), \quad (4.5)$$

where $M(t)$ is the deflection magnitude varying with time, measured by the Hall effect sensor in

volts. Note that $t(f_1) = t(\max_t M(t))$

Similarly, contact speed could be discriminated using deflection duration. Deflection duration was taken as the width of the deflection peak (prominent initial deflection in each trace of Figure 3.7 of Chapter 3). Deflection duration was measured using a threshold crossing on the sensor output. When Hall effect sensor output exceeded 0.05V a timer was initiated (t_1), and when Hall output subsequently fell below this threshold the timer was stopped (t_2). Feature f_2 can be defined as,

$$t_1 = \min\{t : M(t) \geq \gamma\}, \quad (4.6)$$

$$t_2 = \min\{t : M(t) \leq \gamma, t_2 > t_1\}, \quad (4.7)$$

$$f_2 = t_2 - t_1, \quad (4.8)$$

where γ is the threshold and f_2 was measured in ms. Figure 4.1 shows the object-contact space for f_1 and f_2 in graphical format.

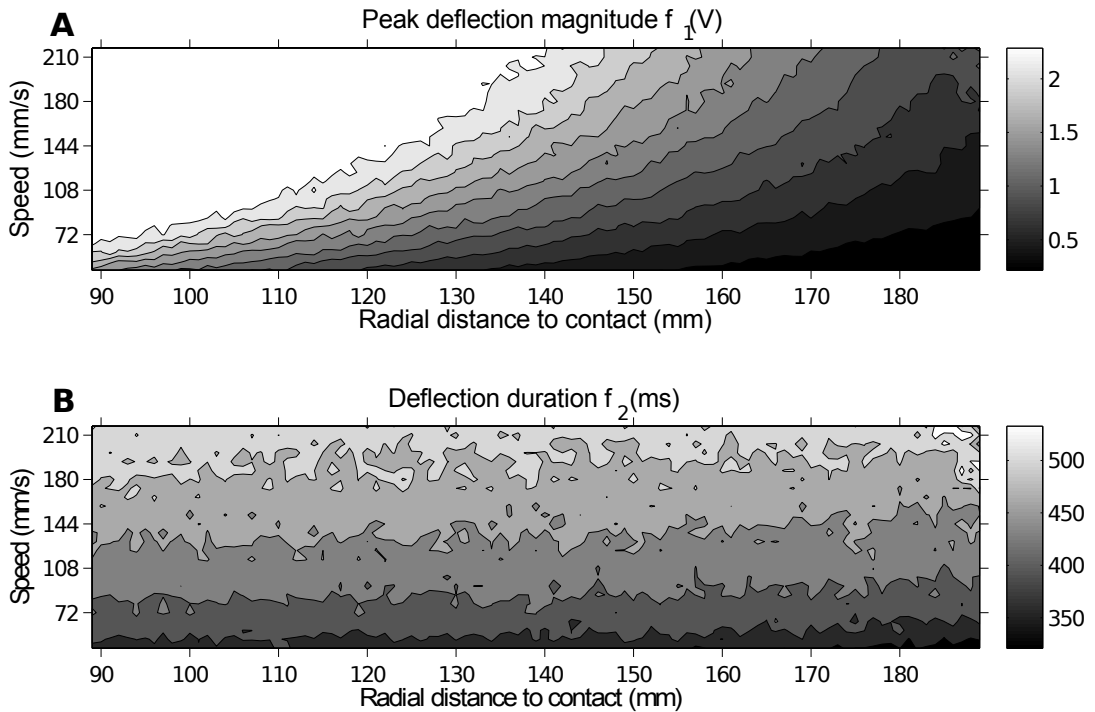


Figure 4.1: A contour plot of peak deflection magnitude and duration for each contact. Each point in the image corresponds to a location in the speed-radial distance space, which is equivalent in both plots. (a) Peak deflection magnitude f_1 , brightness indicates higher deflection magnitude, measured in volts. (b) Deflection duration f_2 , brightness indicates greater duration (measured in ms).

A model was generated of the relationship between each pair of features and the corresponding contact properties with polynomial regression (using `polyfitn` in MATLAB <http://bit.ly/polyfitn>). Using simple linear least squares a model is generated that can be used to classify new data. Only three arguments are required for the model, an array of independent variable values, an array of dependent variable values, and a model specification, namely the degree of the polynomial. A fifth degree polynomial was chosen as preliminary studies showed it provided good results.

The independent variables in this instance were features f_1 and f_2 . To find both radial distance and speed, two models were developed, with dependent variables of radial distance and speed respectively. After the speed and radial distance of a test data file is estimated it is rounded to

the nearest integer (using the MATLAB round function) to more directly compare performance to the other classification methods.

4.3.5 Stationary naïve Bayes classification

Empirically, it was found that whisker velocity traces gave a better localisation of contact speed and distance than raw whisker deflection traces (Lepora et al., 2011). Thus, the positional deflections were converted to velocities for the analysis (by taking their numerical derivative and Gaussian smoothing to reduce noise).

Measurements were quantised into one hundred equal-width intervals that spanned the entire data range of the whisker, then the resulting histogram of sensor measurements smoothed with a Gaussian of width five intervals to correct for sampling errors and normalising by the number of samples to give the likelihood.

A log-likelihood function is generated for each trial in the training set

$$\log P_w(x_i|C_l), \quad (4.9)$$

declaring the probability P_w (w for each whisker) of each sensor measurement x_i occurring, for a given class C_l . These likelihood functions are generated by generating an amplitude histogram from the whisker deflection data, with 501 bins over whisker amplitude range (-2.5V : 2.5V). This number of bins had been chosen from preliminary investigations. The histograms were normalised to sum to 1, and natural logs were taken of the resultant histograms to simplify the later calculations. There are 2626 classes in the complete training set condition, one for each speed and radial distance combination.

For each trial in the test set a classification was achieved using naïve Bayes rule (naïve as it treats each sample as statistically independent) to calculate the posterior probabilities for each of the

possible classes. These posterior probabilities were calculated from the time-independent naïve Bayes rule,

$$\log P(C_l | x_1, \dots, x_n) = \sum_{i=1}^n \log P_w(x_i | C_l), \quad (4.10)$$

for flat priors, a time-independent likelihood and the naïve assumption of statistical independence. More informally, the equation gives the log probability of each class C_l given the sensor data x by taking each sample in the test set and summing it with each stored likelihood histogram to from the posteriors.

The classification is given by the largest log-posterior for each validation trial,

$$R = \operatorname{argmax}_{T_l} \log P(C_l | x_1, \dots, x_n). \quad (4.11)$$

Generally, the distribution of log-posteriors for each trial had an extended curving segment of high values close to the target speed and distance of the test trial, surrounded by a drop-off of values further away from these targets. The class with the largest posterior is most probable and declared the winner.

4.3.6 A comparison of all five classifiers

Classification errors are reported for each classifier, in both speed and radial distance to contact, apart from for the static beam equation, as this method cannot determine the speed of contact. Here radial distance errors are given for each speed instead.

The performance of each method when trained on reduced training set sizes are given, to determine how each classifier performs with impoverished data. Computing time is given for the classification as an additional measure of classifier performance, with a view to comparing candidate methods for real-time operation on a mobile robot (as demonstrated in Chapter 6). Though this is heavily implementation dependent, it provides an insight in to the comparative

computational overhead of each method.

4.4 Results

Results are presented for each classifier in turn for radial distance and speed estimation. The performance is compared by calculating the accuracy and precision of classification of radius and speed. Histograms and scatterplots of radial distance and speed classification errors are given for each classifier, with exception of static beam equation based classification, where mean and standard error for radial distance classification is given for each contact speed in the range.

Performance is assessed for a complete set of training data, as well as for reduced data sets to determine each classifier's robustness and generalisability. Computing time for each classifier is compared, with a view to comparing candidate methods for real-time operation on a mobile robot (as demonstrated in Chapter 6). Conclusions are drawn about the performance of each method with respect to the tactile framework established in Chapter 1.

4.4.1 Static beam equation based classification

Mean classification error for the static beam equation based classifier with measured parameters was 0.25mm, with a standard error of 8.8mm. Mean classification error for the fitted static beam equation based classifier was 0.015mm, with a standard error of 10.4mm. Due to the reduction in mean this is an improvement in total error even though the standard error is higher.

For the equation with measured parameters, a comparison of radial distance classification errors across speeds shows that a best mean error of 0.44mm and standard error of 4.23mm at the median speed. These values increase to -10.22mm and 10.86mm respectively for the most extreme speed.

For the equation with fitted parameters, a comparison of radial distance classification errors across speeds shows that a best mean error of 0.015mm and standard error of 3.87mm at the median speed. These values increase to 9.97mm and 12.67mm respectively for the most extreme speed.

Table 4.1: Static beam equation parameters, measured and fitted

*	E	r_{base}	L	S_f
Measured	2.4GPa	1mm	180mm	0.0031
Fitted	1.5GPa	1.2mm	230mm	0.002

Fig 4.2 shows a histogram of classification errors for radial distance using static beam equation and measured parameters (a), and radial distance classification error for each speed (b). Errors increase as speed deviates from the median.

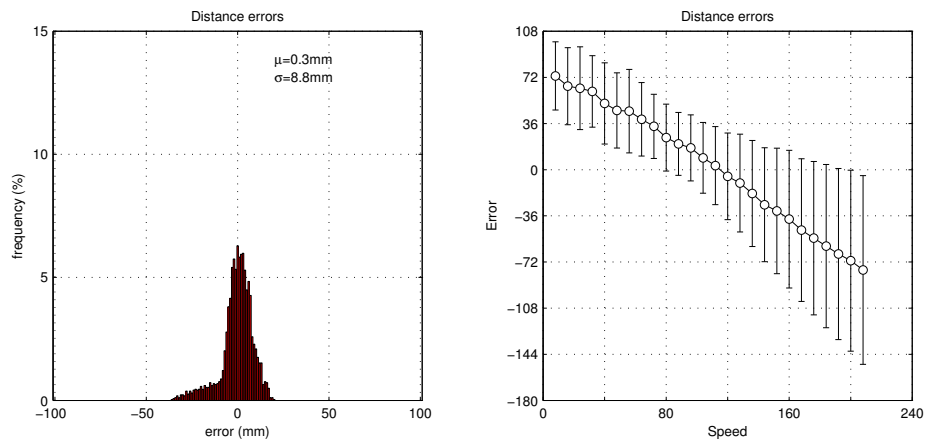


Figure 4.2: (a) Histogram of radial distance classification errors using the fitted static beam equation based classifier. (b) Radial distance classification error for each speed. Error bars are for standard error. Error increases as speed deviates from the median

Fig 4.3 shows a histogram of classification errors for radial distance using static beam equation and fitted parameters (a), and radial distance classification error for each speed (b). Errors increase as speed deviates from the median.

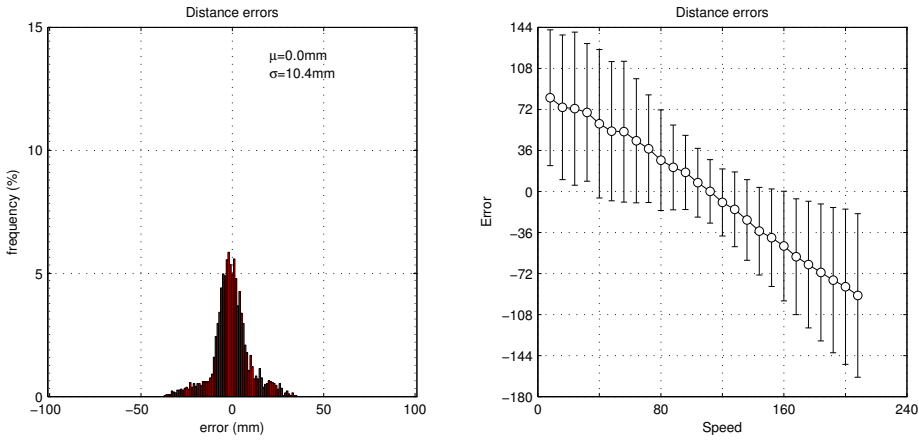


Figure 4.3: (a) Histogram of radial distance classification errors using the fitted static beam equation based classifier. (b) Radial distance classification error for each speed. Error bars are for standard error. Error increases as speed deviates from the median

4.4.2 Oscillation frequency based classification

Table 4.2 shows the results for classification performance with the frequency template classifier in each of the conditions. These results are also shown in Figure 4.4.

Table 4.2: Mean and standard error of frequency template based classification, for different training set sizes. Percentages indicate relative sizes of training subsets from the total.

		5%	10%	20%	40%	60%	80 %	100%
Speed	Mean	-86.17	-57.71	-75.68	-84.30	-87.50	-88.85	-89.98
	Std Err	53.94	56.66	54.64	54.08	53.95	53.98	53.99
Radius	Mean	-3.66	-0.16	-0.50	-4.47	-7.61	-9.32	-1.78
	Std Err	40.90	41.28	41.57	40.89	40.08	40.76	34.33

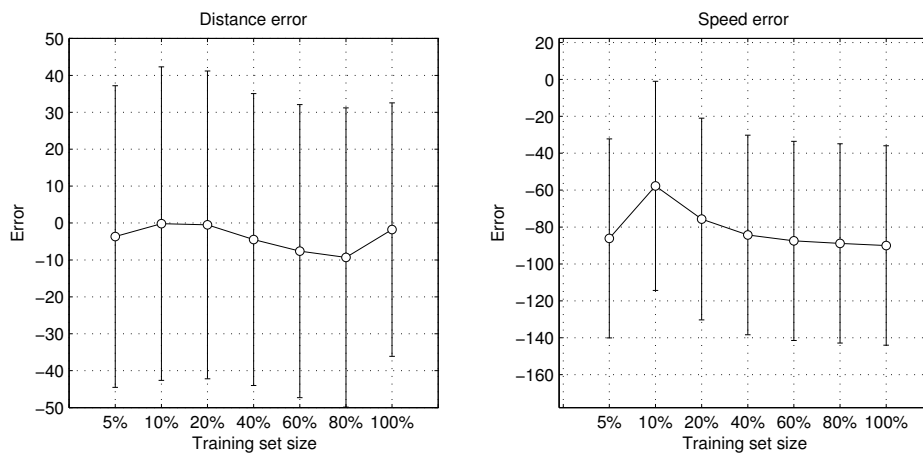


Figure 4.4: Mean classification error of frequency template based classification for different training set sizes, for distance (a) and speed (b). Error bars are for standard error.

Fig 4.5 shows histograms of classification errors for both radial distance (a) and speed (b), and a scatterplot (c) of the errors for each sample in the test set.

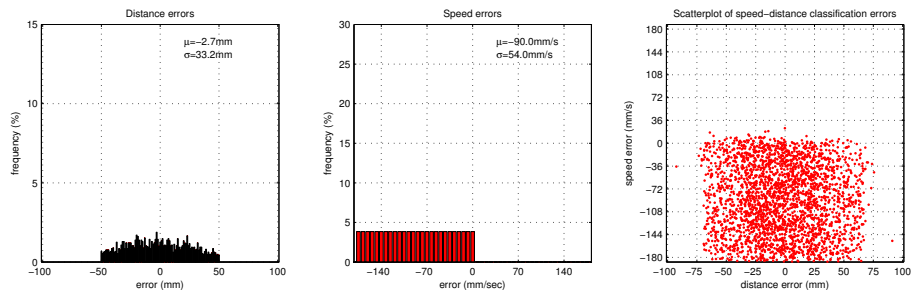


Figure 4.5: (a) and (b) Histograms of radial distance classification errors using the frequency template based classifier. (c) Scatterplot of these errors for each point in the dataset.

4.4.3 Template based classification

Table 4.3 shows the results for classification performance with the template based classifier in each of the conditions. These results are also shown in Figure 4.6.

Table 4.3: Mean and standard error of template based classification, for different training set sizes. Percentages indicate relative sizes of training subsets from the total.

		5%	10%	20%	40%	60%	80 %	100%
Speed	Mean	-1.50	-4.32	-2.23	-1.58	-1.66	-1.38	-1.22
	Std Err	18.71	28.01	23.25	19.73	17.85	16.6	15.70
Radius	Mean	0.38	0.73	0.39	0.45	0.48	0.45	0.4
	Std Err	5.79	8.83	7.36	6.21	5.53	5.17	4.92

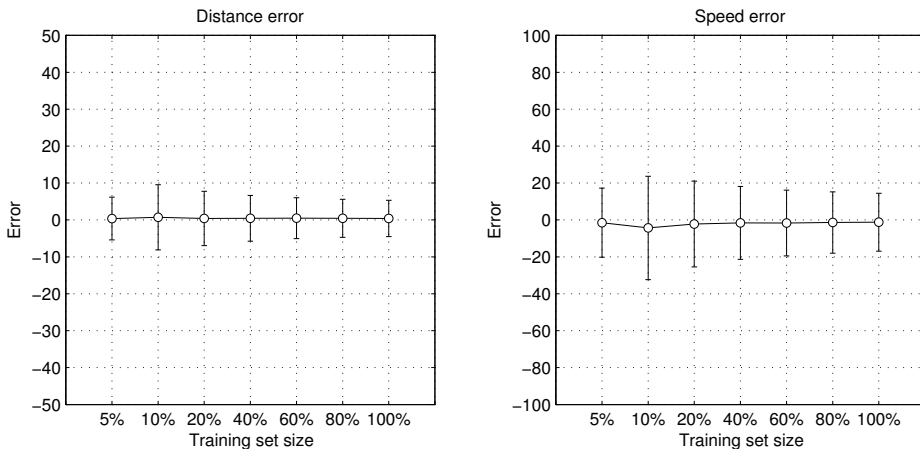


Figure 4.6: Mean classification error of template based classification for different training set sizes, for distance (a) and speed (b). Error bars are for standard error.

Fig.4.9 shows histograms of classification errors for both radial distance (a) and speed (b), and a scatterplot (c) of the errors for each sample in the test set.

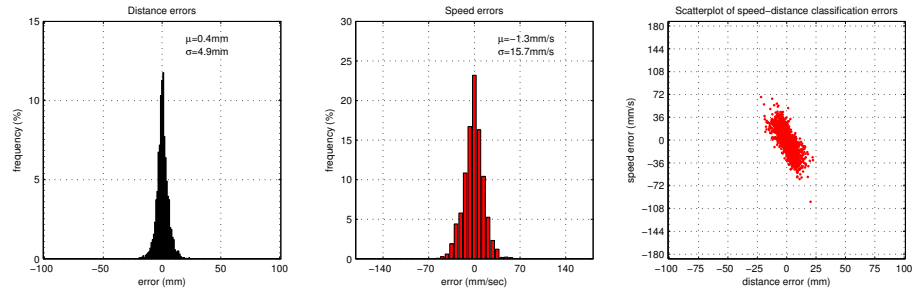


Figure 4.7: (a) and (b). Histograms of radial distance and speed classification errors using the template based classifier. (c) Scatterplot of these errors for each point in the dataset.

4.4.4 Feature based classification

Table 4.4 shows the results for classification performance with the feature based classifier in each of the conditions. These results are also shown in Figure 4.8.

Table 4.4: Mean and standard error of feature based classification, for different training set sizes. Percentages indicate relative sizes of training subsets from the total.

		5%	10%	20%	40%	60%	80 %	100%
Speed	Mean	-1.05	-1.20	-1.35	-0.002	0.05	0.44	0.09
	Std Err	30.35	32.66	31.98	29.01	27.65	26.16	25.80
Radius	Mean	2.14	1.85	1.85	1.42	1.50	1.50	1.65
	Std Err	10.49	10.04	11.32	7.70	8.05	7.99	7.84

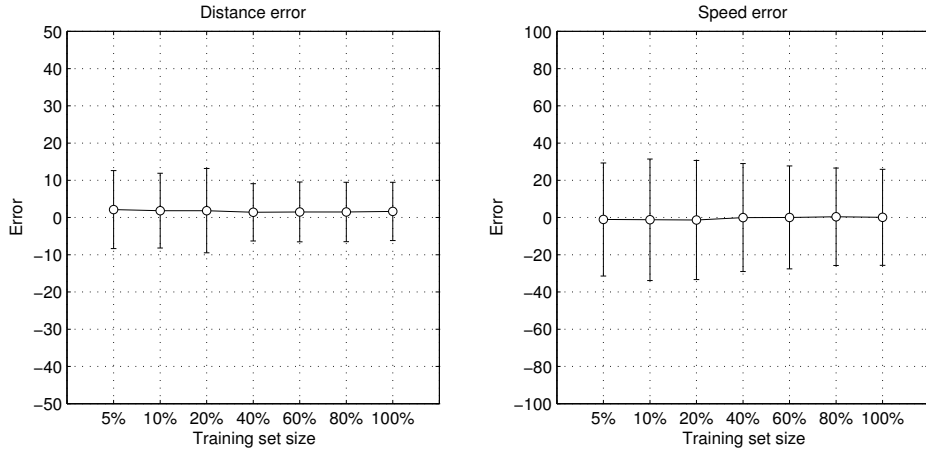


Figure 4.8: Mean classification error of feature based classification for different training set sizes, for distance (a) and speed (b). Error bars are for standard error.

Fig.4.9 shows histograms of classification errors for both radial distance (a) and speed (b), and a scatterplot of the errors for each sample in the test set.

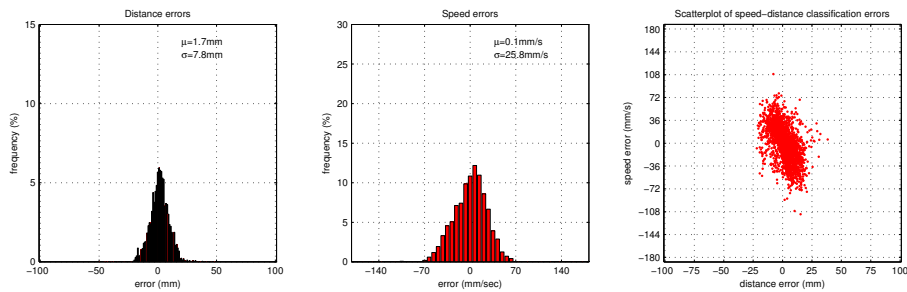


Figure 4.9: (a) and (b). Histograms of radial distance and speed classification errors using the feature based classifier. (c) Scatterplot of these errors for each point in the dataset.

4.4.5 Stationary naïve Bayes classification

Table 4.5 shows the results for classification performance with the naïve Bayes classifier in each of the conditions. These results are also shown in Figure 4.10.

Table 4.5: Mean and standard error of naïve Bayes based classification, for different training set sizes. Percentages indicate relative sizes of training subsets from the total.

		5%	10%	20%	40%	60%	80 %	100%
Speed	Mean	-3.82	-5.47	-4.81	-3.78	-3.76	-3.50	-3.38
	Std Err	13.95	19.2	16.53	14.28	13.62	13.14	12.79
Radius	Mean	0.636	1.23	0.85	0.54	0.54	0.51	0.47
	Std Err	5.27	7.82	6.22	5.41	5.17	4.97	4.85

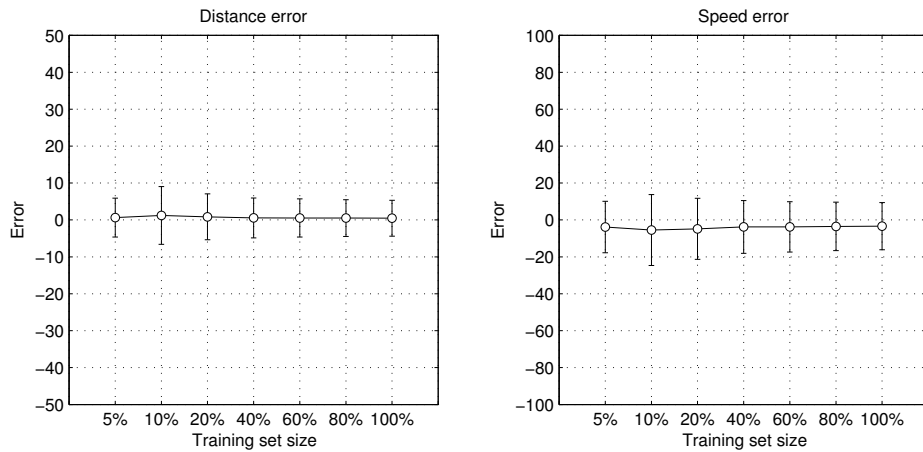


Figure 4.10: Mean classification error of naïve Bayes based classification for different training set sizes, for distance (a) and speed (b). Error bars are for standard error.

Fig. 4.11 shows histograms of classification errors for both radial distance (a) and speed (b), and a scatterplot of the errors for each sample in the test set.

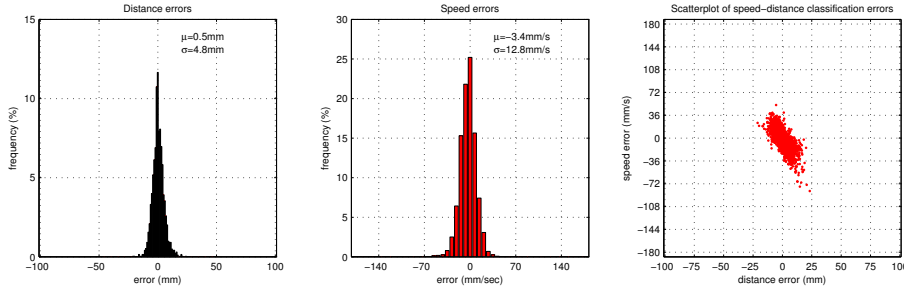


Figure 4.11: (a) and (b). Histograms of radial distance and speed classification errors using the naïve bayes classifier. (c) Scatterplot of these errors for each point in the dataset.

4.4.6 A comparison of all five classifiers

Table 4.6 shows the time to complete the classification for each method on a 2.5 Ghz Intel Core 2 Duo MacBook Pro. Specifically the values are totals for the classification based on training with full training data sets and the classification of 2626 test samples.

Table 4.6: Time to complete classification (2626 test samples)

	Static Beam	Frequency	Template	Feature	Naïve Bayes
Time	1.2s	2mins	4min15s	14.1s	22min24s

Table 4.7 shows the ‘best-case’ classification performance for each classifier under ideal conditions. These results are shown in Figure 4.12

Table 4.7: Classification performance for each classifier under ideal conditions

		Static Beam	Frequency	Template	Feature	Naïve Bayes
Speed	Mean	NA	-89.98	-1.22	0.09	-3.38
	Std Err	NA	53.99	15.70	25.80	12.79
Radius	Mean	0.25	-1.78	0.4	1.65	0.47
	Std Err	8.8	34.33	4.92	7.84	4.85

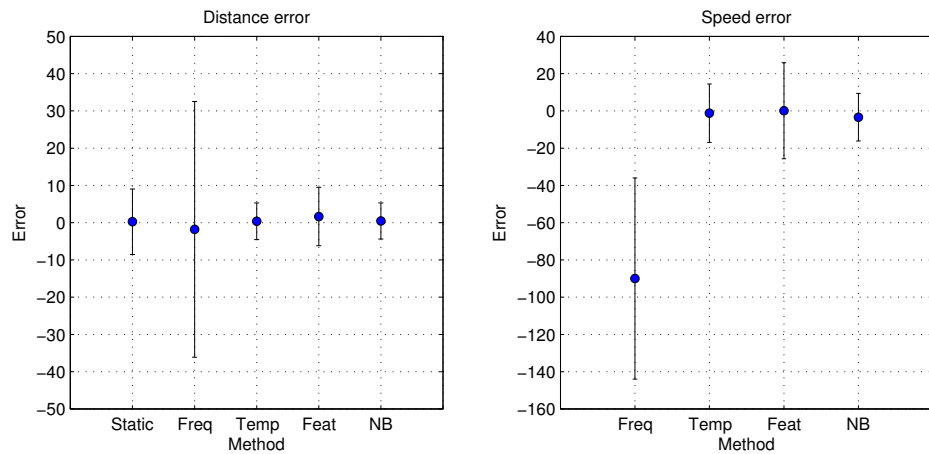


Figure 4.12: Mean classification error of each classifier for distance (a) and speed (b). Error bars are for standard error. Static = static beam equation, Freq = frequency template, Temp = template, Feat = feature, NB = naïve Bayes.

4.5 Discussion of radial distance estimation methods

We have shown that established and novel classifiers can distinguish radial distance to contact along a whisker under conditions of unknown speed, with varying degrees of success.

The most accurate classifiers were the template method and naïve Bayes, followed by a fitted static beam equation, then finally the feature based classifier. It is important to note that feature based classification still performed very well; the only classifier that was unsuccessful was the frequency based classifier, though this is unsurprising considering the reasons given in Section 2.4.3.2.

A static beam equation works very well once the parameters have been fitted. It is interesting to note that the ‘fitted’ values not only work better but may be more accurate values for the parameters. Though the whiskers were designed to have a base radius of 1mm, manufacturing precision of ABS plastic may have resulted in a whisker that is slightly thicker. It’s difficult to determine this without special equipment. In addition a lower Young’s modulus indicates that the whisker was softer, or less elastic, than was first thought. This could be due to a softening over time through extended use, or because the whisker is built up of layers of ABS instead of being cut from a block. Finally, a truncated cone with a radius of 1mm that is 180mm in length and 0.5mm at the tip would be ≈ 230 mm long if it were to taper to zero. Depending on the method used for classification, radial distance detection is confounded with contact speed (see Fig.3.7 in Chapter 3 for a demonstration of this). This ambiguity in the signal cannot be accounted for with a single observation, an additional observation or feature must be found in order to discriminate these two properties of the collision. Successful classification relies either on finding the contact speed before conducting a radial distance estimation, or discriminating both properties simultaneously. Each of the model-free classifiers (template, feature and naïve Bayes) recovers radial distance and speed simultaneously from the data.

On the other hand performance of the static beam equation is critically dependent on knowing the

whisk protraction angle θ . In the results presented in Fig. 4.3 the model's precision decreases as contact speed deviates from the median, but performance would deteriorate if θ was unknown or incorrect. For example if the object was moving towards the agent the actual angle would be shorter than the protracted θ . A similar problem occurs if the θ information is noisy or incomplete: classification would become unreliable.

Naïve Bayes has been shown to out-perform other non-probabilistic classifiers for texture discrimination (Lepora, **Evans, M. H.**, Fox, Diamond, Gurney, and Prescott, 2010b), and performs comparably to or better than the other methods here. It should be noted that this performance does depend upon the pre-processing of the input signal. Classifying speed and radial distance over deflection velocity gave the accurate classification reported here (mean and standard error of 3.38mm/s and 12.79mm/s respectively for speed classification, and 0.47mm and 4.85mm for radial distance estimation).

However, using just raw deflection data led to poorer performance (mean and standard error of 3.16mm/s and 37.08mm/s respectively for speed classification, and -1.25mm and 12.75mm for radial distance estimation). Using a time derivative of the signal improved classification dramatically. One possible reason for this improvement is that using a derivative of the signal provides the classifier with temporal information that is lacking when considering each deflection sample independently. Here the classification is of contact speed, which affects the temporal pattern of the deflection signal, and so it might be expected that velocity information would be better than deflection information for classification purposes.

It is possible that a template classifier would suffer with a noisy signal, where a feature based or naïve Bayes method provides a means for extracting signals from ambiguous background data. For example in another whisker geometry and texture experiment naïve Bayes proved more accurate than a template method in classifying data from the BIOTACT G1 whisking robot (Sullivan, Hutchinson, Pearson, **Evans, M. H.**, Lepora, Fox, Melhuish, and Prescott, 2011, described in detail in Section 6.4 of Chapter 6).

Accuracy is not the only way to compare the models. Large discrepancies exist for time it takes to run the different methods. The static beam equation method is the quickest, though the time shown does not take in to account the fitting of the parameters. In addition, the protraction angle is provided to the classifier so no time is wasted having to infer this information. Naïve Bayes classification is the most time consuming by some distance. This is because of the increased complexity of the algorithms in comparison to the other methods. However most of this time is spent training the classifier, and naïve Bayes is also particularly suited to parallelisation, so computing time is not really an issue for any of these methods in this task.

Perhaps surprisingly the frequency template method is quicker to compute than the raw signal template. This is because the raw signal is filtered, which takes longer than a FFT which utilises MATLAB's own hard coded libraries. If both methods were coded up from scratch, as they would need to be for real time processing on a mobile robot (such as for CrunchBot, Section 6.5 of 6), the results are likely to be different. In this implementation the feature classifier only extracts information that is also available to the template classifier, so increases in accuracy were always unlikely. Classification is not quite as good as for some of the other methods, but the short computation time makes this method attractive for certain mobile robot applications.

Though all the classifiers can be performed in real time (if we use a constraint of 1 classification per second on a mobile robot whisking at 1Hz) on a standard PC, reducing the computational burden could be important for mobile robotics applications, or when attempting to process data from numerous whiskers.

Time savings can be made if reduced training sets are used, and none of the methods appear to suffer too badly from reducing the training set, which is a surprise. However, even small increases in mean or standard error of classification performance result in a significant increase of total error when classifying large test sets. Any performance increase may be worth the extra computing time, especially as a full training set can be used in the classification while preserving real time processing. In some of the classifiers a complete training data set may be causing

over-fitting to the data. For example, the feature classifier’s peak performance for radial distance estimation is when only 40% of the training data is used. It is important, therefore, to be careful when training a classifier to pick an appropriately sized training set for maximum performance.

The results presented here compare favourably with the sensory capabilities of rats. Rats have been shown to be capable of discriminating apertures differing in width by 5mm, corresponding to a radial distance difference of 2.5mm per whisker (Krupa et al., 2001). Since the longest rat whiskers are 50–60mm in length, a 2.5mm discrimination corresponds to an acuity of $\approx 4\text{--}5\%$ of whisker length. A standard error of classification of $\approx 5\text{mm}$ on an 185mm whisker corresponds to an acuity 2.7% of whisker length.

It is important to consider that a rat has ≈ 30 whiskers on each side of its head. Combining information from multiple whiskers may improve the reliability of classification, for example by providing a means to remove independent noise from the signal (Lepora, Evans, M. H., Fox, Diamond, Gurney, and Prescott, 2010b). Alternatively the reports from an array of whiskers could be used to inform gross shape information about the environment. This is an approach we take to determine the angle of a surface on CrunchBot (described in Section ?? of Chapter 3) during a tactile SLAM task. These results are described in Section 6.4 of Chapter 6.

When we consider the tactile framework in Section 2.5 of Chapter 2, a few of these methods could be used for radial distance and speed estimation in the ‘where’ task. Both template and naïve Bayes classification are very accurate, and feature based classification is quite accurate while being very quick to run. The choice of method for application to other robots may be determined more by other task demands, such as computing time and the nature of training data, than strictly by task performance. In Section 6.4 of Chapter 6 we implement the feature based classifier for radial distance estimation on data from CrunchBot. This was because the classifier performs well, while being very simple to implement in C++ code for real-time processing on board the robot.

In the next Chapter we again use the XY positioning robot to generate a large data set, this time for the ‘what’ task in our tactile framework. Specifically for texture discrimination that is invariant of surface angle and contact speed.

Chapter 5

Classification of surface angle and texture estimation under varying contact speeds

5.1 Introduction

We move now to texture discrimination. With respect to the tactile framework (Section 2.5 of Chapter 2), and a goal of developing classifiers for navigation with a mobile robot, texture discrimination is very important for object identification. Texture provides the only surface property for object identification that has been studied extensively in the whisker domain, compared to other object properties such as gross shape or curvature (though shrews are purported to use gross shape recognition in prey capture Anjum et al., 2006). Rats have been shown to be excellent at texture discrimination (Diamond et al., 2008 (a)), and as detailed in Section 2.4.5 of Chapter 2, many approaches have been pursued in the past for texture discrimination, with varying degrees of success. Some approaches have extracted features from the frequency spectrum

for texture discrimination (Hipp et al., 2006). Others have suggested that the pattern and number of high velocity deflections during contact could be used to encode textures (Wolfe et al., 2008), and that neurons responding to these high velocity events have been found in the thalamus (Petersen et al., 2008) and cortex (Arabzadeh et al., 2006) of rats. Data–driven model–free methods have also been used successfully for whisker based texture discrimination, using stationary naïve Bayes (Lepora, **Evans, M. H.**, Fox, Diamond, Gurney, and Prescott, 2010b) and spectral templates (**Evans, M. H.** et al., 2009a) similar to the methods used successfully for radial distance estimation the preceding Chapter.

For the requirements of our tactile framework (Section 2.5 of Chapter 2), texture discrimination needs to be robust to changes in contact speed, and surface orientation. It has been shown previously that texture discrimination is more difficult when whisker–object contact geometry is unknown or variable (Fend, 2005; Fox et al., 2009a; N’Guyen et al., 2010). Whisker movement speed will affect the frequency of oscillations in the whisker in much the same way as a music record played at the wrong speed changes pitch. The angle of the surface affects the amount of friction between the whisker and the texture, changing the pattern of whisker deflections. Surface angle has not been classifier with a whisker from a single brief contact before, though surface contours have been recovered from a series of contacts (Section 2.4.3.1 of Chapter 2). The XY positioning robot also allows us, for the first time, to systematically investigate the effect speed and surface angle have on texture discrimination.

It may be easier to discriminate textures if the classification method can also take the geometry and speed of whisker contact into account. The classifiers presented in this Chapter are tasked with discriminating the speed of contact, and the angle and texture of a surface *simultaneously*, to determine whether such an approach is possible, and if so which methods are most successful. We also report the classification performance of each method where only the texture varies, to show how the inclusion of speed and angle discrimination affects classification.

In this Chapter a dataset is generated on the XY positioning robot (Section 3.3 of Chapter 3)

to generate data for developing, training and testing four methods for surface angle and texture discrimination at different contact speeds. These four methods, in order of presentation, are; Template based classification (Sections 5.3.1 and 5.4.1, reviewed in Section 2.4.4.1 of Chapter 2), Spectral template based classification (Sections 5.3.2 and 5.4.1.6), Feature based classification (Sections 5.3.3 and 5.4.2, reviewed in Section 2.4.4.2 of Chapter 2), and stationary naïve Bayes classification (Sections 5.3.4 and 5.4.3, reviewed in Section 2.4.4.3 of Chapter 2).

Importantly, note that radial distance is not a parameter for this experiment. If we consider the tactile framework (Section 2.5 of Chapter 2), surface contacts are always at the tip of the whisker. Therefore any texture discrimination that the rat performs does not need to be invariant for radial distance.

Template (Section 4.3.3 of Chapter 4) and stationary naïve Bayes (Section 4.3.5 of Chapter 4) based classification methods, that have been used for radial distance and speed estimation in Chapter 4, may be improved by making some texture specific modifications. It has been proposed that rats may encode textures by the number, magnitude or timing of high velocity ‘stick-slip’ events (Wolfe et al., 2008). It may be possible to discriminate textures more accurately if a classifier has information about the velocity or acceleration events within the signal. To test this hypothesis we compared the performance of template (Section 5.3.1) and stationary naïve Bayes classifiers (Section 5.3.4) based on filtered raw signals against versions using the first and second derivatives of the signals as input. Spectral templates have previously been demonstrated for texture discrimination on data collected on a whiskered mobile robot (**Evans, M. H.** et al., 2009a, Section 6.2 of Chapter 6). This methodology is applied here, with the aim of texture discrimination under conditions of varying speed and surface angle, as well as for determining whether information from the spectral domain can be useful for speed and surface angle discrimination.

Having already developed features based classifiers for discriminating certain parameters of the contact, such as radial distance and speed (Chapter 4), we look to doing the same here for surface

angle and texture under conditions of varying contact speed. Certain feature based methods have been shown to be particularly useful when whisker contact geometry is unknown, (Fox et al., 2009a; Fend, 2005). Fend (2005) and Hipp et al. (2006) extracted spectro-temporal features from the fast Fourier transform (FFT) of the whisker deflection signal, namely the frequency with the most power in the spectrum, the power at that frequency, and the total power spectral density (PSD) of the signal. We seek to implement these so called ‘centroid energy’ features (features of the frequency spectrum) for texture discrimination on data from the XY positioning robot, and then combine them to improve texture discrimination using multinomial regression. We also also develop features for surface angle and speed estimation suggested by preliminary investigations on the XY positioning robot (**Evans, M. H.** et al., 2009b), namely the magnitude of whisker deflection and the latency to peak deflection.

5.2 Data collection for angle, speed and texture estimation

A right angled corner stimulus was designed for presenting textures to the whisker on the XY positioning robot (described in Section 3.3 of Chapter 3). This textured object is shown in Figure 5.1. The stimulus consists of an angled strip of aluminium suspended from the XY positioning robot on an pole. Textured sandpapers were affixed to the aluminium surface using double sided adhesive tape.

Compared to the radial distance discrimination experiment (Chapter 4) a smaller range of contact speeds was used to limit any damage that could occur to the whisker from the large stimulus during high velocity impacts. 6mm/s was the lower bound on speed, with an upper bound of \approx 106mm/s, with an interval of \approx 7mm/s, providing 11 different speeds. Surface angle ranged from 10° – 80° , in increments of 10° . When the stimulus was angled at 0° or 90° the contact was equivalent to a point contact along the shaft so was not considered a tip–surface contact for this experiment. Four textures were chosen, three grades of sandpaper (P80, P180, and P600) and a

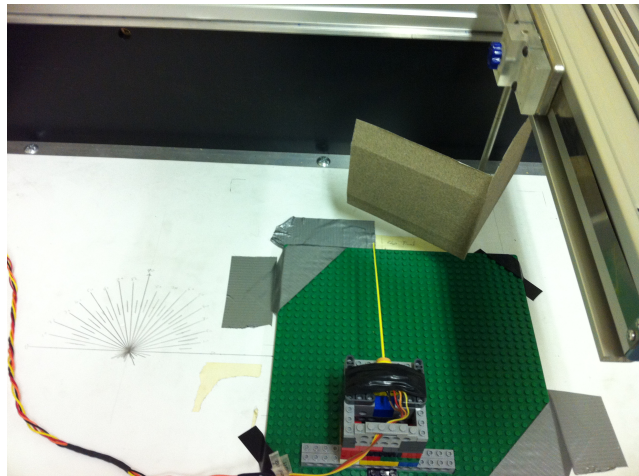


Figure 5.1: Angled corner stimulus mounted on the XY positioning robot. Textured surfaces were fixed to the stimulus and presented the whisker at different angles and speeds

smooth aluminium surface. Eleven speeds, eight angles and four textures results in 352 different combinations. Contact combinations were randomly interleaved during data acquisition to limit any affects of changing whisker properties during the trial.

For each contact combination the whisker was deflected by the robot in both a clockwise and anticlockwise directions (-ve and +ve in x), ensuring that the whisker did not bend over time through repeated unilateral deflections. The experiment was performed twice to generate sufficient data for classification. As for the radial distance experiment (Chapter 4) Minimal impingement (described in Section 2.2.2 of Chapter 2) was implemented by instructing the robot to move an object into the whisker at a given speed until a deflection threshold is crossed, at which point the robot retracts the object as fast as possible (720mm/s). Temporal latency for the loop is ≈ 300 ms from initial contact due to the controller duty cycle. Whisker deflections were processed in the same manner as for the radial distance experiment, with the exception that data was sampled at 4kHz instead of 1kHz to ensure any texture related high frequency vibrations weren't lost. Data from each trial was stored separately. Deflections from the clockwise robot movement trials (-ve in x) were converted so all data samples were equivalent. Trials were ordered into arrays by robot movement direction, contact speed, surface angle and texture. Each

trial was aligned to peak deflection, and shortened to only the 6000ms either side of the peak deflection (1.5s).

5.3 Classifier specification

Data was separated into training and test sets that were each complete data sets of 8 angles, 11 speeds, and 4 textures. Signals were placed in the training or test sets at random from the original data. In each case classifiers were developed on the training sets, and performance was determined on the test set.

5.3.1 Time-domain template based classification

If the temporal pattern of whisker deflections is important for texture discrimination, as has been suggested by the kinetic signature hypothesis (described in Section 2.4.5.2 of Chapter 2) template based classifiers could be successful. Briefly, the kinetic signature hypothesis of texture encoding in rats suggests that cells in the whisker system have been shown to respond strongly and accurately to high velocity whisker deflections (Arabzadeh et al., 2005). It is thought that recording the timing, magnitude, frequency or pattern of these high-velocity ‘stick-slip’ events would allow the rat to encode a surface efficiently (Arabzadeh et al., 2006), as different textures elicit a unique ‘kinetic signature’ in the temporal profile of deflection velocity. In support of this hypothesis Panzeri et al. (2001) and Foffani et al. (2009) found that patterns of spike timing in somatosensory cortex is a better predictor of surface texture than spike number alone.

A template classifier preserves the temporal pattern and order of oscillations in a whisker deflection, allowing the classifier to make use of these events when making a discrimination. Different filtering operations could also reveal which aspects of the signal, for example low versus high frequency oscillations, are most useful in discriminating surface textures or angles.

We have previously shown that this approach can be successfully applied to data collected from a whisking robot, where contact geometry and texture vary together (Sullivan, Mitchinson, Pearson, **Evans, M. H.**, Lepora, Fox, Melhuish, and Prescott, 2011, Section 6.4 of Chapter 6).

A number of different template based classifiers were tested, in an attempt to understand which parameters, proposed by the literature and signal inspection, were most important for successful classification.

First a raw data signal template classifier was implemented, as used for radial distance estimation (Sections 5.3.1 and 4.4.3 of Chapter 4).

As in the radial distance estimation case, an input signal is stored as a template, then compared to new data from the test set. During the test phase, trials were taken at random from the test set as inputs to the classifier. An element-wise sum of squared errors calculation was made between the input I and each template T_i ,

$$e(I, T_i) = \sum_{t=1}^n (I(t) - T_i(t))^2. \quad (5.1)$$

where n is the length of the template in samples. The template with the lowest sum of squared error was determined the winner, and a recording was made in an output array of the estimated speed and radial distance to contact of the input trial.

Different groups of rat primary afferent neurons fire preferentially for long duration deflections (named slowly adapting (SA) cells), or short duration deflections (named rapidly adapting (RA) cells, Gibson and Welker, 1983; Lichtenstein et al., 1990; Stuttgen et al., 2006). We aimed to determine whether applying different filters to the raw signal could reflect this low and high frequency decomposition of the whisker signal, and whether this decomposition can improve classification of angle, speed or texture.

Inspection of the raw data also suggests that filtering the signal may affect classification. As was seen in the case of radial distance and speed estimation (Chapter 4) contact parameters such as

speed or the location of an object affect the gross shape of the whisker deflection.

If information about a surface's orientation affects the data in the same way, then a low pass filtered signal could allow for better angle discrimination. A third-order low pass Butterworth filter with a 20Hz cutoff frequency was used to remove any texture-induced high frequency vibrations from the data. An additional second order infinite impulse response (IIR) notch filter with frequency 30 and bandwidth 20dB was applied to remove the resonant frequency of the whisker from the signal (identified by inspection of the fast Fourier transform (FFT)).

A separate classifier based on high pass filtered signals was also built to reflect the response properties of RA cells. Inspection of the signals also suggested that surface texture affected the high frequency oscillations in the signal. A tenth-order high pass Butterworth filter with a 35Hz cutoff frequency was used to remove any contact-geometry induced low frequency vibrations from the data. As in the low pass filtered case an additional second order IIR notch filter with frequency 30Hz and bandwidth 20dB was applied to remove the resonant frequency of the whisker from the signal, which was still present after applying the high-pass filter.

Some research has shown the pattern and number of high velocity deflections during contact could be used to encode textures (Wolfe et al., 2008), and that neurons responding to these high velocity events have been found in the thalamus (Petersen et al., 2008) and cortex (Arabzadeh et al., 2006) of rats. This so called 'kinetic signature' hypothesis of texture discrimination has proven popular in the neuroscience community. A template classifier using the first or second derivatives of the raw signal as input may be an analogous method to kinetic signature, as classification would be based on the magnitude and pattern of velocity and acceleration events in an incoming signal's similarity to stored signals.

The methodology for both of these classifiers is the same as detailed above for raw signal classification, but with an additional pre-processing step of taking either the first or second derivative of the signal as input to the classifier for a velocity or acceleration based classifier, respectively.

5.3.2 Spectral template based classification

Previous work from our own lab (**Evans, M. H.** et al., 2009a, Section 6.2 of Chapter 6) has shown that a spectral template classifier could be successfully applied to the task of whisker based texture discrimination, and unsuccessfully for radial distance estimation in Chapter 4 of this thesis.

Here a FFT was performed on the filtered data, and stored to compare with the FFT of incoming signals using the method outlined in Chapter 4.3.2.

5.3.3 Feature based classification

Inspection of the data showed that peak deflection magnitude could be used as a feature for speed discrimination under conditions of varying contact angle and texture. Deflection magnitude was taken as the Hall effect sensor output voltage at peak deflection, which is proportional to the bending moment M . Feature f_1 can be defined as,

$$f_1 = \max_t M(t), \quad (5.2)$$

where $M(t)$ is the deflection magnitude varying with time, measured by the Hall effect sensor in volts. Note that $t(f_1) = t(\max_t M(t))$

In previous preliminary work (**Evans, M. H.** et al., 2009b) it was shown that the latency to peak or slope of the initial whisker deflection could be used as a measure of surface angle. To test this idea comprehensively we implemented the same classifier here. Taking the amplitude of deflection f_1 , and the time of peak deflection $t(f_1)$, we can find feature f_2 the slope of deflection,

$$f_2 = \frac{f_1}{t(f_1)}. \quad (5.3)$$

To perform a feature based classification for texture discrimination, centroid energy features such as those described in Hipp et al. (2006) and Fox et al. (2009a) were extracted from the signal. After the data had been IIR notch filtered to remove the resonant frequency the modulation centroid, f_3 , was taken as the frequency with most energy in the DFT (X, see equation eq:FFT) of the signal x after X_{1-5Hz} is set to zero,

$$f_3 = \arg \max \text{ abs}(X_{[6Hz-1kHz]}). \quad (5.4)$$

The modulation energy, f_4 , was defined as the energy of the DFT at the modulation centroid (the magnitude of energy at f_3),

$$f_4 = \max \text{ abs}(X_{[6Hz-1kHz]}). \quad (5.5)$$

Finally a total power feature, f_5 , was defined as the total energy in the FFT below 1kHz,

$$f_5 = \sum_{6Hz}^{1kHz} |X|, \quad (5.6)$$

where FFT(1:5Hz) were set to 0.

In both the contact geometry and frequency case a model was generated of the relationship between each feature and the corresponding contact property with regression, (using the polyfit toolbox in MATLAB <http://bit.ly/polyfitn>). Using simple linear least squares a model is generated that can be used to classify new data. Only three arguments are required for generating the model, a vector of independent variable values, a vector of dependent variable values, and a model specification, namely the degree of the polynomial. A second degree polynomial was chosen as preliminary studies showed it provided good results. The independent variables for contact geometry were features f_1 for contact speed, f_2 for surface angle, f_3 , f_4 and f_5 for surface texture.

An additional combined feature classifier was built to see if combining the texture features f_3 ,

f_4 and f_5 into a single model could improve classification. Polynomial regression was used to develop a model comprising all three texture features, as above. A fourth degree polynomial was chosen as preliminary studies showed it provided good results. After the angle, speed and texture of a test data file is estimated with the model the output is rounded to the nearest integer (using the MATLAB round function) to make a classification.

5.3.4 Stationary naïve Bayes classification

Stationary naïve bayes classification has been successful in both texture discrimination, in determining geometric properties of contacts such as radial distance and speed, and in situations where texture and contact geometry are varied together (Sullivan, Mitchinson, Pearson, **Evans, M. H.**, Lepora, Fox, Melhuish, and Prescott, 2011, described in Section 6.4 of Chapter 6). In each instance the methodology remains principally the same (as described in Section 4.3.5 of Chapter 4).

Previous work (Lepora, Fox, **Evans, M. H.**, Mitchinson, Motiwala, Sullivan, Pearson, Welsby, Pipe, Gurney, and Prescott, 2011) has shown that using the first derivative of a signal can improve classification if the variables to be discriminated have a temporal component. This was also demonstrated in the Chapters of this thesis addressing radial distance estimation (Sections 4.3.5 and 4.4.5 of Chapter 4, respectively). A stationary naïve Bayes classifier was implemented on raw data, a first derivative and second derivative of the data, to see whether information about velocity or acceleration events could improve classification in line with the kinetic signature hypothesis of texture discrimination described in Section 2.4.5.2 of Chapter 2.

5.3.5 Combination of classifiers for full contact parameter estimation

Finally the best classifiers in each condition are combined, performing each part of the classification together on a single input file to determine whether texture classification can be improved

if contact geometry and speed can be taken into account.

5.3.6 A note on the analysis

Confusion matrices, means and standard errors are shown for each classification. In a confusion matrix the output of classification is marked on a grid. Rows in the matrix correspond to the true class of an observation, while columns in the matrix correspond to the predicted class of an observation by a classifier. In this way it is easy to see how often a correct classification is made, and what kind of errors the classifier is making. Perfect classification results in all outputs lying along the diagonal of the grid. Because so many methods are being compared here, the confusion matrices are given as imaged arrays only, and not with the actual values on the grids. This is to give a visual indication of how well each classifier has performed.

Cohen's Kappa κ (Cohen et al., 1960) is given as a summary statistic. Cohen's κ provides a measure of classification accuracy that is scaled for the number of classes involved. For example, in a two choice task a hit rate of 50% is no better than chance, but in a situation where there are 10 possibilities a 50% would be a good result. Formally κ is defined in terms of total accuracy (hit rate or P_O , O for observed value), and chance performance P_E (E for expected value) by,

$$\kappa = \frac{P_O - P_E}{1 - P_E}. \quad (5.7)$$

In this way performance can be compared for each of the contact parameters even though they are over different classification ranges (Forbes, 1995). The value will fall between 0 and 1, with 1 indicating perfect classification and 0 indicating chance performance. Scores below 0.2 are deemed poor classification. In a 2 choice discrimination, where 50% hit rate is chance performance, a κ of 0.5 would be equivalent to a hit rate of 75%.

Cohen's κ is given for each classifier when discriminating speed, angle and texture simultaneously, as well as texture alone. To generate this second value each classifier was trained for each

speed–angle combination, and results of classification in this reduced preparation were added together to give an overall score for texture discrimination independent of contact geometry.

5.4 Results

Results are presented for each classifier in turn for surface angle, speed and texture estimation. The performance is compared by calculating the accuracy and precision of angle, speed and texture classification by the reporting of mean and standard errors for classification. Confusion matrices are given for each classifier.

Typical whisker deflections for each condition are shown in Figure 5.2.

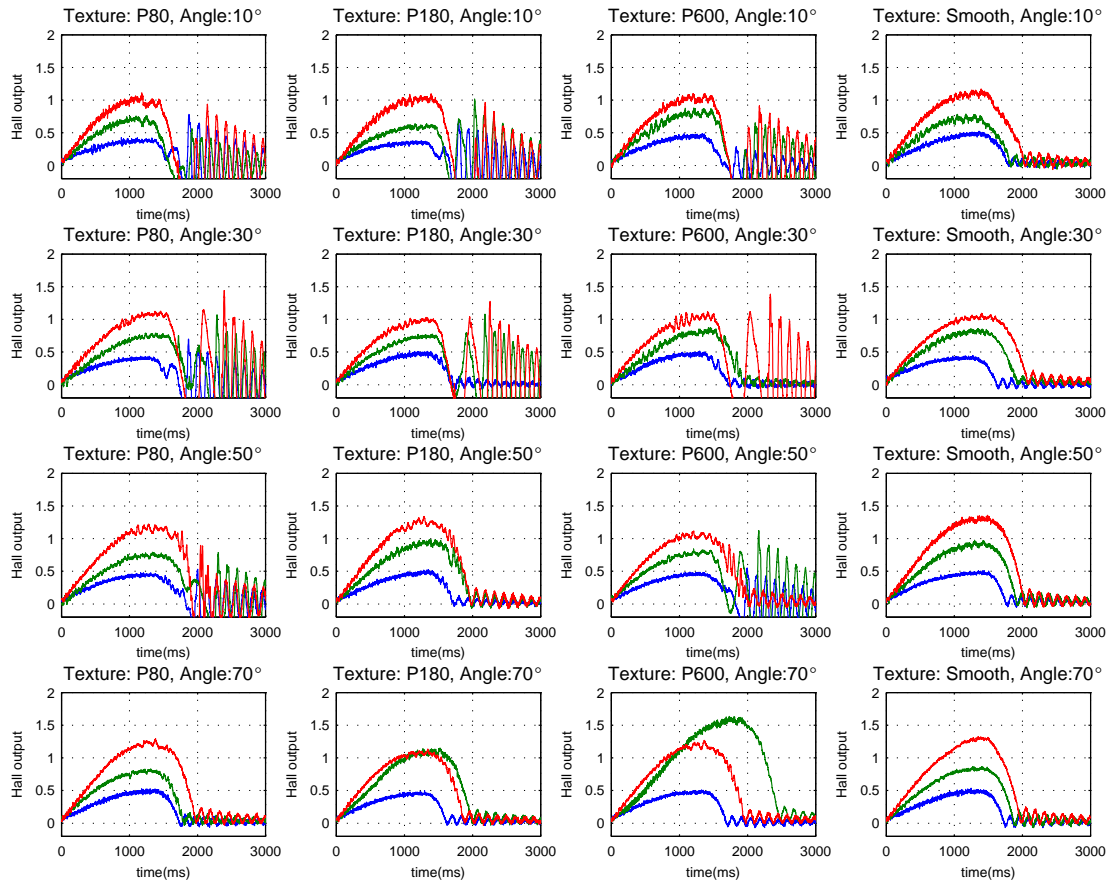


Figure 5.2: Typical whisker deflections from the artificial whisker, for different angles, speeds and textures. Texture varies by column, angle varies by row. Colour indicates contact speed, blue = 36mm/s, green = 72mm/s, red = 108mm/s. Note large differences in the amount of oscillatory ringing in some trials.

5.4.1 Template based classification

Presented here are the results of template based classification of angle, speed and texture. Results are presented, in order, for templates based on low pass filtered signals (Section 5.4.1.2), high pass filtered signals (Section 5.4.1.3), first derivatives of signals (Section 5.4.1.4), and second derivatives of signals (Section 5.4.1.5).

5.4.1.1 Raw signal template classification

Figure 5.3 shows the confusion matrices for simultaneous angle, speed and texture classification using a template classifier on raw data. Cohen's κ for each parameter: Angle = 0.27, Speed = 0.25, Texture = 0.24. Cohen's κ for texture independent of contact geometry = 0.24. Mean and standard errors for classification, when classified simultaneously, are given in table 5.1.

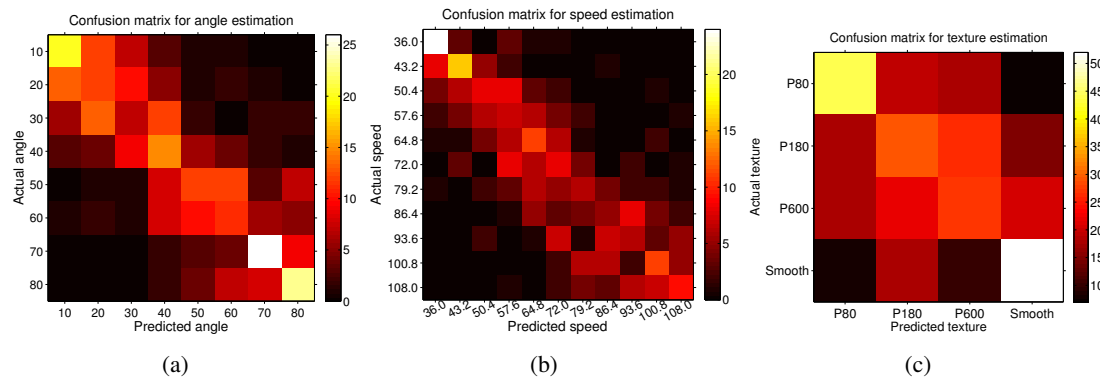


Figure 5.3: Confusion matrices for classification of angle (a), speed (b), and texture (c) with the raw signal template classifier over all contacts. Brightness indicates larger numbers, and better classification

Table 5.1: Mean and standard deviations of classification error, when classified simultaneously, for the raw signal template

	Angle	Speed	Texture
Mean	0.71°	-2.7mm/s	-0.0199
Std Err	15.6°	14.22mm/s	1.23

5.4.1.2 Low pass filtered template classification

Figure 5.4 shows the confusion matrices for simultaneous angle, speed and texture classification using a template classifier on low pass filtered data. Cohen's κ for each parameter: Angle = 0.30, Speed = 0.23, Texture = 0.21. Cohen's κ for texture independent of contact geometry = 0.24. Mean and standard errors for classification, when classified simultaneously, are given in table 5.2.

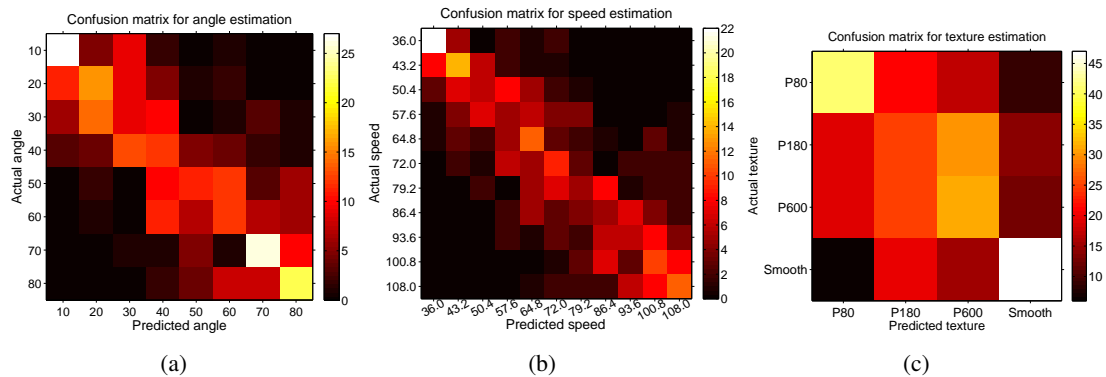


Figure 5.4: Confusion matrices for classification of angle (a), speed (b), and texture (c) with the low pass filtered signal template classifier over all contacts. Brightness indicates larger numbers, and better classification

Table 5.2: Mean and standard deviations of classification error, when classified simultaneously, for the low pass filter template

	Angle	Speed	Texture
Mean	0.1°	-0.61mm/s	-0.01
Std Err	14.8°	14.12mm/s	1.24

5.4.1.3 High pass filtered template classification

Figure 5.5 shows the confusion matrices for simultaneous angle, speed and texture classification using a template classifier on low pass filtered data. Cohen's κ for each parameter: Angle = 0.25, Speed = 0.19, Texture = 0.30. Cohen's κ for texture independent of contact geometry = 0.16. Mean and standard errors for classification, when classified simultaneously, are given in table 5.3.

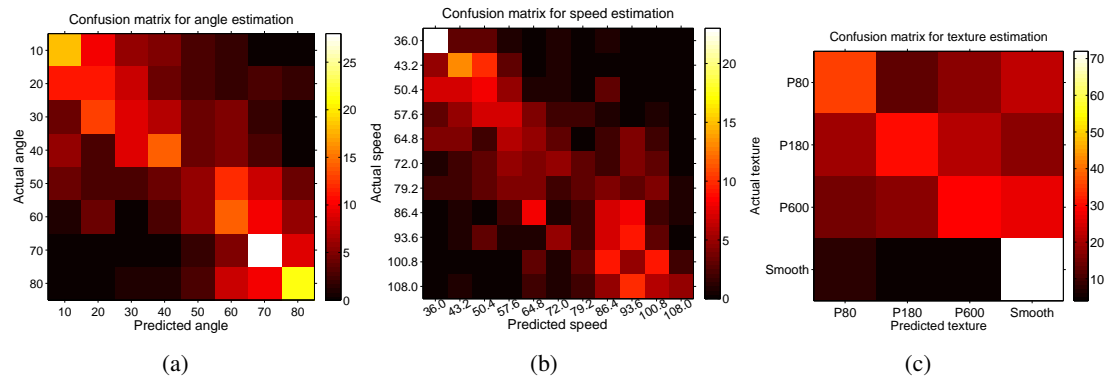


Figure 5.5: Confusion matrices for classification of angle (a), speed (b), and texture (c) with the high pass filtered signal template classifier over all contacts. Brightness indicates larger numbers, and better classification

Table 5.3: Mean and standard deviations of classification error, when classified simultaneously, for the high pass filter template

	Angle	Speed	Texture
Mean	1.9 °	-4.18mm/s	-0.28
Std Err	17.9°	16.85mm/s	1.27

5.4.1.4 First derivative template classification

Figure 5.6 shows the confusion matrices for simultaneous angle, speed and texture classification using a template classifier based on the first derivative of raw data. Cohen's κ for each parameter: Angle = 0.15, Speed = 0.08, Texture = 0.21. Cohen's κ for texture independent of contact geometry = 0.11. Mean and standard errors for classification, when classified simultaneously, are given in table 5.4.

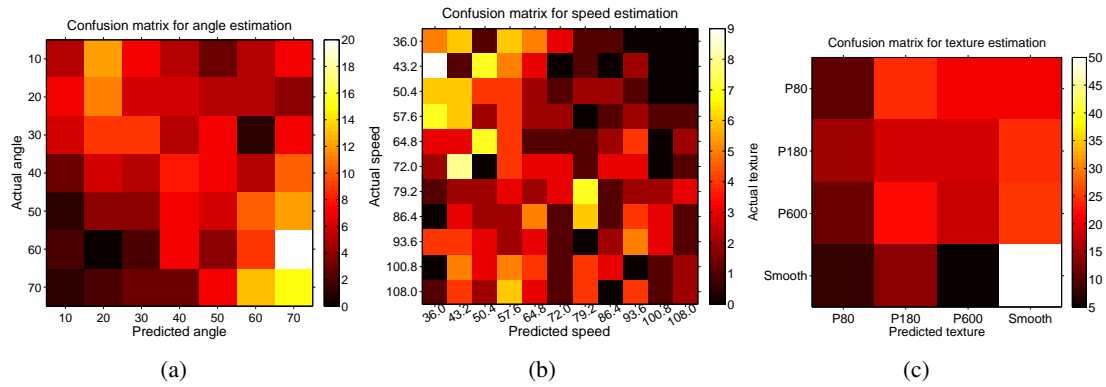


Figure 5.6: Confusion matrices for classification of angle (a), speed (b), and texture (c) with the first derivative template classifier over all contacts. Brightness indicates larger numbers, and better classification

Table 5.4: Mean and standard deviations of classification error, when classified simultaneously, for the first derivative template

	Angle	Speed	Texture
Mean	-1.19°	-5.5mm/s	0.33
Std Err	20.2°	23.9mm/s	1.35

5.4.1.5 Second derivative template classification

Figure 5.6 shows the confusion matrices for simultaneous angle, speed and texture classification using a template classifier based on the second derivative of raw data. Cohen's κ for each parameter: Angle = 0.07, Speed = 0.04, Texture = 0. Cohen's κ for texture independent of contact geometry = 0.05. Mean and standard errors for classification, when classified simultaneously, are given in table 5.5.

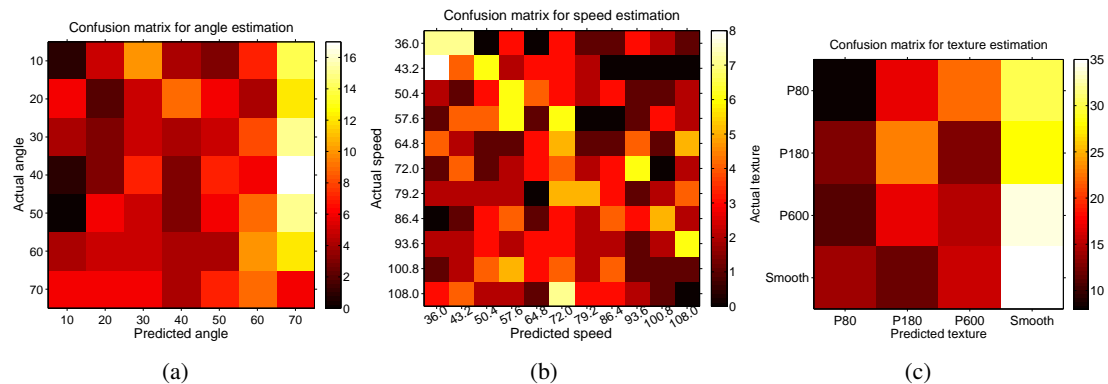


Figure 5.7: Confusion matrices for classification of angle (a), speed (b), and texture (c) with the second derivative template classifier over all contacts. Brightness indicates larger numbers, and better classification

Table 5.5: Mean and standard deviations of classification error, when classified simultaneously, for the second derivative template

	Angle	Speed	Texture
Mean	21.3°	-3.99mm/s	0.70
Std Err	25.6°	29.5mm/s	1.51

5.4.1.6 Spectral template based classification

Figure 5.8 shows the confusion matrices for simultaneous angle, speed and texture classification using a template classifier on low pass filtered data. Cohen's κ for each parameter: Angle = 0.44, Speed = 0.14, Texture = 0.46. Cohen's κ for texture independent of contact geometry = 0.42. Mean and standard errors for classification are given in table 5.6.

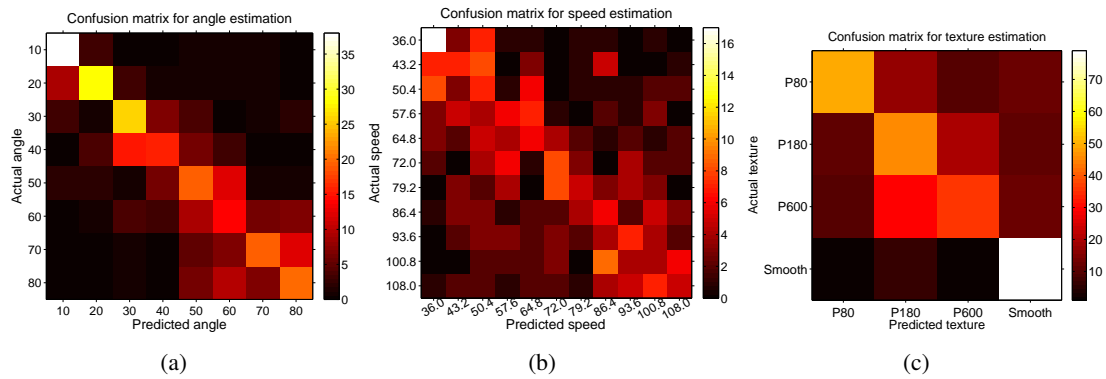


Figure 5.8: Confusion matrix for classification of texture with a spectral template based classification. Brightness indicates larger numbers, and better classification.

Table 5.6: Mean and standard deviations of classification error, when classified simultaneously, for the spectral template classifier

	Angle	Speed	Texture
Mean	-1.08°	-2.78mm/s	0.14
Std Err	13.8°	22.4mm/s	1.00

5.4.2 Feature based classification

Figure 5.9 shows the confusion matrices for feature based speed and angle classification using features f_1 (magnitude of deflection), f_2 (slope of deflection), and texture classification using features f_3 (modulation centroid), f_4 (centroid energy) and f_5 (total energy). Cohen's κ for each parameter; angle = 0.11, speed = 0.43, texture (f_3) = 0.06, texture (f_4) = 0.03, texture (f_5) = 0.15. Cohen's κ for each parameter independent of each other; angle = 0.3, speed = 0.25, texture (f_3) = 0.08, texture (f_4) = 0.21, texture (f_5) = 0.27.

Table 5.7 shows the mean and standard error for classification with each feature, when classified simultaneously.

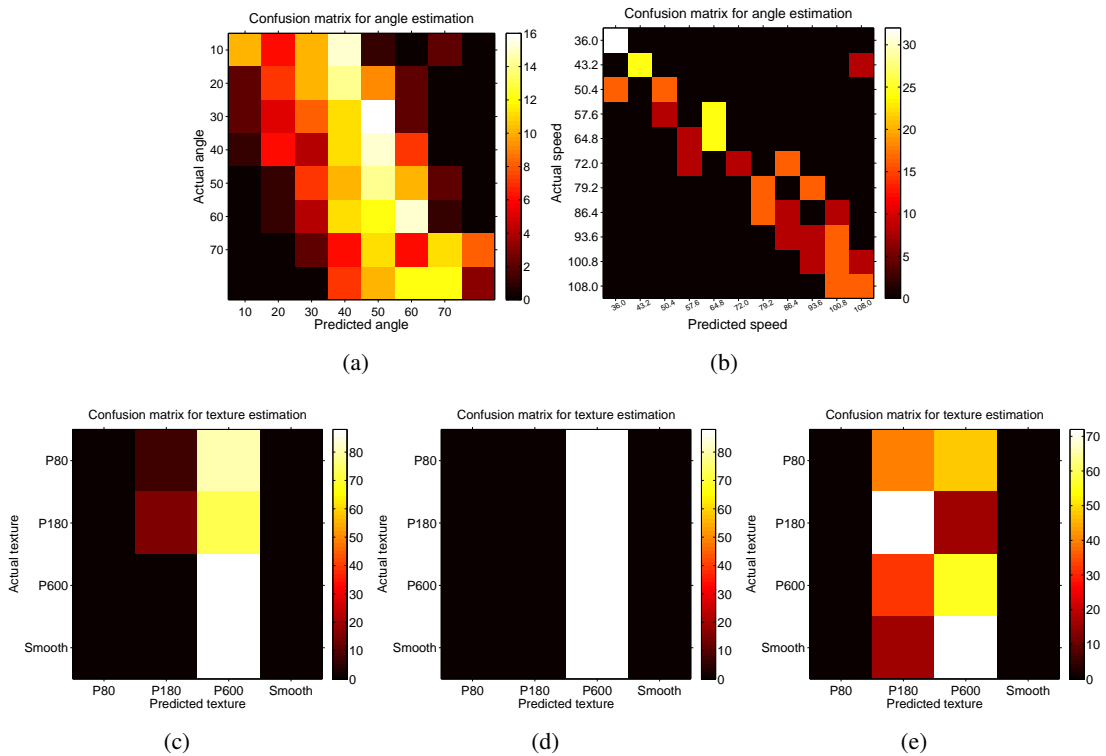


Figure 5.9: Confusion matrices for classification with the feature based classifier; of angle with f_2 (a), speed with f_1 (b), and texture with f_3 (c), f_4 (d) and f_5 (e). Brightness indicates larger numbers, and better classification

Table 5.7: Mean and standard deviations of classification error for feature based classification, for all five features when classified simultaneously.

	f_1	f_2	f_3	f_4	f_5
Mean	1.80mm/s	0.17°	0.43	-0.07	0.05
Std Err	12.12mm/s	18.6°	1.10	1.22	1.09

Figure 5.10 shows histograms of classification error, when classified simultaneously, for each of the five features.

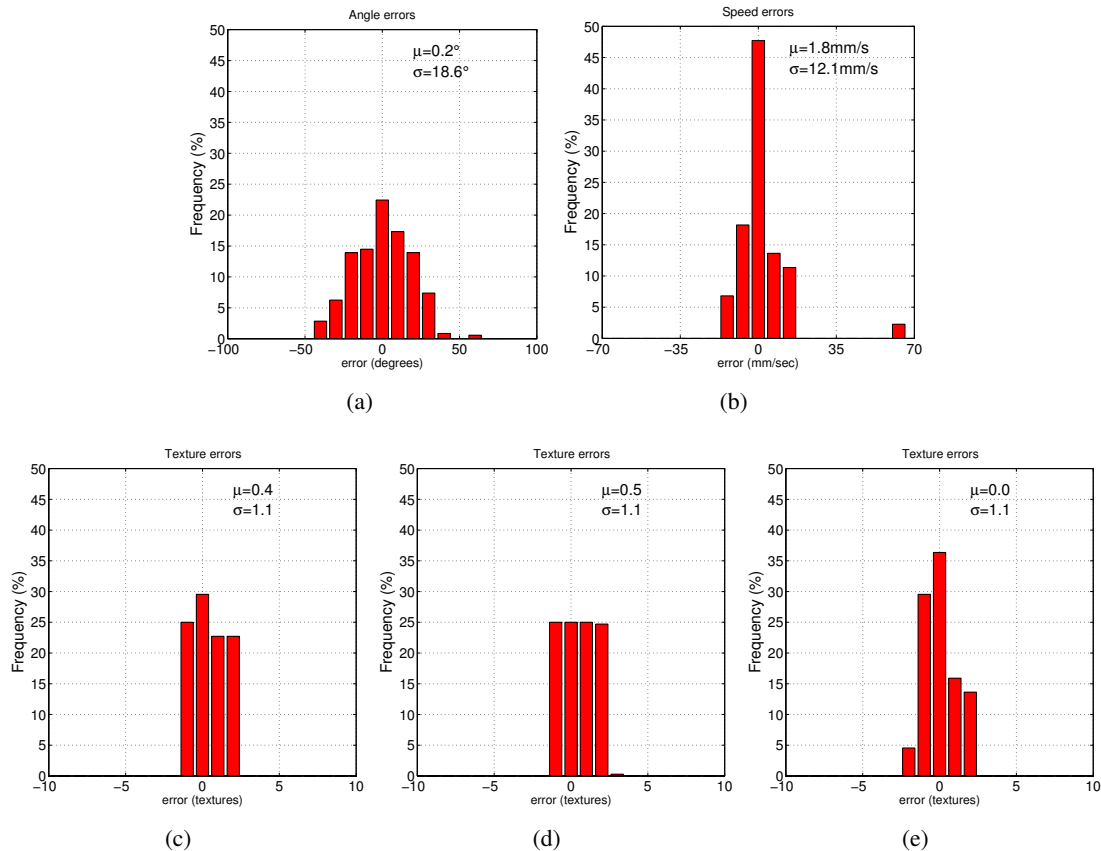


Figure 5.10: Histograms for classification error with the feature based classifier; of angle with f_2 (a), speed with f_1 (b), and texture with f_3 (c), f_4 (d) and f_5 (e).

5.4.2.1 Combining features with multinomial regression

Figure 5.11 shows the confusion matrix for texture classification using the multinomial feature classifier. Mean error was -0.09, standard error was 0.97. Cohen's κ for texture discrimination was 0.12.

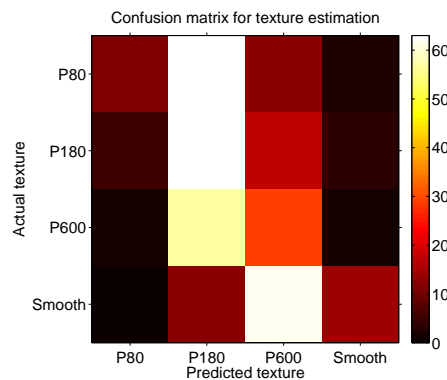


Figure 5.11: Confusion matrix for classification of texture with the multinomial feature based classifier, using features f_3 , f_4 and f_5 over all contacts. Brightness indicates larger numbers, and better classification

5.4.3 Stationary naïve Bayes based classification

Figure 5.12 shows the confusion matrices for simultaneous angle, speed and texture classification using a naïve Bayes classifier on filtered raw data. Cohen's κ for each parameter: Angle = 0.18, Speed = 0.08, Texture = 0.11. Cohen's κ for texture independent of contact geometry = 0.22. Mean and standard errors for classification, when classified simultaneously, are given in table 5.8.

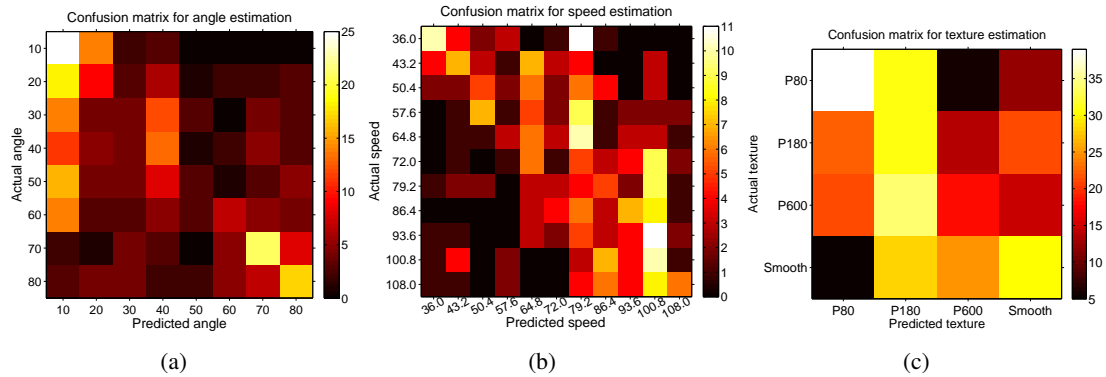


Figure 5.12: Confusion matrices for classification of angle (a), speed (b), and texture (c) with the naïve Bayes classifier over all contacts. Brightness indicates larger numbers, and better classification

Table 5.8: Mean and standard deviations of classification error, when classified simultaneously, for the spectral template classifier

	Angle	Speed	Texture
Mean	-6.6°	-5.0mm/s	0.13
Std Err	24.5°	22.6mm/s	1.3

5.4.3.1 Naïve Bayes based classification using velocity signals

Figure 5.13 shows the confusion matrices for simultaneous angle, speed and texture classification using a template classifier on low pass filtered data. Cohen's κ for each parameter: Angle = 0.39, Speed = 0.18, Texture = 0.38. Cohen's κ for texture independent of contact geometry = 0.37. Mean and standard errors for classification, when classified simultaneously, are given in table 5.9

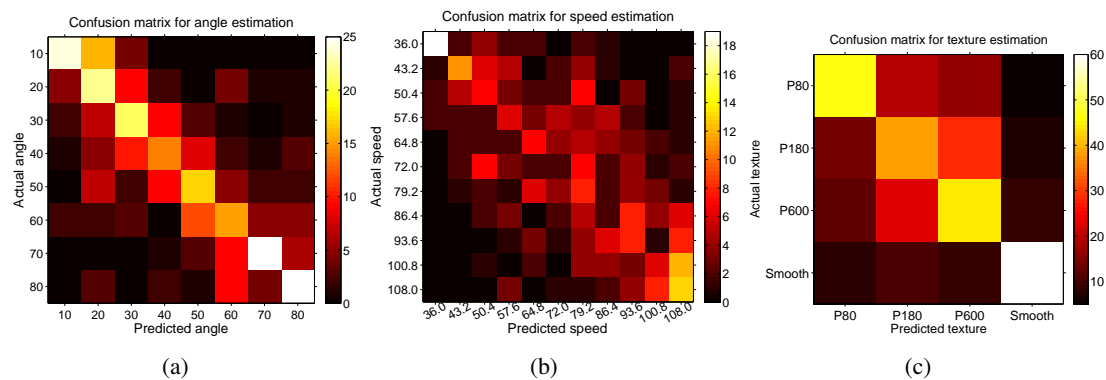


Figure 5.13: Confusion matrices for classification of angle (a), speed (b), and texture (c) with the naïve Bayes classifier using velocity signals, over all contacts. Brightness indicates larger numbers, and better classification

Table 5.9: Mean and standard deviations of classification error, when classified simultaneously, for the naïve Bayes classifier using velocity signals

	Angle	Speed	Texture
Mean	-0.9°	3.2mm/s	0.01
Std Err	15.5°	18.8mm/s	1.08

5.4.3.2 Naïve Bayes based classification using acceleration signals

Figure 5.14 shows the confusion matrices for simultaneous angle, speed and texture classification using a template classifier on low pass filtered data. Cohen's κ for each parameter: Angle = 0.25; Speed = 0.12; Texture = 0.27. Cohen's κ for texture independent of contact geometry = 0.28. Mean and standard errors for classification, when classified simultaneously, are given in table 5.10

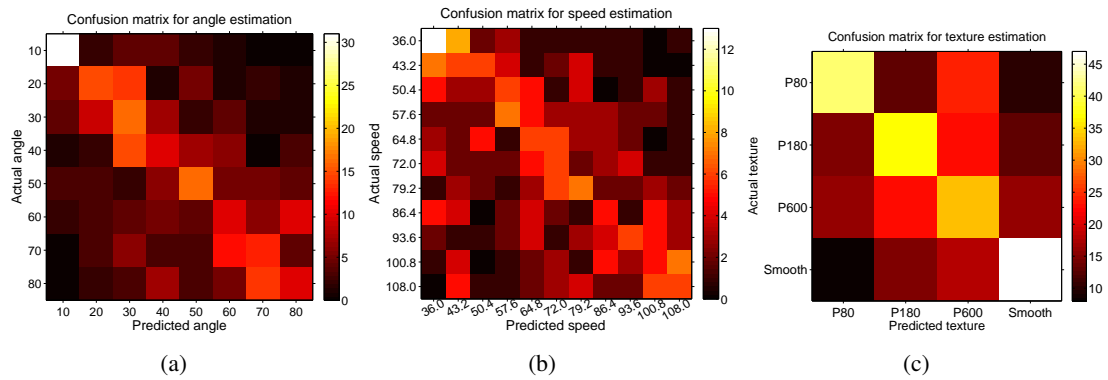


Figure 5.14: Confusion matrices for classification of angle (a), speed (b), and texture (c) with the naïve Bayes classifier using acceleration signals, over all contacts. Brightness indicates larger numbers, and better classification

Table 5.10: Mean and standard deviations of classification error, when classified simultaneously, for the naïve Bayes classifier using acceleration signals

	Angle	Speed	Texture
Mean	-2.0°	-2.64mm/s	0.04
Std Err	19.9°	24.45mm/s	1.24

5.4.4 Comparing the classifiers

Figure 5.15 compares Cohen's κ for the best version of each method, namely the low pass filtered template, the frequency template, a ‘best case’ feature classifier (f_1 for speed, f_2 for angle and f_5 for texture), and the velocity based naïve Bayes classifier. Mean and standard errors for each method is compared in Figure 5.16.

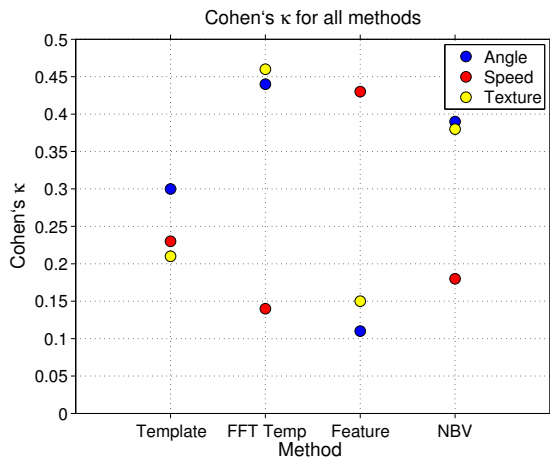


Figure 5.15: Cohen's κ for the best version of each method for angle (blue), speed (red) and texture (yellow). Template: Low pass filtered template; FFT Temp: the frequency template; Feat: a ‘best case’ feature classifier (f_1 for speed, f_2 for angle and f_5 for texture); NBV: velocity based naïve Bayes classifier.

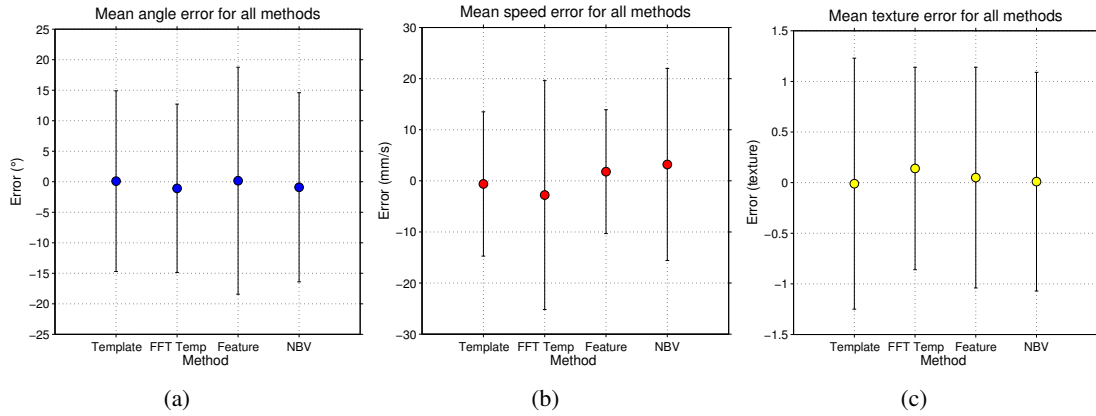


Figure 5.16: Mean and standard error of classification for the best version of each method for angle (a), speed (b) and texture (c). Template: Low pass filtered template; FFT Temp: the frequency template; Feat: a ‘best case’ feature classifier (f_1 for speed, f_2 for angle and f_5 for texture); NBV: velocity based naïve Bayes classifier.

5.4.5 Combining the classifiers

The best classifiers were combined into a single system to see whether taking contact speed or surface angle could improve classification. The classifiers chosen were a feature based classifier

for speed, and a naïve Bayes of velocity classifier for angle and texture discrimination.

For a given input file the speed of contact is determined with the feature based classifier (amplitude of deflection, f_1). This contact speed is then used as an index into the array of stored log likelihoods for naïve Bayes classification. With classification of speed accounted for the input signal is then compared to 32 stored likelihoods, instead of 352 for the whole set, to determine the angle and texture of the surface. Finally the angle of the surface is used, along with speed, as indices into the array of stored likelihoods. This leaves a 4 way texture classification.

Figure 5.17 shows the confusion matrices for simultaneous angle and texture classification using the combined feature and naïve Bayes classifier. Results for speed classification are not shown as they are identical to those shown in Figure 5.9 (b) of Section 5.4.2. Cohen's κ for each parameter using the combined classifier was: Speed = 0.43; Angle = 0.26; Texture (speed fixed) = 0.18; Texture (speed and angle fixed) = 0.18.

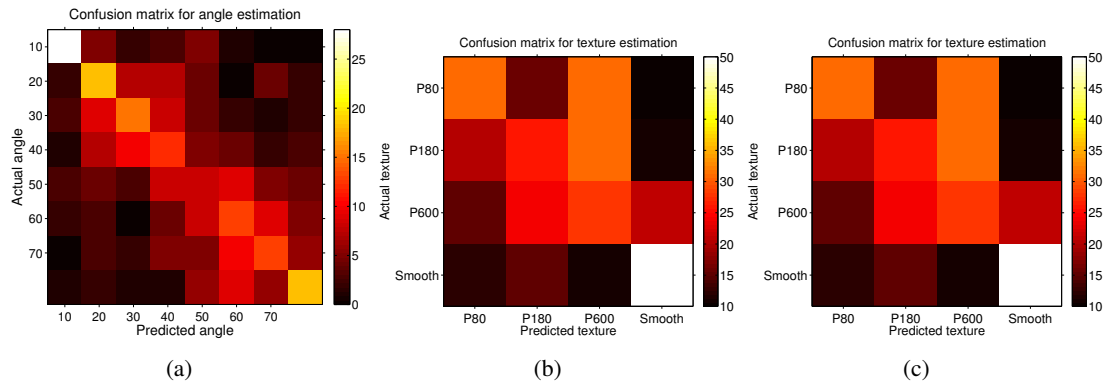


Figure 5.17: Confusion matrices for classification with the combined classifier; of angle with fixed speed (a), of texture with fixed speed (b), and of texture with fixed speed and angle (c) . Brightness indicates larger numbers, and better classification

Mean and standard error for classification of each variable is given in Table 5.11.

Table 5.11: Mean and standard deviations of classification error for the combined feature and naïve Bayes classifier

	Speed	Angle	Texture 1	Texture 2
Mean	1.8mm/s	-0.5°	0.09	0.09
Std Err	12.12mm/s	20.1°	1.31	1.31

5.5 Discussion

We have shown that established and novel classifiers can distinguish surface angle and texture under conditions of unknown speed, with varying degrees of success. Classification results vary a great deal across the different methods, with most classifiers performing better for some parameters than for others. No method performed well across all conditions.

The best classifier for angle estimation was spectral templates, followed by velocity based stationary naïve Bayes. The same spectral template and naïve Bayes methods were also most successful in texture discrimination. Naïve Bayes classification has proven to be successful at texture discrimination on a number of whiskered robots (work described in Chapter 6), therefore it is no surprise that it is successful here. Speed classification was most accurate with the feature based classifier, with all other methods performing poorly. Again this may be expected in light of the success had with feature based speed discrimination in Chapter 4. This split in classifier success between different methods for different parameters may indicate that the salient features in the signals for texture and angle vary together, while speed discrimination is somehow orthogonal. More work needs to be done develop a clearer understanding of the way surface angles and textures, and contact speeds affect whisker deflections, and how these effects interact.

When inspecting the raw data, different surface angles only subtly change the shape of the whisker deflection. It may not be surprising therefore that the a feature based method was not successful for angle estimation. Using the first and second derivatives did not improve template based classification, though stationary naïve Bayes classification is improved by taking

derivatives. In the case of radial distance classification (Chapter 4) it was shown that naïve Bayes classification is improved to be comparable to template based classification if a temporal derivative is taken during pre-processing. It was proposed that taking a derivative provided the classifier with important temporal information that is unavailable when considering each data sample independently. The same operation may be resulting in removing some of the information about the magnitude of deflection which is important for discrimination with the raw signal template based classifier.

Including a speed discrimination step (Section 5.4.5) did not improve angle or texture discrimination, which is perhaps surprising. In addition, mixed results were achieved when the classifying texture independently of contact speed and surface angle. Here five classifiers improved their performance when classifying texture independently of the other parameters (Low pass filtered templates, second derivative templates, raw-signal stationary naïve Bayes, and feature based classification with features f_4 and f_5), while two classifiers performed worse (High pass filtered templates, first derivative templates) and the other methods performed about the same as in the 3-parameter simultaneous classification. In many of these results however Cohen's κ remains below 0.2, and is a poor classification (0 is chance performance), indicating that the features and classifiers presented here are not succeeding in classifying the data. In previous studies it has been shown that information about the whisker-object contact geometry can improve whisker sensing (work reviewed in Section 2.4.5 of Chapter 2). It is difficult to determine why this has not been the case in the present experiment.

It may be that better classifiers could be built, or more successful features could be extracted. In previous studies a Gaussian classifier was used for feature based texture discrimination (Fox et al., 2009a, described in Section 2.4.5 of Chapter 2). This kind of classifier may be more effective at combining information from a number of features, or for discriminating properties that interact. In the future we hope to pursue more robust classifiers, and more powerful classifiers for feature combination. In addition, larger data sets may be useful for training classifiers

to be robust to small within-trial variations. Inspection of the raw signals in Figure 5.2 shows oscillatory ringing after contact on some trials but not others. This ringing does not seem to be associated with a particular contact parameter, but may be due to the whisker tip interacting with a surface uniquely on different trials. Collecting more example data could alleviate these problems.

Another reason for poor angle discrimination performance could be that the whisker used in this experiment was too stiff. A stiff whisker keeps its shape during deflection, and the tip of the whisker remains in contact with the surface throughout. If the whisker were less stiff the tip would bend during contact, causing the radial distance along the whisker to become shorter. The rate of this shortening could then be used to determine the angle of the surface. It may also be the case that surface angle is too difficult to discriminate with a single whisker, and is one of the reasons why rodents have dozens of whiskers. Tracking the timing of contacts across the array would be a useful metric of surface angle or shape. Multiple copies of similar signals may also be enough to reduce common noise to the point that angle discrimination is possible on a single whisker basis. Moving forward we look towards multi-whisker classifiers for surface angle discrimination on a mobile robot (Chapter 6).

Contact duration in this experiment is quite short (\approx 300ms), so any effect caused by the surface do not have much time to take effect. Contacts in the rat are much shorter (tens of ms), but biological whiskers are also much smaller and it may be that contact duration needs to scale in proportion to whisker size for effective sensing. In Chapter 6 the BIOTACT G1 robot (described in Section 3.4 of Chapter 3) is used to evaluate the effect of different biologically inspired whisker movement strategies on sensing. A future extension of this work may look to address the optimal duration for a whisker contact for good classification performance.

Another parameter where scale could be important is texture discrimination. Inspection of the confusion matrices shows that discrimination between rough and smooth surfaces is fairly robust in the present analysis but discrimination between different sandpapers is less successful. This

could be due to a number of factors such as contact duration, and the effect movement speed and surface angle is having on the signal. However scale could be a factor again. Deflection signals transduced by a whisker from the surface texture will reflect the way the whisker tip interacted with the object. Textures of different coarseness will have bumps along their surface of different scale. This is how sandpapers are graded, for example P180 sandpaper has mean grain size of 63–90 μm , and P80 has a mean grain size of 180–212 μm (Orvis and Grissino-Mayer, 2002). If the tip of the whisker is smaller than the grain of a surface, the whisker will catch on the bump before slipping and ringing to the next bump. If the tip of the whisker is larger than the grain of a surface, the whisker will slide over the bump. The number and magnitude of these slips is transduced to the whisker base through vibration, and these vibrations can be used to determine the texture of the surface. If the grain of different surfaces are all smaller than the whisker tip they will be difficult to discriminate. The same could be said for different surfaces where the grain is always larger than the whisker tip. In this experiment the surface coarseness may not be optimally tuned to the sensitivities of the whisker. This is a consideration that we could pursue in the future.

Each parameter is classified best by a different classifier, which is interesting. This could be for a number of reasons. Naïve Bayes performs well in the texture discrimination, a task it has proven excellent at in the past (Lepora, Pearson, Mitchinson, **Evans, M. H.**, Fox, Pipe, Gurney, and Prescott, 2010a). When implementing the naïve Bayes classifier the likelihoods are generated from amplitude histograms of the data, and each sample is treated as independent. In this way the temporal structure of the data is lost. Texture classification may not be reliant upon the temporal structure or pattern of the data, as had been suggested by the ‘kinetic signature’ hypothesis described earlier. However, the temporal information may be of great importance for determining the speed of contact, as it is the duration of contact that is most clearly affected by changing the contact speed (this was demonstrated in Chapter 4). As a result the naïve assumption of sample independence may underly the Bayesian classifier’s poor classification of speed in this experiment. An important development of this work would involve finding

an appropriate method of including the temporal structure of the data in the likelihoods for classification with Bayes rule. One method is to generate two likelihoods, one an amplitude histogram as described in this thesis, and the other a normalised template. The classifier could then use the joint likelihood to combine both in the classification.

Contact speed can be classified very effectively using a feature based classifier, again a result that has been shown before (**Evans, M. H.** et al., 2010a, Chapter 4 of this thesis). As all contacts are at the tip of the whisker the maximum amplitude of deflection is a good predictor of contact speed. Interestingly this is a different feature than was found in the radial distance estimation case. It is unclear why the duration of contact does not reliably increase with contact speed as it does in the radial distance case. It may be due to the shape of the object, causing contacts over larger regions of the whisker as speed increases. More work needs to be done on this front, for example through high speed videography of the whisker during contact to assess how the whisker tip interacts with the object. More thorough work of this kind may determine which aspects of the signal are due to the contact parameters, and which are trial to trial noise. This would allow more appropriate filtering to be applied to the signals before classification, and would guide the amount of training data that is appropriate for capturing this variability. It may be the case that the amount of training data used in this experiment was not sufficient, which would have had a detrimental effect on some of the classifiers. The naïve Bayes classifier is well suited to being trained on large data sets, as additional information is simply added to the likelihood function. Training the template classifiers with more data is more problematic as averaging over templates ends up blurring them, reducing their accuracy. This effect is demonstrated on data from the BIOTACT G1 sensor in the next Chapter. A potential solution is to store all trials in the training set as additional template, with more than one template stored for each parameter combination. The classification could then be based on a winner-takes-all operation as in the present experiment, or by first averaging over the scores on each pool of templates for a given parameter combination. This would increase the computational overhead at run time but might improve classification.

In the combined classifier case, using the feature based method for speed discrimination to reduce the number of likelihoods that are used in a naïve Bayes classifier does not improve classification. It is unclear why this is the case. For situations where a number of parameters need to be classified simultaneously a holistic approach seems to be best. Complementary classifiers could be used, with each reporting its own belief of a parameter's identity. A separate observer may then effectively weight the report by a classifier by the accuracy of that observation. Such ‘mixture-of-experts’ methods have been used extensively in other tasks.

We have seen that though contact speed can be reliably discriminated from this dataset, this information is not useful for improving texture discrimination. In the case of radial distance estimation (Chapter 4), varying the speed of contact had a predictable effect on the whisker deflections. The effect of contact speed on measures of radial distance (the amplitude of deflection) could also be predicted, and classification of contact speed could improve radial distance estimation. In the case of angle and texture discrimination, presented in this and the previous chapter, the effect of contact speed on the signal can be predicted, but its effect on measures of the other parameters cannot. At this stage we still do not have a good enough understanding of how surface angle and texture affect whisker deflections to predict how variable contact speed will affect them. In the future we hope to develop more reliable features for surface angle and texture to improve classification when groups of parameters change concurrently.

Though the results presented in this chapter do not directly support the finding that knowledge of whisker-contact geometry and speed can improve sensing (described in Section 2.4.5 of Chapter 2), there are a number of contributing factors that suggest that these results do not disprove them either. The nature of whisker-object interaction may be more complex than had been anticipated, and additional work needs to be done to uncover the underlying principles of this interaction.

One way of perhaps having a clearer picture of classifier performance in ordered classifications, such as those presented here, is to use a weighted Cohen's κ statistic (Cohen, 1968). Here miss-

classifications are weighted by their distance from the true value instead of being simply marked as incorrect. The classifier essentially is ‘rewarded’ for making small errors over larger ones. A clearer measure of each classifier’s performance may then be given, though the relative ranking of the methods themselves, for example in Figure 5.15, may not change.

It may be that trying to classify so many parameters effectively and at the same time may be too difficult a task for one whisker making a single brief contact. This may be the limit of single whisker sensing, and improvements would no doubt be gained through pooling of information across whiskers. Stationary naïve Bayes classification, as a probabilistic method, is ideally suited to optimally combining information from a number of sources, as has been demonstrated before in whisker based ‘novelty’ detection (Lepora, Pearson, Mitchinson, **Evans, M. H.**, Fox, Pipe, Gurney, and Prescott, 2010a). In the next Chapter (Section 6.5) we develop a multi-whisker template classifier for surface angle detection on a mobile robot. On our mobile robot CrunchBot (described in Section ?? of Chapter 3) different groups of whiskers make contact with the walls of an arena depending on the angle of approach to the surface. By utilising a multi-whisker template based classifier it is possible to combine whisker identity, contact timing and deflection magnitude information simultaneously to improve classification. Going forward we hope to develop classifiers within the tactile framework (Section 2.5 of Chapter 1) that can utilise more sources of information to perform more complex tactile discriminations.

In the next Chapter we apply some of the classifiers that have been presented in the preceding Chapters to data collected on a range of robots developed to address specific problems within whisker based tactile sensing. These robots (described in Chapter 3) provide the next step in the development of these classifiers, by testing their applicability to different whisker motion protocols, real-time operation, and reliability for a tactile simultaneous localisation and mapping (SLAM) task.

Chapter 6

Classification with embedded models on whiskered robots

6.1 Introduction

Models are important tools for understanding complex systems. Models provide a level of abstraction from the complexities of the system of interest. Hypotheses can be tested, and experiments can be conducted in ways that are not possible in the intact system. By building computational models we make our assumptions explicit, and gaps in our understanding can be exposed. However software models can only be as accurate as the simulation environment they are developed in. Carefully collected data from a robot can be used to test a model more thoroughly, as the richness of real-world data is difficult to simulate, especially in the domain of whisker sensing.

Embedding a computational model on a mobile robot is the ultimate test of robustness, accuracy and suitability to a task. The classifiers discussed in the literature review (Section 2.4 of Chapter 2) were all successful in their own experimental conditions, but it is difficult to compare them

fairly. The whiskers, sensors and robot platforms are all different, and they were each developed with specific goals in mind.

In the preceding two Chapters an XY positioning robot (Section 3.3 of Chapter 3) was used to develop and test a number of classifiers for whisker based tactile discriminations, to fulfil the criteria required in the tactile framework (Section 2.5 of Chapter 2). In Chapter 4 classifiers were built, tested and compared for estimating the radial distance to contact of an object along a whisker, under conditions of variable contact speed. In Chapter 5 classifiers were built, tested and compared for estimating the angle and texture of a surface that has been contacted by a whisker, under conditions of variable contact speed.

In this Chapter we apply some of these classifiers to other, less restricted robots developed in a collaboration between the Active Touch Laboratory at the University of Sheffield (ATL@S) and the Bristol Robotics Laboratory (BRL). These robots are detailed in Chapter 3. These robots test the classifiers in different ways, and address different questions about whisker based tactile discrimination. SCRATCHbot is a biomimetic whiskered robot built to integrate state of the art computational models on a system capable of accurate whisker control (Pearson et al. (2010), Section 3.2 of Chapter 3). In this Chapter data from SCRATCHbot is used to verify that features developed on the XY positioning robot for radial distance estimation are present in data generated on a whisking robot (Section 6.3). A SCRATCHbot whisker was fixed to a Roomba vacuum cleaner robot to test texture classifiers on real-world floor textures (Section 6.2). The BIOTACT G1 robot was developed with industrial whisker sensing applications in mind (Sullivan, Mitchinson, Pearson, **Evans, M. H.**, Lepora, Fox, Melhuish, and Prescott, 2011, Section 3.4 of Chapter 3). In this Chapter data is collected on the BIOTACT G1 robot to explore the effect biomimetic whisking strategies have on texture and contact geometry discrimination (6.4).

In most instances the classifiers are applied to data collected on the different robots. In the case of CrunchBot (Section 3.5 of Chapter 3) the classifiers are first trained off line on data collected on the robot, but are then implemented in real-time on board the robot for a series of localisation

and mapping tasks (Section 6.5,Fox, **Evans, M. H.**, Lepora, Pearson, Ham, and Prescott, 2011; Fox, **Evans, M. H.**, Pearson, and Prescott, 2012).

6.2 Floor texture discrimination on a Roomba: (Evans, M. H. et al., 2009a)

To explore how texture discrimination is affected when whisker–surface movement is unconstrained an artificial whisker was attached to an iRobot Roomba vacuum cleaner robot (www.irobot.com) and whisker deflections were recorded while the robot moved across four floor surfaces. The robot was commanded to rotate clockwise or anti-clockwise for 16 seconds, or a pre-programmed ‘spot’ cleaning behaviour was executed, which varied from run to run. This provided a range of movement patterns that could be compared. The floor surfaces encountered, and typical data recorded from the surfaces are shown in Figs. 6.1 and 6.2 respectively.

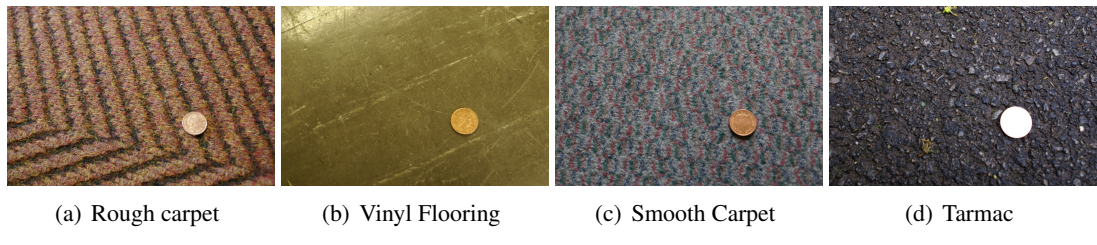


Figure 6.1: Photos of all the surfaces, with 1p coins for scale.

6.2.1 Analysis

For each behavioural condition the Labjack sampled data while the robot moved in a specific direction for 16 seconds. Each 16-second trial was then repeated 4 times for each of the behavioural conditions, and 4 times for the spot command. Data from the Labjack is passed to the computer in packets of 160 recordings each (at 2kHz. 0.08s, or 200 packets per 16 second trial) to ensure seamless acquisition of the data with no bottleneck at the Labjack. When the

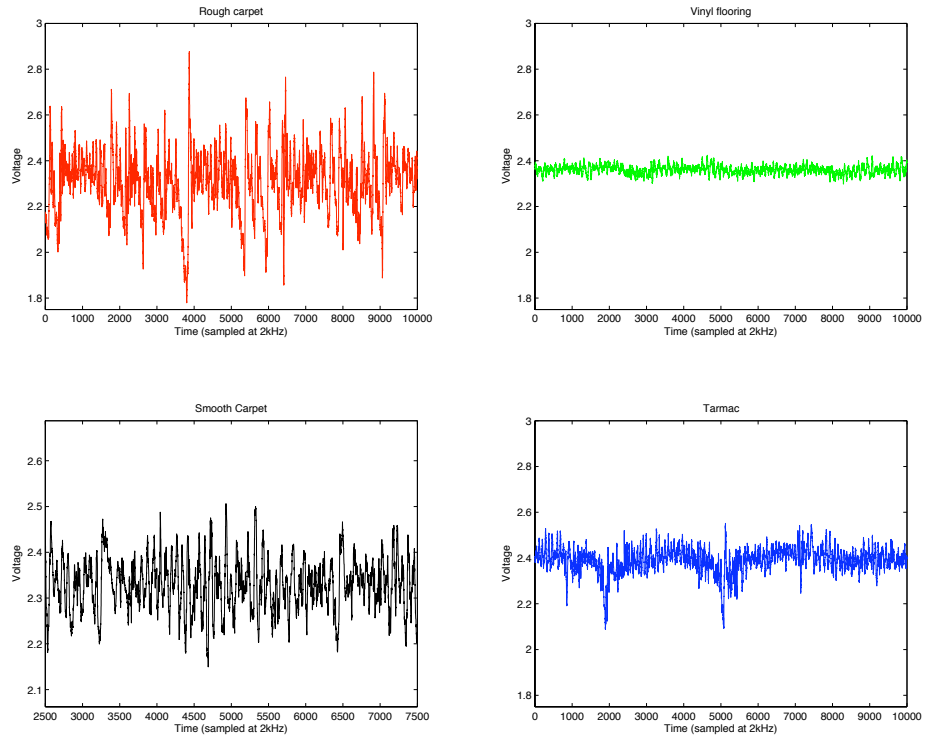


Figure 6.2: Example signals from the artificial whisker sampled from the four floor surfaces.

data is sampled there is no guarantee that the robot will be moving, so to aid the classification the packets acquired when the robot was stationary were removed. A MATLAB script was written to remove any packets where the variance in the signal was below 5×10^{-5} . This automated process provided a clean signal for classification. The remaining packets were restructured to windows for classification that were 800 recordings long (0.4s, or 40 per 16 second trial). These restructured windows were then separated evenly into training and test data sets by assigning all odd numbered samples to the training set, and all even numbered samples to the test set. Only the training set was then used to develop any classifiers. Classifiers were then applied to the test set, and their performance measured using confusion matrices.

Classification was performed using a spectral template based classifier, as was described in Sec-

tion 5.3.2 of Chapter 5. Figure 6.3 shows the templates generated from the data.

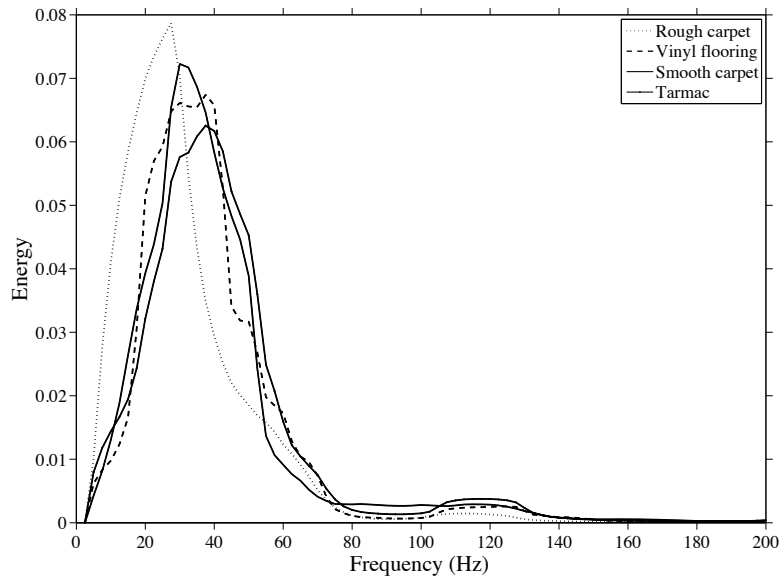


Figure 6.3: Templates used for surface classification in the clockwise movement condition

6.2.2 Results

Tables (6.1) and (6.2) show confusion matrices for four-way texture discrimination in the anti-clockwise and clockwise movement conditions respectively. Though mean classification performance is good in both movement conditions, there is quite a significant difference in performance between the conditions. Overall, classification in the anti-clockwise movement condition is better (Mean correct = 72%, vs 64%), though classification of the vinyl flooring is more accurate in the clockwise condition (79% vs 68% correct). Smooth carpet classification is extremely poor in the clockwise movement condition (33% correct), as can be seen in the third column of table (6.2).

Table (6.3) shows the performance of the classifier in the spot program movement condition.

Table 6.1: Confusion matrix for classification in the anti-clockwise direction of movement condition. Mean correct = 72%

<i>AC</i>	Rough carpet	Vinyl	Smooth carpet	Tarmac
Rough carpet	78	6	12	10
Vinyl	1	54	4	12
Smooth carpet	0	1	43	4
Tarmac	1	19	21	54
Correct %	97.5%	67.5%	54%	67.5%

Table 6.2: Confusion matrix for classification in the clockwise direction of movement condition. Mean correct = 64%

<i>C</i>	Rough carpet	Vinyl	Smooth carpet	Tarmac
Rough carpet	64	6	26	11
Vinyl	0	63	0	9
Smooth carpet	11	1	27	8
Tarmac	5	10	27	52
Correct %	80%	79%	33%	65%

Table 6.3: Confusion matrix for classification in the ‘spot’ movement condition. Mean correct = 56%

<i>Spot</i>	Rough carpet	Vinyl	Smooth carpet	Tarmac
Rough carpet	60	7	48	7
Vinyl	0	48	1	2
Smooth carpet	13	3	9	9
Tarmac	7	22	22	62
Correct %	75%	60%	11%	77.5%

Though overall performance is poorer in this condition than the previous single direction of movement tests, it is still well above chance. Also, the confusion matrix clearly shows that performance overall is very good in three of the four conditions, with misclassification of smooth carpet (11% correct) accounting for the low mean correct score.

In a further analysis, we tried classifying each behavioural condition with the templates from the other, clockwise templates on the anti-clockwise data and vice versa, to see how robust these templates were. The performance in this test was much poorer, with the mean correct scores on both datasets falling to 52%.

6.2.3 Discussion

These results show that the performance of these classifiers are dependent on the movement of the robot. Though classification performance is good on most surfaces across all conditions, movement would need to be taken into account for classification of all surfaces to be optimised. Given that any robot movement would be controlled by the same system that is hoping to process the whisker information, this motor–efference signal would be available making deciphering the signals easier. Robot movement could be controlled to accentuate certain aspects of the signal, in this case by turning in the most discriminating direction. This sort of active sensing can work to get the most from the sensory apparatus and from the stimuli. As discussed in Section 2.2.2 of Chapter 2, rats adjust the movement of their whiskers to extract the most information possible from the surface by ensuring frequent and numerous light touches (Mitchinson et al., 2007), and by controlling the speed and spread of the whiskers before initial contact and between multiple contacts (Grant et al., 2009).

It may be possible to both control the movement of the robot and extract contact geometry features from the signal to maximise the sensitivity of the system for texture discrimination.

This same dataset has been used as input to a stationary naïve Bayes classifier, as described in

Sections 2.4.4.3, 4.3.5 and 5.3.4 of Chapters 2, 4 and 5, respectively. We showed that performing a classification with this method on the histograms of raw data it was possible to achieve almost perfect performance ($> 90\%$ hit rate) under a number of conditions (Lepora, **Evans, M. H.**, Fox, Diamond, Gurney, and Prescott, 2010b), and on different whisking robots (Lepora, Pearson, Mitchinson, **Evans, M. H.**, Fox, Pipe, Gurney, and Prescott, 2010a; Lepora, Fox, **Evans, M. H.**, Mitchinson, Motiwala, Sullivan, Pearson, Welsby, Pipe, Gurney, and Prescott, 2011).

6.3 Radial distance estimation on SCRATCHbot: (Evans, M. H. et al., 2010a)

Having developed a feature based classifier for radial distance and speed estimation (**Evans, M. H.** et al., 2010a, Chapters 4 and 5) a small data set was collected on the SCRATCHbot whiskered robot platform (Described in 6.3 of Chapter 3, Prescott et al., 2010; Pearson et al., 2010) to verify that the same signal features (amplitude and duration of contact) were present in signals from other robots.

The robot was kept stationary while it whisked into a vertical pole at three different radial distances (70, 100 and 130mm), and 3 whisk speeds (2, 4 and 6Hz). This dataset is too small to do an analysis similar to that conducted on the XY positioning robot data, but some useful insights can be gained from it. SCRATCHbot data was inspected to see whether the same features found in the XY positioning robot generated signals would be present in a less well constrained situation (see Figure 6.4). A key difference between data from SCRATCHbot and that from the XY positioning robot is the way whisker speed affects contact duration. Contact duration on the XY positioning robot increases as object speed increases, as object retraction is controlled by a feedback loop of a fixed duration. The faster the object moves, the further the whisker is deflected before a retraction is initiated. This increases contact duration in proportion to an increase in speed (as described in Section 4.3.4 of Chapter 4. Since SCRATCHbot is performing

active whisking, increased whisk speed results in a shorter contact duration. However, though the direction of the relationship is reversed, whisk speed still predictably affects contact duration. As in the XY positioning robot data, whisking at the same speed but different radial distances affects peak deflection magnitude (as can be seen in Figure 6.5(b)). On SCRATCHbot, as on the XY positioning robot (Chapter 4), accurate radial distance estimation must involve taking whisker contact speed into account.

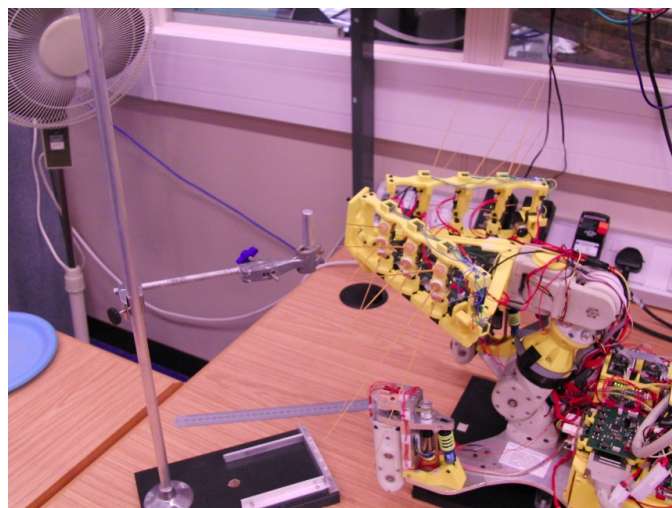


Figure 6.4: The SCRATCHbot whiskered mobile robot. To collect data for this experiment the robot platform was kept stationary while it whisked into a pole at varying radial distances to contact, and whisk speed.

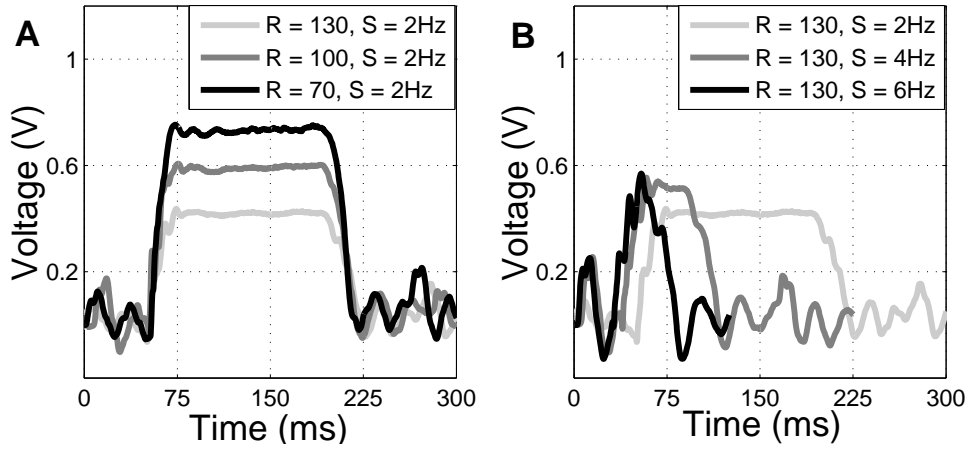


Figure 6.5: Properties of the deflections match closely to those from the XY positioning robot (Compare with Figure 3.7 of Chapter 3). (a) 3 deflections at different radial distances (R , in mm), but the same speed (S , in Hz). Peak deflection height varies predictably with radial distance. (b) 3 deflections at the same radial distance but at different speeds. Contact duration varies predictably with speed.

6.4 Texture discrimination on the BIOTACT G1 robot: (Sullivan, Mitchinson, Pearson, Evans, M. H., Lepora, Fox, Melhuish, and Prescott, 2011)

The BIOTACT G1 sensor (described in Section 3.4 of Chapter 3) is complementary to the XY positioning robot as the whiskers are of the same design on both robots, but the BIOTACT G1 has many more degrees of freedom. The whiskers are actuated, and the array can be moved to cover a volume of space or positioned to perform stationary sensing of an object. These degrees of freedom in the system introduce a great deal of complexity in the whisker deflection signal, so it is necessary to develop classifiers in the carefully controlled XY positioning robot environment. Once a classifier has been developed it is then important to test performance on data from robots like the BIOTACT G1 sensor, to see how classification is affected by changing the contact geometry parameters.

Of particular interest is the effect that biomimetic whisker movement strategies can have on classification. A number of experiments were conducted with this prototype showing, in particular, how biomimetic whisker control can be implemented (as described in Section 3.4 of Chapter 3), and how properties, such as surface texture and radial distance to contact, can be extracted from sensor signals (detailed in the next Section). Here the impact of active control on whisker based tactile sensing is discussed in the context of our twin goals of furthering the understanding of biological whisker systems, and developing classifiers for the tactile framework outlined in Section 2.5 of Chapter 2.

Although a number of active sensing strategies have been demonstrated on earlier whiskered robot platforms (Section 2.3.3 of Chapter 2), the consequences of this active control for sensory discrimination has not previously been investigated or measured.

6.4.1 Texture classification experiments

Following from the work presented in Chapters 4 and 5, two contact parameters were changed simultaneously, namely the horizontal (axial) distance to the contacted surface and the texture of that surface, under varying whisker control strategies: with and without whisking modulation using the rapid cessation of protraction (RCP, described in Section 3.4 of Chapter 3). Horizontal distance varies the angle that whiskers meet the surface, as larger distances cause the whiskers to be more protracted before they meet the surface. This is analogous to the angle parameter in Chapter 5.

Two different classification methods were tested; template based classification (Sections 2.4.4.1, 4.3.3 and 5.3.1 of Chapters 2, 4 and 5, respectively), and stationary naïve Bayes classification (Sections 2.4.4.3, 4.3.5 and 5.4.3 of Chapters 2, 4 and 5, respectively),

A set of textured surfaces were fixed in a vertical plane and rigidly attached to the robot arms support post. The arm trajectory was pre-programmed to bring the front of the sensor to within

a specified horizontal axial distance from the surface (5mm, 10mm or 15mm) with the two rows of whiskers aligned in a horizontal plane. All experiments were carried out with a whisk frequency (f_w) of 2Hz. This is slower than the whisking frequency of rats (dominant frequency 8Hz, Section 2.2.2 of Chapter 2), but not unreasonably so, given the greater length of the artificial whiskers. Three different textures were used; a smooth plastic surface and two grades of commercial abrasive sandpaper (3M silicon carbide ‘Wetordry Tri-M-ite’). The combination of three distances and three textures gave a total of nine distinct classes to be discriminated.

Three different whisking strategies were implemented:

Unmodulated: The whisker pattern generator output, unperturbed by feedback from sensors.

RCP7: Motor drive signal modulated with RCP, using a moderate gain factor ($\sigma_z = 0.7$, see Equation 3.3 in Chapter 3)

RCP9: Motor drive signal modulated with RCP, using a stronger gain factor ($\sigma_z = 0.9$, see Equation 3.3 in Chapter 3)

The goal was to determine whether RCP gain modulation was effective in improving the accuracy and robustness of classification and not to determine optimal values of the equation parameters. Values were chosen which were known to have a clearly visible effect on the output whisker movement patterns.

6.4.2 Stationary naïve Bayes classification

Classification was performed using the same methodology as in Section 4.4.5 of Chapter 4, with a few changes. Measurements were quantised into one hundred equal-width intervals that

spanned the entire data range of each whisker, then the resulting histogram of sensor measurements smoothed with a Gaussian of width 5 intervals to correct for sampling errors and normalising by the number of samples to give the likelihood. This led to $n_w \times n_C$ log-likelihood functions, for each of the $n_w = 12$ whisker inputs (two sensor directions for each of the six whiskers) and $n_C = 9$ texture/distance classes.

6.4.3 Template-based classification

As we have seen elsewhere in this thesis (Sections 2.4.4.1, 4.3.3 and 5.3.1 of Chapters 2, 4 and 5, respectively), template based classification involves recording example sensory data as templates during a training phase, and comparing the stored templates to new data during the test phase. The same methodology was used here.

From the training data set an array of templates were generated by storing the average of the signals for each whisker in each class in the training set. This gave rise to 9 sets of 12 templates.

A sum of squared errors from the 12 templates in each set were taken, and compared across the 9 classes. The class with the lowest total sum of squared errors was determined the winner, and a recording was made in an output array of the estimated texture and distance to contact of the input trial.

6.4.4 Classification results

6.4.4.1 Overall classification performance (unmodulated whisking dataset)

The hit rates over multiple validation trials were first calculated for the unmodulated whisking data set. From one to eight training whiskers were used. Because a total of twelve (training and validation) whiskers were measured, from 11×9 to 4×9 single whiskers remained for valida-

tion over all nine texture/distance classes. The hit rate for each whisk number was then plotted against the number of training whisks (Figures 6.6(a) and 6.7(a), solid black lines). Both classifiers show classification accuracy increasing with numbers of training whisks and reaching a maximum after 4 or 5 training whisks. Thereafter, increasing the number of whisks leads to similar performance.

6.4.4.2 Comparative performance of unmodulated whisking, RCP7 and RCP9 datasets

The unmodulated whisking dataset discussed in the preceding study was compared with results from the RCP datasets. Hit rates for each whisk number are plotted in Figures 6.6(a) and 6.7(a), dashed and dotted lines.

For both classifiers, the RCP modulated whiskers give higher hit rates after one or two training whisks than the un-modulated, with RCP7 giving the highest accuracy. However, the two classifiers behave differently as the number of training whisks increases; using the stationary Bayesian method RCP7 continues increasing, reaching 100% accuracy after seven training whisks, whereas with the template classifier, RCP7 shows little improvement and RCP9 begins to lose accuracy with increased training but suddenly improves after six training whisks.

6.4.4.3 Classification performance for just textures or distances (unmodulated whisking dataset)

Classifiers for texture or distance (three classes of each) were then constructed by concatenating all training data for each distance or each texture. (Equivalently, the likelihoods could be averaged.) Once again, the number of training whisks was varied from one to eight and the hit rates plotted against whisk number (Figures 6.6(b),(c) and 6.7(b),(c) solid lines).

Using the stationary naïve Bayes method, classification for both features again reached high accuracy after about three/four training whisks. Roughly speaking, the hit rate for the single

classifier texture/distance classifier was about equal to multiplying the hit rates for the individual classifiers, so there was no advantage apparent from considering either the single 9-class method or the double 3-class methods to distinguish both texture and distance. It should be noted that the double method is more efficient computationally, because a total of six classes are considered rather than nine. The template-based method performed similarly on the distance classification task but only reached 75% hit rate on the texture classification.

6.4.4.4 Comparative performance for just textures or distances of unmodulated whisking, RCP7 and RCP9 datasets

Finally, the single-classifiers of texture or distance were applied to the RCP7 and RCP9 datasets and the hit rate plotted against training whisk number (Figures 6.6(b),(c) and 6.7(b),(c) dashed and dotted lines).

With the stationary naïve Bayes method, the same pattern of RCP7 being the best classifier, followed by RCP9 and then unmodulated whisking was again found, with the classification performance reaching a maximum at four whisks. With the template-based method, RCP9 gave higher classification accuracy in texture classification. This was also the case in distance classification with less than 3 training whisks, but RCP modulated whisking resulted in lower accuracy than unmodulated with more training contacts.

6.4.5 Discussion

Based on these early results we appear to see an advantage for active control (rapid cessation of protraction – RCP, described in Section 2.2.2 of Chapter 2) for classification after fewer training whisk cycles, particularly when using the stationary naïve Bayes method. This outcome is perhaps surprising in that RCP tends to reduce rather than increase the duration of contact between the whisker and the surface. It therefore suggests that the benefit of RCP may be to increase

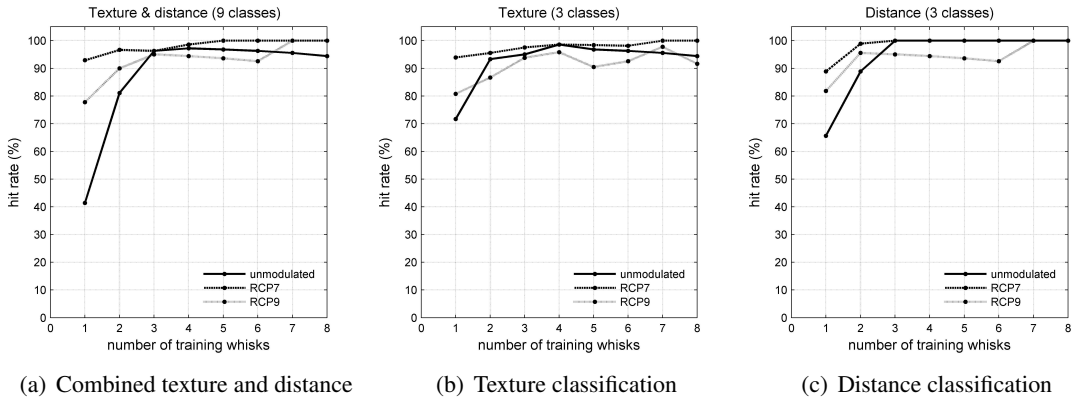


Figure 6.6: Classification performance using naïve Bayes.

Panel A compares the performance of the unmodulated, RCP7 and RCP9 datasets for classifying both texture and distance together. Panels B and C are analogous to panel A, but for a single classification of either texture or distance. Classification accuracy is measured by hit rate, which is the ratio of successful classifications to validation whisks.

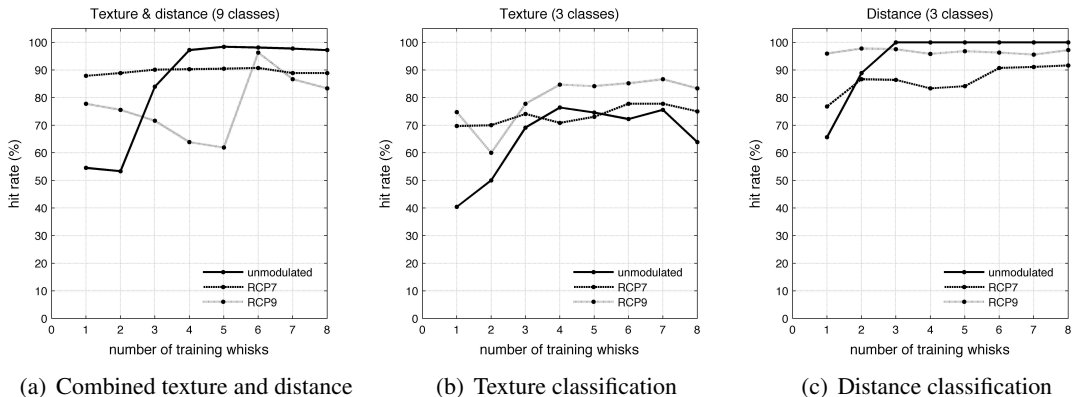


Figure 6.7: Classification performance using template based classifier.

Classification accuracy is measured by hit rate, which is the ratio of successful classifications to validation whisks.

the repeatability of whisker-surface contacts. The advantage is not clearly demonstrated when using the template based method and more than 2 training whisks; under which circumstances classification of distance was actually less accurate when RCP modulation was applied.

Further experiments both with artificial vibrissae and perhaps, using *in vivo* electrophysiology in animals, could usefully investigate the specific consequence of varying RCP gain (i.e. whisker retraction speed) that might lead to improved discriminative capabilities. A moderate gain may

keep the whisker contact forces within a consistent range, while ensuring contact duration is still long enough to gather enough information from the surface. One of the advantages of the BIOTACT G1 sensor, over other systems such as those detailed in Section 2.3 of Chapter 2, is that the whiskers are individually actuated; therefore, sensor movement can potentially be modulated by sensory feedback on a per-whisker basis. Although this possibility is yet to be explored, some experimental work with rats suggests that whisker velocity can be differentially controlled for more anterior and posterior whiskers in a manner that affects the angular spread of the whiskers (Grant et al., 2009). A difference of up to 5 milliseconds was found in the timing of RCP, with posterior whiskers beginning to retract later than more anterior ones (Grant et al., 2009). The classification results from the BIOTACT G1 presented in this Section suggest that such differences, whilst subtle, could be impacting on the discrimination capabilities of the whiskers. Further experiments looking at some of the other control strategies employed by rats (described in Section 2.2.2 of Chapter 2) with the BIOTACT G1 could continue to shed light on the reasons for such careful whisker control, and how it affects sensing.

6.5 CrunchBot: a mobile whiskered robot platform

An autonomous mobile robot presents additional challenges for the classifiers presented in this thesis. Processing must be performed in real-time, robot movement can be noisy leading to unusual artefacts in the whisker deflections, and the reports must be reliable enough to be used in whatever task the robot is engaged with. Crunchbot (Fox, **Evans, M. H.**, Lepora, Pearson, Ham, and Prescott, 2011, Section 3.5 of Chapter 3) allows the integration of a complete tactile sensory system on a mobile robot while keeping the degrees of freedom to a minimum. Robust reports of local object features can be generated in real time, that can then be used as inputs to a system for tactile based navigation or simultaneous localisation and mapping (SLAM Dissanayake et al., 2001; Thrun, 2002, Fox, **Evans, M. H.**, Lepora, Pearson, Ham, and Prescott, 2011). A SLAM algorithm builds up a map of the environment, and localises the agent within that newly formed

map, a task that is very useful for autonomous robots. SLAM is an important field in robotics, where visual (Newman and Ho, 2005), or laser rangefinder sensors (Montemerlo et al., 2002), are often used as input devices. Touch based SLAM is a very different and difficult task, and poses some unique problems. For instance touch information is very sparse, and landmarks cannot be used. Once an agent moves away from an object all information is lost. It is important to generate tactile reports that are rich in information for efficient map building and navigation. One of the most informative object properties that can be extracted is the orientation of a surface, as these reports can inform likelihood estimations of wall sections either side of the contacted point.

We decided to implement a range of classifiers that have been developed in Chapters 4 and 5 of this thesis to run in real-time on CrunchBot, providing tactile reports that could be used as input to a system of tactile SLAM. The classifiers implemented were naïve Bayes texture discrimination (Sections 2.4.4.3 and 5.4.3 of Chapters 2 and 5, respectively), feature based radial distance estimation (Section 4.3.4 of Chapter 4), and template based surface angle estimation (Section 5.3.1 of Chapter 5) alongside two other simple surface angle methods to show the advantages of the rich reports available with template methods.

As has been discussed throughout this thesis, information about whisker-object contact geometry can aid tactile discrimination. Information about angle could improve texture discrimination, though the precise nature of this improvement is still unclear (Chapter 5). Surface orientation estimation is also very useful in touch based navigation and mapping. Touch information is inherently sparse. Information about the environment must be gathered one touch at a time. Object contours can be recovered by determining the location of contact across iterative contacts (Russell and Wijaya, 2003; Kim and Moller, 2007; Gopal and Hartmann, 2007). An alternative method is to combine rich tactile information extraction with strong priors about surfaces and objects (Fox and Prescott, 2011). A report of surface angle could be fused with the knowledge that surfaces tend to continue beyond the immediate region. In this way it is possible to build up

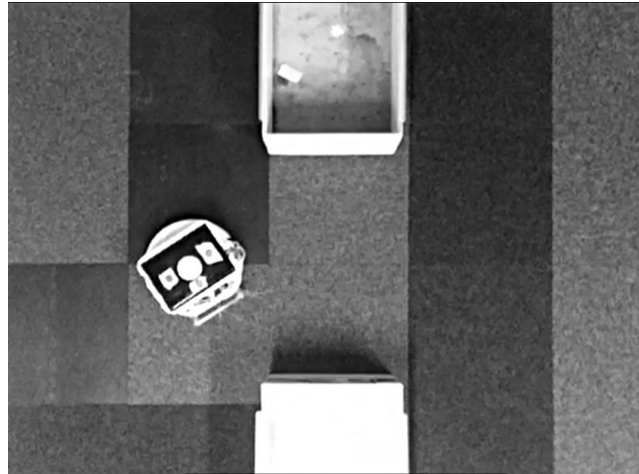


Figure 6.8: Overhead view of Crunchbot in the arena environment. Different carpet tile textures can be seen on the floor along with square obstacles.

maps of the environment from only a few touches.

In the remainder of this section the CrunchBot data collection paradigms are described, along with a finite state machine (FSM) for robot control. The results of classifiers from this thesis, developed for the tactile framework (Section 2.5 of Chapter 2), are reported. Finally, example maps generated by a navigation system utilising different object orientation strategies are shown, to illustrate the advantages of an accurate surface orientation classification for tactile SLAM.

6.5.1 Exploratory behaviour

Figure 3.10(b) shows the arena environment used in the texture discrimination and radial distance estimation experiments. The arena is a $2.5\text{m} \times 2.5\text{m}$ square, surrounded by walls and paved with twenty five $0.5\text{m} \times 0.5\text{m}$ tiles. There are three types of tiles with different textures: vinyl, smooth carpet and rough carpet (see Figure 3.10(c)). A few $0.5\text{m} \times 0.5\text{m}$ square obstacles are also placed over some carpet tiles.

As demonstrated in Chapter 4 accurate object localisation with a whisker requires some measure

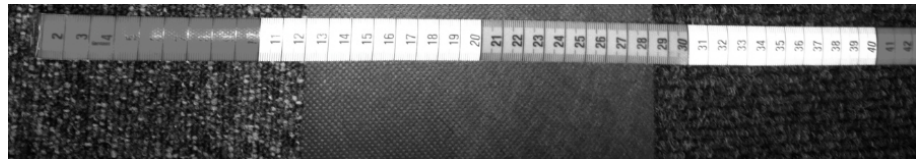


Figure 6.9: Textured floor tiles used in the experiment. From left to right; smooth carpet, vinyl and rough carpet.

of contact speed, or of the applied forces and bending moments at the base of the whisker (discussed in Section 2.4.3.1 of Chapter 2), values that are not always available in the mobile case as agent movement will affect these contact properties. To address these points a ‘body whisk’ behaviour was included in the robot program. As the whiskers were not actuated the whole robot must rotate in a systematic way to simulated the whisking behaviour of rats. As we have seen in Section 6.4 of this Chapter, careful whisking movement can lead to improved tactile discrimination accuracy. Upon initial contact with an object the robot first reverses away a short distance before rotating at $\pi/24$ radians per second towards the object for one second, then rotating at $\pi/24$ radians per second away from the object for one second. This allows this whiskers to move over the surface of the contact object, collecting data about the radial distance, orientation and texture of the surface. After the whisk the robot reverses again to clear the object, then rotates in a random direction and moves forward again.

6.5.2 Floor texture discrimination

The outer two of CrunchBot’s six whiskers are angled downwards to make a light, brushing contact with the floor surface that CrunchBot is travelling over (Figure 3.10). Classification software on the netbook then seeks to classify the whisker deflection signals into previously learnt classes (for example, vinyl or rough carpet), to infer which surface the robot is travelling over. In the current configuration, the signals from the two outer whiskers are classified individually, so that the robot can determine whether the left and right sides are on the same or different textures.

Due to previous success in classifying continuous data a stationary naïve Bayes algorithm was used to infer the surface texture from the whisker contacts (Sections 2.4.4.3, 4.3.5 and 5.4.3 of Chapters 2, 4 and 5, respectively). The methodology is the same as that outlined in Section 4.3.5 of Chapter 4.

However, in the other implementations in this thesis, the likelihoods generated from the data were fed into Bayes rule to give the posterior probabilities of the probabilities for each texture having generated the window of data. Instead, the present method feeds the likelihoods directly into the navigation system for the robot, to be used to infer navigation information.

Another principal difference from our previous applications of stationary naïve Bayes, is that the present implementation requires that the classification be done in real-time on board the robot. Moreover, the texture that the robot is sensing can change during the motion, as the robot moves from one tile to the next. For these reasons, only the most recent 100ms (200 sample) window of texture data was classified, to give good classification reliability while minimising possible boundary crossing. Fortunately, the algorithmic complexity of the classifier is low, so that classification times were much less than the inter-classification intervals of 100ms.

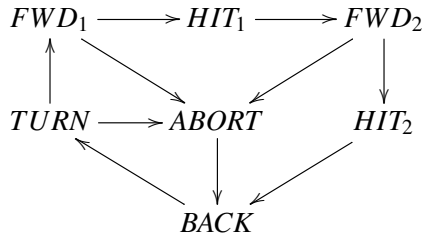
Training data for floor texture discrimination was collected by running the robot over lengths of five floor tiles of a single texture. Test data was collected in a similar fashion, but with texture changing during the run, to show how the classifier would perform when running in a navigation task.

6.5.3 Finite state machine for tactile SLAM

For the simultaneous localisation and mapping (SLAM) task the robot was placed in a small $1.25\text{m} \times 1.25\text{m}$ square arena shown in Fig. 6.8, containing several square objects. This was so the robot could cover the whole arena within a relatively short period of time (6 minute runs). Robot movement was controlled by a finite state machine (FSM Gill, 1962), which is used

to control the robot in a logical if:then type formalism similar to a subsumption architecture (Brooks, 1986). This is an alternative solution to the action-selection problem of motor systems with high degrees of freedom, that the basal ganglia is proposed to solve in biological systems (Gurney et al., 2004).

This diagram of the FSM shows how the states are ordered;



The FSM moves the robot forward in a straight line (FWD_1) *repeatedly* until a whisker hits something (HIT_1). The FSM then moves the robot forward again at a slower speed (FWD_2) until either a second whisker makes contact (HIT_2), or the strain in any whisker exceeds a safety threshold ($ABORT$). The robot then reverses ($BACK$) and turns on the spot ($TURN$). Turn angles (rotations) are drawn from a mixture of two Gaussians, one of which has a small mean and variance ($0.14\pi, 0$) to encourage wall following and the other a large mean and variance ($0.3\pi, 0.25\pi$) to encourage movement away from walls to explore other parts of the arena. Each FWD_1 , FWD_2 and $BACK$ step of the FSM lasts for 0.5s, the FWD_1 and $BACK$ state moves at 0.05 m/s and the FWD_2 state moves at 0.02 m/s for safety. Turning is at 0.3 rad/s. Within each 0.5s FSM step, the whisker strains are monitored regularly for strains exceeding the safety threshold – if this occurs, the motion is terminated early and the FSM switches to the $ABORT$ state, then $BACK$ to escape. Under these behaviours, the robot tends to move anticlockwise overall around the arena, interspersed with periods of wall following and exploration, and typically makes around 3 or 4 circuits (and hopefully loop closures) in a 6 minute run. Combined odometry and radial distance reports are sent after every FSM step with the exception of $BACK$ states, which revisit recently visited locations in the environment and would double-count recent

observations there if their likelihoods were fused into localisation and mapping.

A tactile SLAM system (Fox and Prescott, 2011; Fox, **Evans, M. H.**, Pearson, and Prescott, 2012) was implemented on a remote PC, integrating sensory and odometry data (accurate to $\approx 10\%$ of any movement) from CrunchBot into a standard particle filter algorithm (Gordon et al., 1993; Thrun et al., 2006). 100 particles are maintained, each of which carries a continuous-valued pose (2D location and orientation) and a grid cell map, $m[x,y]$, of the environment. We use a 50×50 grid cell map covering a $2.5m \times 2.5m$ space (double the dimensions of the arena to allow for overspill; 50mm cells). Updates occur at each FSM step.

6.5.4 Radial distance to contact

To determine whether an object has made contact with the a whisker at the tip or the shaft, and to discriminate between contacts with the surfaces or corners of objects, radial distance to contact was implemented. The feature method outlined in Section 4.3.4 of Chapter 4 was used due to it's speed and adaptability.

During the training phase a dataset was collected for each whisker, consisting of 5 contacts at each point along the whisker at 10mm intervals over a 50mm range from the tip of the whisker. Though the whisker is 160mm long, only 140mm is external to the ‘follicle’. A model was then generated of the relationship between the deflection magnitude and the corresponding radial distance to contact by fitting a linear equation to the training data in MATLAB, as in Chapter 4 except a linear regression was used as it was sufficient for accurate classification in this instance.

6.5.5 Surface orientation

Three methods were compared to determine the advantages gained for mapping with strong surface orientation predictions. These methods are ‘blob’ based, multi-whisker contact geometry

based and template based mapping.

6.5.5.1 Blob-based mapping

The simplest whiskered mapping method would treat each contact as an observation of a single grid cell at the contact location, and assume independence between cells. Preliminary experiments showed this is impractical, as there are many grid cells and only a small number of contacts (e.g. 30) during a run (of 6 minutes). A simple extension of this idea is to assume a local correlation between grid cells, as in a Markov Random Field. Under this assumption, a single contact observation gives rise to a small local Gaussian Δm likelihood to be added into the grid map m ,

$$\Delta m[x, y] = \Delta[x_c, y_c] \exp \left\{ -\frac{(x - x_c)^2 + (y - y_c)^2}{2\sigma^2} \right\}, \quad (6.1)$$

where (x_c, y_c) are the coordinates of the contact cell, σ is set to make the resulting blob affect a radius of about two pixels, and $\Delta m[x_c, y_c]$ is the likelihood of the original contact cell occupancy given the current particle and observation (set to a constant > 0.5).

Whiskers that do not make contact also carry likelihoods that grid cells along their lengths are empty. We approximate this by a single Gaussian as in Equation 6.1, but with $\Delta m[x_c, y_c] < 0.5$, and (x_c, y_c) in the center of the whisker shaft. Furthermore, we know that the region occupied by the robot's current body position cannot be occupied by another object, so we can also fuse a similar negative evidence Gaussian centred on the robot body location.

6.5.5.2 Angle-based maps with multi-whisker contact geometry

A more sophisticated mapping strategy is to exploit prior knowledge about the structure of the world, coupled with using features from multiple whiskers together. Previous work (Zhang et al., 2010) made the strong assumption that all objects in the environment have straight edges aligned along Cartesian axes, exploiting the fact that many man-made environments are based

on square grids. Strong hierarchical object priors were used by Fox and Prescott (2011) to constrain the interpretation of contacts as known 3D object forms. Here we use a prior whose strength lies somewhere between these strong prior approaches and the weak prior blob method of Section 6.5.5.1. We assume that the environment is made up mostly of long, straight edges, but do not impose a Cartesian grid on their poses or make assumptions about the 3D forms of objects. So rather than placing Gaussian blobs at contact points, we place a blur of long, oriented edges.

We and others have previously investigated the recovery of surface angle information from *individual* whisker data (Kim and Moller, 2007; **Evans, M. H.** et al., 2009b, Chapter 5 of this thesis).

A simple approach for *multi*-whiskered robots is to locate two contact points on the same surface with two different whiskers, then compute the angle between them. Assuming that edges in the world are locally straight at this scale, then this angle gives the angle of the surface. The two contacts can be read during the FSM states HIT_1 and HIT_2 as described in Section 6.5.5. (In some cases the FWD_2 state terminates to $ABORT$ without a second contact due to a strain safety threshold being exceeded. In these cases, we revert to mapping a single Gaussian blob at the first contact point only as in sec. 6.5.5.1.)

When an oriented surface is found in this way, we add a blur of long oriented edges into the map,

$$\Delta m[x, y] = \Delta[x_c, y_c] \exp \left\{ -\frac{R^2}{2\sigma_R^2} - \frac{(\theta - \theta_c)^2}{2\sigma_\theta^2} \right\}, \quad (6.2)$$

where (R, θ) are radial coordinates centered on the contact midpoint (x_c, y_c) and estimated surface angle θ_c . We use $\sigma_R = 0.25$ and $\sigma_\theta = \pi/12$. Importantly, this produces a *long* (0.25m) blurred edge in the map around the contact point.

6.5.5.3 Angle-based mapping with multi-whisker templates

We have shown in this thesis that simple template classifiers can be used to infer contact parameters such as the radial distance to contact with a single whisker (Chapter 4). On CrunchBot we have access to four whiskers together, so we can train templates corresponding to contact *angle* classes from the 8-dimensional time series from the whole *multi-whisker* set (four whiskers, each with vertical and horizontal channels). The rationale for this approach is that the geometric multi-whisker method of Section 6.5.5.2 must assume that the estimated contact locations are accurate – which is not necessarily true – and is restricted to utilising data from only two contact whisker locations. In contrast, a template method can utilise bulk data from all whiskers to find similar surface angles, and without any geometric assumptions. It is a purely data-driven method. Oriented edges as in Equation 6.2 may again be added to the map once surface angles are found using templates.

Figure 6.10 (a) shows the experimental setup for collecting training data for orientation estimation. Offline training data was collected by programming the robot to drive into a wall at fifteen different angles ($20^\circ:160^\circ$ in 10° intervals) four times. Data was aligned to initial contacts (at HIT_1 occurrence), low pass filtered (17Hz) to remove oscillations caused by robot body movement, recorded for 2s, and smoothed with a five-point moving average. Templates were generated by averaging across the four sets for each angle. Templates for each angle comprised data of all eight channels from the four whiskers to allow multi-whisker information to inform classification.

During online SLAM, strain time-series data was logged from immediately after each HIT_1 to the following HIT_2 then sent to the classifier at HIT_2 . The average squared error for each template is computed over the stored data points as for the methodology in Section 4.3.3 of Chapter 4. The angle of the winning template was used in Equation 6.2 to fuse an oriented long edge into the map.

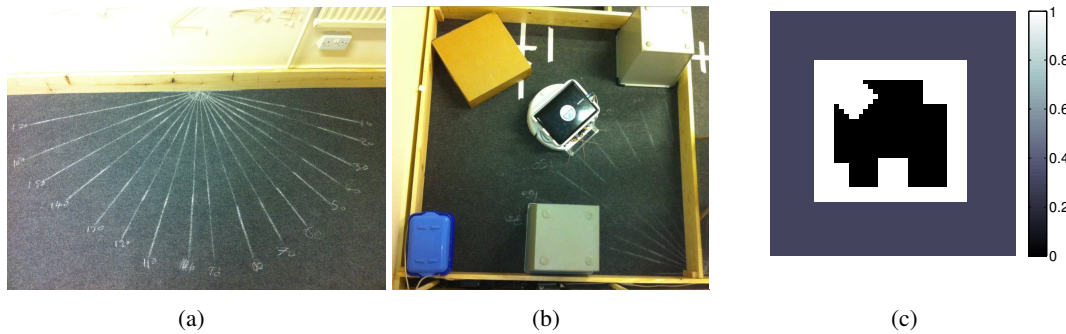


Figure 6.10: (a) Experimental set up for collecting orientation data. (b) Arena used in map building experiments (c) Ground truth grid map based on the arena used for comparison with generated maps. Brightness indicates occupancy.

6.5.6 CrunchBot Results

6.5.6.1 Floor texture discrimination

Robot performance at real-time texture classification was assessed by having the robot follow a course in the arena where it traverses different textures. For an initial investigation, only two surface textures were considered, corresponding to a smooth vinyl and rough carpet. The classification algorithms were trained by presenting the robot with just a single texture, from which a central controller determined the corresponding texture likelihoods for that surface. These were then stored for use in general classification.

A typical example of the classification performance is shown in Figure 6.11. The course consisted of a tile of rough carpet, then a tile of smooth vinyl, and finally a tile of rough carpet. The approximate times when the robot was traversing each texture are marked on the Figure, with rough carpet shaded and smooth vinyl unshaded. As is visible from the Figure, both whiskers reliably reported the correct texture.

One general feature that we observed is that the texture classifier can produce sporadic results near texture boundaries, with the whiskers disagreeing about which texture is being encountered (Figure 6.11 top panel, borders of shaded regions). Examining the whisker deflection traces,

reveals that large deflections of the whisker can occur in these regions that last over a second. We diagnosed this issue as due to the whisker catching on the boundary between two tiles of different heights, and so this feature is actually a signature of a change in texture. In general, catching the whisker on the floor surface caused problems for the classification, because these are infrequent events that can last several hundred milliseconds or more. Hence, we sought to position the whisker to angle as far back as possible to minimise such events, which emphasises that the way in which the whisker contacts the floor can be important for how reliably a classifier can perform.

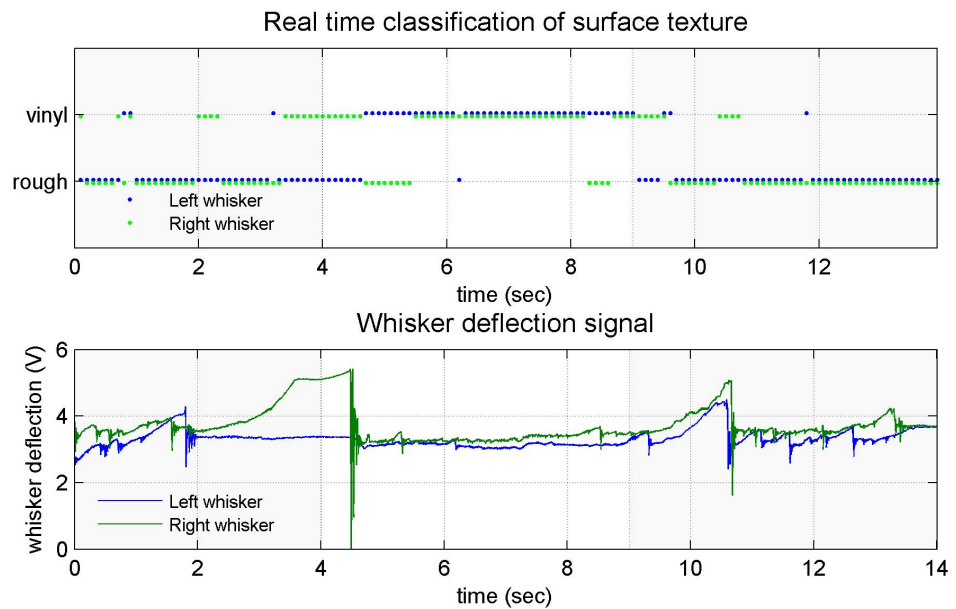


Figure 6.11: Real-time classification of surface texture.
The top panel shows the classification results for the left (blue) and right (green) whiskers traversing a course over rough carpet (shaded regions), then vinyl (unshaded region) and back to rough carpet. The bottom panel shows the deflections associated with each whisker.

6.5.6.2 Radial distance estimation

Peak deflection magnitude for each contact is shown in Figure 6.12. Standard deviation of error for radial distance estimation is shown in the table below.

	Whisker 1	Whisker 2	Whisker 3	Whisker 4	Combined
Std error	5.68mm	2.78mm	1.82mm	4.37mm	4.98mm

Standard classification error is very low, typically less than 5mm over the 60mm range tested. For some whiskers classification error is even lower, below 2mm. These results compare favourably with results from controlled conditions on the XY positioning robot where speed was variable (4). This indicates that the noise in the odometry is low enough to ensure a consistent contact force and speed on this mobile robot.

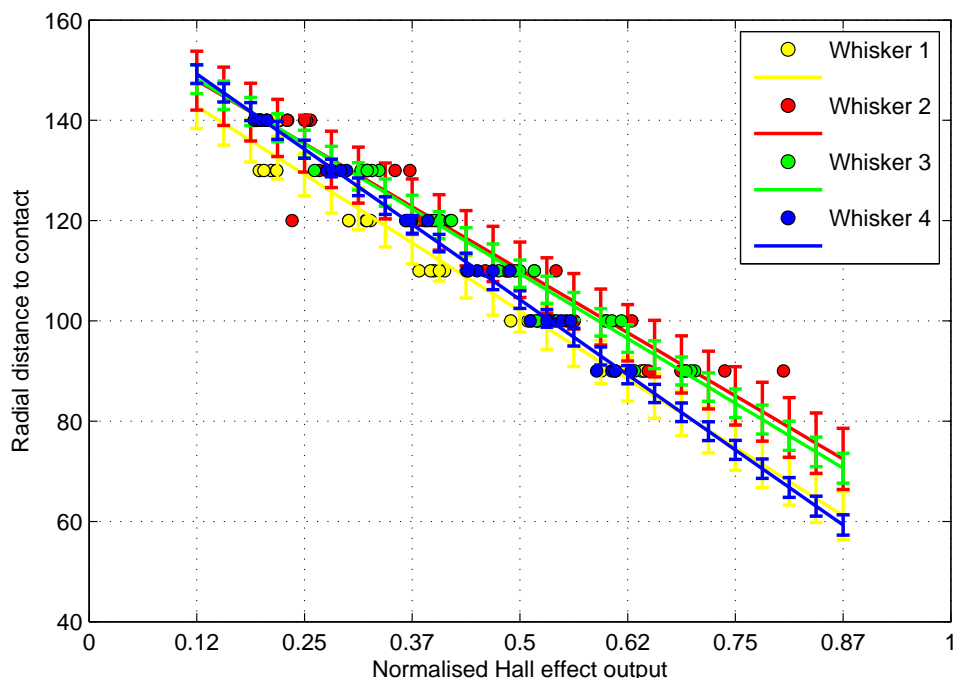


Figure 6.12: Peak deflection magnitude for contacts along the shaft of the whisker (dots), and standard error for the regression (errorbars) for each whisker.

6.5.6.3 Orientation of a surface

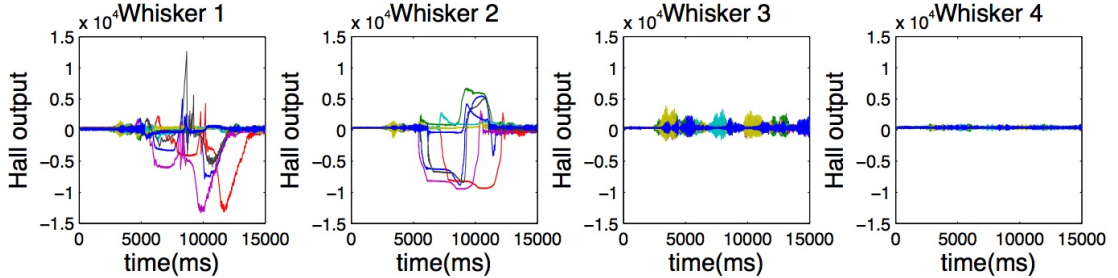


Figure 6.13: Typical data from Cruchbot, contacting the arena wall at 70° anticlockwise from the direction of travel. Different traces in each plot correspond to different trials

Results are presented for mapping using the three methods: blobs, geometric multi-whisker and template multi-whisker. In each instance the robot was programmed to run for twenty trials of six minutes (6 hours of data in total). The resulting grid maps are compared to a ground truth grid map (Figure 6.10 (c); as built by a human observer – which is then smoothed with a 5×5 cell Gaussian filter, standard deviation 2.5). Occupancy in the grid map is represented by a 1 (object present) or a 0 (object not present). Unexplored areas are marked with 0.3 as this is approximately the mean occupancy of the arena. Grid maps, $m[x,y]$, are compared by an element-wise sum of absolute errors calculation to the ground truth map, $gt[x,y]$,

$$\frac{1}{N} \sum_{t=1}^n \frac{1}{50} \sum_{x=1}^{50} \frac{1}{50} \sum_{y=1}^{50} |m[x,y] - gt[x,y]|. \quad (6.3)$$

The mean error per grid cell is reported for each map. For baseline comparison, error for a random map populated from a Bernoulli distribution ($p = 0.5$) is 0.47 (normalised difference of probability).

Figure 6.14(a) shows the average map generated from running the robot with the blob based mapping system. Mean occupancy error was 0.40. Figure 6.14(b) shows the average map generated from running with the geometric multi-whisker based mapping system. Mean occupancy

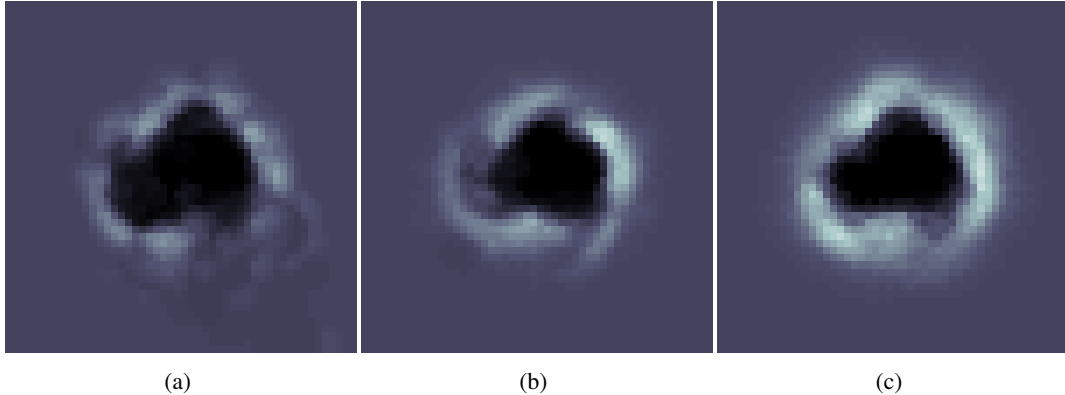


Figure 6.14: (a) Average grid map generated when using blob based mapping over twenty trials. Note grid occupancy outside of the area of the arena and low mean grid occupancy (dark occupied regions). (b) Average grid map generated when using multi-whisker angle based mapping over twenty trials. Note grid occupancy restricted to the area of the arena and high mean grid occupancy (brighter occupied regions). (c) Average grid map generated when using template based mapping over twenty trials. Note grid occupancy restricted to the area of the arena and high mean grid occupancy (brightest occupied regions). Brightness indicates occupancy, all maps are drawn on the same occupancy scale (0:1)

error was 0.39. Figure 6.14 shows the average map generated from running with the template based mapping system. Mean occupancy error was 0.37.

6.5.7 CrunchBot Discussion

We have demonstrated an initial implementation of our framework for whiskered perception and navigation, showing how real-time signal processing, texture classification, distance estimation and navigation can be combined on an inexpensive mobile platform.

Real-time radial distance and texture discrimination performance on CrunchBot was comparable to results presented in Chapters 4 and 5. Though a mobile robot can introduce a large amount of variation in whisker-object contact geometry (which has proven problematic in tactile discrimination experiments in the past Fend, 2005; Fox et al., 2009a), the application of a tactile framework (Section 2.5 of Chapter 2) inspired finite state machine (FSM) and ‘mini-whisk’ robot control strategy restricted whisker contacts. Simplifying the nature of whisker-object con-

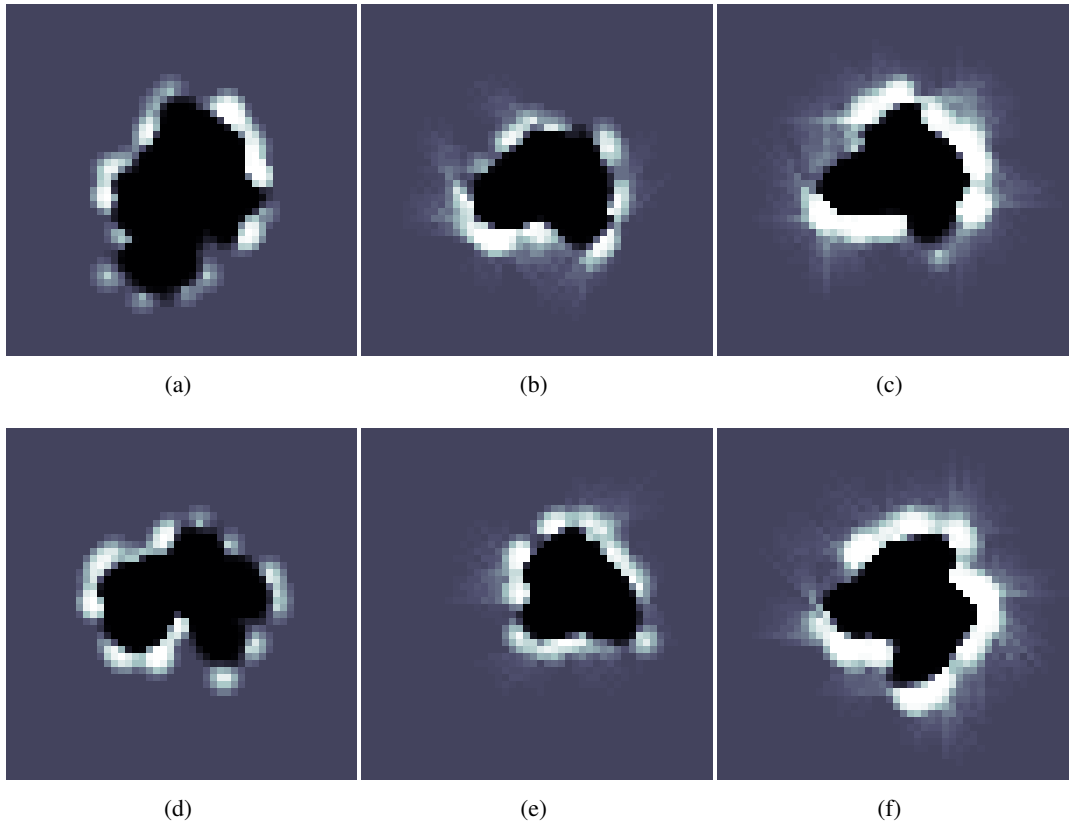


Figure 6.15: Grid maps generated on individual trials for blob based mapping ((a) and (d)), multi whisker geometry based mapping ((b) and (e)), and template based mapping ((c) and (f)). Brightness indicates occupancy.

tacts in this manner allowed high classification performance with simple classifiers implemented in real-time.

In the surface angle experiment, all three methods performed reasonably well. The template method was the best and blob-based was the worst under the metric of Equation 6.3. This seems to be because errors in localisation meant the robot became lost and occupied the map with objects outside of the area of the arena (as can be seen when comparing the lower right quadrants of Figure 6.10 (c) and Figure 6.14(a)). Geometric multi-whisker angle mapping was an improvement on blob based mapping, with grid occupation being restricted to the area of the arena, and surface contours were recovered partially (white patches in Figure 6.14(b)).

The best performance came from the template method. Mapping was restricted to the area of the arena and large sections of surface contours are recovered (prominent white patches in Figure 6.14(c)). Templates were especially useful as they provided strong predictions of surface angle even when only single whisker contacts were made – unlike the geometric method. Templates therefore can extract more information from impoverished whisker data, informing stronger predictions of object contours, leading to a greater occupancy in the grid maps.

Differences between the mapping performance of the three methods can be seen more clearly in the maps generated on individual trials. Figure 6.15 shows typical maps generated in each of the three conditions. Blob based mapping (Figure 6.15 (a) and (d)) resulted in sparse object location reports, and unreliable localisation resulting in mapping outside of the area of the arena. Geometric multi-whisker based mapping (Figure 6.15 (b) and (e)) generated predictions of object contours, and these improved localisation to restrict mapping to the bounds of the arena. Template based mapping (Figure 6.15 (c) and (f)) generated more, better predictions of object contours (white areas in the grid maps), improving localisation. Object features such as sharp corners can also be seen in the template based grid maps (lower region of Figure 6.15 (c) and (f)).

The template classifier was able to discriminate the orientation of a surface but was not trained to discriminate other sorts of contacts, for example with the corners of objects. In principle it is possible to train a template classifier on every possible contact in the arena. However collecting such a data set would be impractical, and the computations involved in comparing incoming data to templates for every possible contact could be cumbersome. An alternative approach is to extract features from the tactile data, as has been done in the field of haptic touch (Stansfield, 1986; Sinclair et al., 2000) and is commonly used in vision (Juan and Gwun, 2010), and audition (Bello and Sandler, 2000). It has been proposed that cells in the thalamus and cortex of the rat are encoding ‘kinetic’ features in the whisker deflection (Petersen et al., 2008; Jadhav et al., 2009) in this way. As detailed in Chapters 4 and 5 we have developed features for whisker based

tactile sensing of contact geometry and texture. In the future we hope to be able to combine features for more diverse tactile properties in rich environments into a coherent tactile–framework system onboard a whisking mobile robot such as SCRATCHbot (Section 6.3). We hope that adding reports of object texture with classifiers similar to those detailed in Chapter 5 will allow the development of richer maps that could be used in more complex goal oriented tasks. However, it is important to consider interactions between components when integrating systems. For example, we found it useful to disable both odometry reports and texture classification while performing mini-whisks when using this information in navigation (Fox, Evans, M. H., Lepora, Pearson, Ham, and Prescott, 2011).

6.6 General discussion

In this Chapter a number of experiments have been presented that test the classifiers developed in Chapters 4 and 5 of this thesis on a range of whiskered robots. Each robot provided unique challenges in the development of whisker based tactile sensing, and the results could potentially provide insights in a number of ways. In the Roomba texture discrimination experiment (Section 6.2) it was shown that whisker sensors and simple classifiers could be used to discriminate ‘real–world’ textures, of the sort a robot may encounter when navigating the environment. Good classification performance was possible when robot motion was unpredictable (spot condition), but performance improved when movement is restricted to certain trajectories. This result supports ideas from biology about why rats seem to control whisker movement (Section 2.2.2 of Chapter 2), and results presented in the texture discrimination work in this thesis (Chapter 5).

This work was expanded to data on the BIOTACT G1 robot (Section 6.4). Classifiers described in Chapters 4 and 5 were applied to data collected from a whiskered robot with much greater degrees of freedom, to answer a pertinent question from the biology: what effect does biologically–

inspired whisker movement (such as that detailed in Section 2.2.2 of Chapter 2) have on sensing? It was demonstrated that certain whisker movement parameters, such as the speed and strength of a rapid cessation of protraction upon initial contact, could improve sensing in certain conditions. In the future other whisker movement strategies will be investigated to develop a clearer picture of the reasons for, and benefits of, the rich whisker movement strategies observed in rats (described in Section 2.2.2 of Chapter 2).

It has been shown previously that whisker-based texture discrimination is critically dependent on whisker-object contact geometry (Fend, 2005; Fox et al., 2009a), and the results presented in Chapter 5 suggest the relationship between surface properties, contact geometry and whisker movement is quite unintuitive and complex. In the BIOTACT G1 experiment (Section 6.4), inspection of the raw signals for each class reveals greater within class variation for contacts with a given texture than at a given distance. This is because contacts at different distances result in stereotypical gross changes in whisker deflection amplitude, as seen in the reliable features extracted for radial distance and speed in Chapter 4, and the SCRATCHbot experiment detailed in Section 6.3 of this Chapter. Texture-dependent features involve smaller and more variable deflections of the whisker, either by their direct contact with random particles on the rough surface, or by an oscillatory ‘ringing’ of the whisker as it draws away from the surface (Figure 5.2 in Chapter 5 shows this). This variation could perhaps explain why the template-based classifier considered here did not generalise well across conditions when attempting to classify texture, compared to the stationary naïve Bayes classifier (compare Figures 6.6(b) and 6.7(b)).

Section 6.5 detailed how data processed in real time on CrunchBot can be used in a localisation and mapping task, and previously it has been shown that the floor texture discrimination described here is accurate and precise enough to give real time updates that can be used for robot localisation (Fox, Evans, M. H., Lepora, Pearson, Ham, and Prescott, 2011).

The results presented in Section 6.5 show that, for our implementation, being able to determine the location and angle of a surface allows a tactile SLAM system to build maps of and navigate

a simple environment more effectively than is possible with other Gaussian blob or whisker geometry based methods.

The results presented here do not solve the tactile SLAM problem. Though the algorithm presented in Section 6.5 allows the robot to simultaneously build a map and localise itself within that map, the environment and subsequent maps are rather simple. This means that the algorithms cannot distinguish one area of the environment from another. This is quite different to the examples of visual SLAM with salient features for loop closures, for example Newman and Ho (2005). In the future we hope to increase the richness of the representations in the maps, such as regions of different texture or the locations of specific objects. Tests for loop closures, or way finding after forced ‘teleportation’ would be possible.

As noted throughout this thesis, whisker movement and contact location confounds surface property discrimination (Chapters 2, 4 and 5) and on CrunchBot we have implemented active sensing behaviours which position the robot so as to obtain standardised contact types to aid sensing. Placing action at the heart of the perceptual process in this way is only possible with integrated mobile systems, rather than the statically mounted whiskers that have been used in previous single component laboratory tests (Gopal and Hartmann, 2007; Russell and Wijaya, 2003). Controlling whisker movement, such as on the BIOTACT G1, SCRATCHbot or CrunchBot, has limitations in guiding whisker sensing. With no external sensory information it is not possible to guide whiskers onto a surface at a desired angle before initially determining the location and orientation of the surface. An initial ‘report’ must be taken and processed to effectively guide subsequent whisker movements. We have shown that this is possible, from analysing the whisker deflection signal, to extract this surface location and angle information, which could then inform and potentially improve texture discrimination (as was shown in the BIOTACT G1 experiment).

We hope to use rich tactile reports developed on the XY positioning robot as inputs to larger scale tactile SLAM systems, which build up representations of objects in the environment (such

as in Fox and Prescott, 2011), and with a better understanding of the role of whisker movement in sensing from experiments on the BIOTACT G1, use this sensing information to guide more efficient exploratory behaviours.

Chapter 7

Conclusion

This thesis is about whisker based tactile discrimination. The overall aim of the thesis is to develop an understanding of whisker based tactile sensing sufficient for a robot to navigate an unfamiliar environment (as described in Chapter 1). To achieve this goal, inspiration was taken from biological whisker systems – specifically the rat whisker system (Section 2.2 of Chapter 2). The tactile discrimination and navigation task–performance of rats (reviewed in Section 2.4 of Chapter 2) was used as an ‘existence proof’ and benchmark for whisker based tactile discrimination. By reviewing the physical structure of the rat whisker system; whisker morphology and mechanical properties, actuation mechanisms; and the control strategies employed by the animal (all in Section 2.2 of Chapter 2), specific questions about the whisker system were formulated.

1. What kinds of tactile information can be extracted from the environment with a whisker?
2. What methods or algorithms could be implemented to achieve these tactile discriminations?
3. What effect does whisker movement have on tactile sensing?
4. How can the problem of discriminating the identity and location of a surface in the environment be simplified for implementation on a mobile robot?

To answer each of these questions a series of whiskered robots (described in Chapter 3) were

developed to collect data for testing candidate mechanisms for tactile discrimination (reviewed in Section 2.4 of Chapter 2), and move beyond the robotic hardware that had been developed in the past (reviewed in Section 2.3 of Chapter 2).

In answer to Question 1: a review of the literature suggested that rats could reliably discriminate the location of a whisker contact in space (Sections 2.4.1 and 2.4.2 of Chapter 2) and the texture of a surface (Section 2.4.5 of Chapter 2). These two tactile ‘where’ and ‘what’ discriminations were used as the foundations of a new framework (Section 2.5 of Chapter 2) for tactile sensing. This framework was designed to begin answering Question 4 by simplifying the task of tactile discrimination. In the framework the task of tactile sensing is reduced to a series of ‘where’ and ‘what’ discriminations.

In answer to Question 2, candidate methods for tactile discriminations suggested in the literature (Section 2.4 of Chapter 2) were identified for testing and comparison. An XY positioning robot and a biomimetic artificial whisker (Sections 3.3 and 3.2.2 of Chapter 3, respectively) were used to generate large data sets to explore whisker–object interactions more comprehensively than had been possible in the past. Data from the XY positioning robot was used to develop, train and test classifiers for radial distance estimation (Chapter 4), and surface angle and texture discrimination (Chapter 5), under conditions of varying contact speed.

To begin answering Question 3, it was shown that contact speed predictably affects the duration and magnitude of a whisker deflection (Chapters 4 and 5), and this information could be reliably extracted to improve radial distance estimation. However, having information about the speed of a contact did not reliably improve texture discrimination with the classifiers presented in Chapter 5, indicating that nature of whisker–object contact is quite complex in the texture domain. Whisker properties, contact duration, whisker movement patterns and whisker deflection transduction may all have a role in determining the nature of a whisker deflection(as discussed in Section 5.5 of Chapter 5). Future investigations may go further to explaining precisely how surface angle and contact speed affect texture–induced whisker deflections.

To expand upon Question 3, and to test the classifiers developed in Chapters 4 and 5 further, additional whiskered robots were used to generate artificial whisker data (Chapter 6). Data from an artificial whisker mounted on a Roomba (Section 6.2 of Chapter 6) showed that spectral template and naïve Bayes classifiers could reliably discriminate ‘real-world’ textures under varying contact conditions. Data from SCRATCHbot (Section 6.3 of Chapter 6) showed that features extracted from artificial whisker data from the XY positioning robot (Chapter 4) can be found in data generated on a whisking robot. The BIOTACT G1 robot (Section 6.4 of Chapter 6) was used to show that biologically-inspired whisker movement strategies (described in Section 2.2.2 of Chapter 2) could improve texture discrimination with certain classifiers, under particular conditions. This work will be expanded in future to address how different whisker movement strategies can be utilised to improve whisker based tactile sensing.

Finally, to answer Question 4 and move towards our aim of developing an understanding of whisker sensing sufficient for tactile navigation a number of classifiers were implemented on CrunchBot, a simple mobile whiskered robot (Section 6.5 of Chapter 6). Taking the tactile framework (Section 2.5 of Chapter 2) as a basis the movement of CrunchBot was carefully controlled with a finite state machine (FSM) to restrict the possible whisker movement patterns during object-contacts. In this way template, feature and naïve Bayes classifiers (described in Chapters 4 and 5) were successfully implemented for real-time surface angle, radial distance and texture discriminations, respectively. These tactile reports were used as input to a system for tactile simultaneous localisation and mapping (SLAM), showing that more accurate maps could be generated when effective classifiers were being utilised.

In this thesis we have aimed to develop a more comprehensive understanding of whisker sensing. It is clear that a complete understanding of how objects in the world can be encoded with whiskers remains a goal for the future. We have seen that whisker movement plays a critical role in sensing. Whisker movement can improve classification (as in the case of texture discrimination on the BIOTACT G1 robot in Section 6.4 of Chapter 6), but it can also affect certain contact

induced features in the deflection such as to confound classifications (as in the case of radial distance estimation with static beam equations in Section 4.3.1 of Chapter 4). We have seen that certain contact parameters can be classified reliably together, such as radial distance to contact and object speed (Chapter 4), but others, such as surface texture and angle, may need to be classified separately in future (Chapter 5). We have also seen that rich reports of surface properties (such as surface angle), combined with carefully controlled whisker and robot movement, can be used to successfully perform tactile SLAM.

7.1 Limitations of the current approach

Great efforts were taken in the design of the robot platforms used in this thesis to address the limitations of previous efforts. The use of a range of robots in a complementary and comparative approach goes some way to ensure that the limitations of one platform are accounted for by a different platform. For example the XY positioning robot is not mobile, therefore classifiers need to be verified on a robot like Crunchbot.

Whisker design was common for all the robots used in this thesis. These whiskers were designed with the limitations of previous designs in mind, and these design choices were detailed in Chapter 3. However, as all the whiskers used in this thesis are similar in design the conclusions must be taken with these whisker design choices in mind.

7.1.1 Whisker design

Only two different whisker designs were used on the robots presented in this thesis. In Chapter 2 whisker mechanics was discussed. It has been shown that a whisker's material properties have a large effect on the signals that are produced during a deflection (Lungarella et al., 2002), Birdwell et al. (2007). N'Guyen et al. (2010) have recently shown that an array of whiskers with different shapes, sizes and material (and as a result different mechanical properties) can be more effective

for discriminating textures than any of the individual whiskers alone. It may be the case that the whiskers used in the experiments in this thesis, though modelled as closely to the physical properties of rodent whiskers as possible, are not the best at that particular task. For example a stiffer whisker may be better for texture discrimination, or a whisker with more damping may produce less noisy signals.

All of the robots detailed in this thesis use Hall effect sensors to measure whisker deflections. Hall effect sensors have been useful as they are robust and respond both to high frequency deflections and large amplitude low frequency deflections. Kim and Moller (2004) compared Hall effect sensors to piezo electric sensors and found that certain texture discriminations were more accurate using the piezo sensors. It may be that Hall effect sensors may not have a wide enough bandwidth to pick up all the texture induced vibrations in the signal. Bending moments have been proposed as important measures of whisker deflection Solomon and Hartmann (2011) and, thought Hall effect output is proportional to bending moment, an explicit bend sensor may provide additional information. The Hall effect sensors used in this thesis output 2-D deflection information in the plane perpendicular to the whisker shaft. Some recent results have shown that rat trigeminal ganglion neurons respond to longitudinal whisker deflections (i.e. along the shaft into the animal's face Stütten et al. 2008). This longitudinal force may be an additional and important source of information for tactile discriminations, especially for properties such as radial distance or surface angle identification. Future whisker designs should aim to capture these additional deflection parameters, either by utilising multi-axis Hall effect sensors, or groups of sensors mounted at different orientations. In this way more information will be available to the classifiers, and performance may improve.

7.1.2 Single whisker contacts

Experimental protocols in this thesis were designed to establish a benchmark for whisker based tactile discrimination. Certain decisions were made that have had a bearing on the results, and

ultimately may limit the conclusions that can be drawn.

With the exception of surface angle classification on CrunchBot in Section 6.5 of Chapter 6, all of the classifiers developed in this thesis are based on data from single whiskers and single contacts. The reason for this approach was to establish a benchmark for whisker based classification in the most basic whisker-object contact case. A goal throughout this thesis has been to determine what kinds of contact-parameter classifications are possible with a whisker sensor, and beginning with a single whisker, single contact condition provides a baseline. Biological whisker systems, such as in rats and mice, have numerous whiskers. The exploratory whisker movements of these animals appear to attempt to maximise the number of whiskers that make contact with an object, and ‘bouts’ of whisking involve 8-10 whisks in brief succession (Carvell and Simons, 1990). Psychophysics results show that classification performance improves after whisker trimming in some tests, though rats cannot learn the task if they only have one whisker during training Szwed et al. (2003). Well trained rats and naive hunting shrews often make a single whisk before making a decision Arabzadeh et al. (2005); Anjum et al. (2006).

Together these results suggest that though rodents seem to maximise the number of whisker-object contacts when exploring an object, and very rarely make decisions based on a single whisker and single contact, they are capable of making such discriminations. Biological whisker systems, therefore, may be constructed in such a way that the cells projecting from each individual whisker are capable of discriminating object properties such as texture or position, but rats combine information across the whisker array to improve their accuracy and efficiency.

Many of the classifiers in this thesis are successful despite only utilising information from single whisker contacts; a relatively small amount of information compared to that available to the exploring rat. This initial benchmark may be improved by utilising information from multiple whiskers and numerous whisker contacts. Some of the poorer classifications, notably for texture discrimination in Chapter 5, may also be improved in this manner.

A key aspect of future research will be to determine how to construct a system capable of pre-

serving accurate single whisker, single contact based classifications, but is able to optimally combine information across whiskers and contacts over time. Probabilistic methods, such as the naïve Bayes classifier presented in this thesis, are ideally suited to combining information or evidence from multiple sources. Sequential analysis Gold and Shadlen (2001); Lepora et al. (2012) is another promising decision making algorithm. Instead of using a discrete decision window, in sequential analysis evidence is accumulated until a decision threshold is reached. If evidence is thought of as reports from classifiers based on individual whisker contacts, the decision making algorithm could balance the relative certainty of those reports with combining them over time to make accurate decisions.

7.2 Future work

The tactile framework presented in Section 2.5 of Chapter 2 in this thesis is the first attempt to develop a single system for general purpose whisker based tactile sensing. The framework was useful for condensing the literature into fewer categories (object localisation and identification, the tactile ‘what’ and ‘where’ problems), for generating problems to investigate (such as how to solve the tactile ‘what’ and ‘where’ problems), and to guide mobile robot control in a navigation task (the FSM and mini-whisk of CrunchBot described in Section 6.5 of Chapter 6). We hope that future research on whisker-based tactile discrimination, especially in task-focused mobile robotics, utilises and expands upon this framework.

Two obvious avenues for future work are to combine the contact localisation and surface identification classifiers from Chapters 4 and 5 in to a single system. The second development would be to apply the approaches developed in this thesis to data from a robot featuring both a mobile platform and actuated whiskers. Both of these lines of work could be combined in to a single system for whisker based tactile sensing on board a mobile robot. Using the tactile framework presented throughout this thesis as a guide a mobile whisking robot would be able to determine

upon initial contact with a surface whether the contact was at the tip of the whisker or not. After any necessary repositioning a surface geometry and identity discrimination could be made, and this information could be used for building a map or construct a model of a large object. Utilising probabilistic methods of evidence accumulation described above to combine information across contacts over time would allow the development of more complex hierarchical representations of objects and environments (Fox and Prescott, 2011).

The XY positioning robot could be used to generate larger sets of data to more comprehensively train the classifiers presented in this thesis. In this way, within-trial noise can be accounted for, and more robust features can be developed (as discussed in Section 5.5 of Chapter 5). Additional experiments carefully varying the movement of the stimulus object could shed light on the nature of whisker-object interactions and their effect on sensing. Though in this thesis we have varied the speed of contact in the classifications, we have not sought to determine which speeds are most useful or effective. It may be that specific whisker movement speeds allow for better classification of certain textures, due to the effects of whisker resonance at certain speeds. There may also be a trade-off between few, long-duration contacts against many, short-duration contacts for whisker sensing, and that rats are aiming to balance this trade-off by modulating whisk speeds (Section 2.2.2 of Chapter 2). Experiments on a whisking robot such as the BIOTACT G1 may provide additional insights in this regard.

The classifiers presented in this thesis have all been either model-based (such as static beam equations in Section 4.3.1 of Chapter 4), or supervised data-driven classifiers (such as the template classifiers in Chapters 4 and 5). It may be possible to develop different systems based on unsupervised learning, such as the principle component's analysis based features discussed in Section 2.4.6 of Chapter 2. With large datasets, such as those that can be generated on the XY positioning robot, it may be possible to determine which features in the whisker deflections can be reliably extracted for a given change in surface properties, or which whisker movement paradigms result in the clearest signals for classification.

7.3 General conclusions, principles and predictions

Whisker movement seems to be of critical importance, to the rat and for tactile discrimination. In future robotics experiments great care should be taken to control the movement of whiskers, and the way whiskers interact with surfaces, to simplify and improve sensing. Further experimentation with the whiskered robots presented in this thesis (described in Chapter 3) could aid a great deal in this research.

More specifically it seems that the interaction between radial distance estimation and speed of contact that is seen in data from the XY positioning robot in Chapter 4 and also in data from ScratchBot and CrunchBot in Chapter 6 is a general property of whisker-object interactions. Other effects seen in data from this thesis, and results reported here seem more a product of a the mechanical properties of a particular whisker, the way that whisker interacts with the surface on that trial, or a chosen classifier's implementation. At this early stage it is difficult therefore to draw general conclusions for whisker sensing on robotic platforms, or biological whisker sensors.

Great progress may be made in understanding the biological system, and in the development of effective artificial whisker systems, if research is focused on understanding the role of whisker movement in active touch. An example would be to make recordings in the trigeminal ganglion of awake rats exploring a surface. It would be possible to determine how different whisker movement strategies (from video inspection) translate in to changes in the spike trains. This approach would also highlight the amounts of trial to trial noise in the spike trains, both for individual whiskers over time and between whiskers. Based on the work presented in this thesis and inspection of artificial whisker deflection signals we would predict that activity in the whisker primary afferents would be affected a great deal by the speed and force of contacts. As in artificial whisker systems, contact related effects in the signal such as increased firing rates for closer radial distances to contact Szwed et al. (2006) will be confounded by whisker movement

effects. A rat's discrimination of parameters such as radial distance and texture would then rely on including some motor efferent signal in the decision at higher processing levels such as the barrel cortex.

Though information about the location and identity of objects and surfaces are processed separately in biological systems Diamond et al. (2008 (a)), it would be interesting to see whether rats suffer from the same 'where' and 'what' separation problems as artificial systems do. This kind of effect is difficult to investigate in rats. It may be that sensing in biological whisker systems is critically dependent on knowledge of whisker movement and contact positioning. However rats seemingly control their whiskers very carefully, so rats have the movement and contact position information at all times. In this way rats ensure that whisker-object contact properties such as surface angle or contact speeds do not affect subsequent texture discriminations. If it was possible to set up tactile illusions for the rats by presenting textures on moving surfaces, or to perturb the movement of the whiskers somehow, we would predict that rats would make systematic errors where the motor afferent signals become unreliable determinants of whisker-object contact parameters.

Finally, biological whisker systems do not operate in isolation. Rats and other whiskered mammals are multimodal systems, capable of integrating information in real time across sensory domains and use historical information to guide sensing from impoverished information. The strict tests presented in this thesis of discriminations based on small amounts of tactile information may serve as building blocks for such a system. The role of a tactile system within a mobile, cognisant, resourceful agent is likely to be very different to that of a tactile system operating in isolation. We hope that the work presented in this thesis demonstrates that this role can be a reliable one.

Bibliography

- Afonso, V.X. (1993), “ECG QRS Detection.” *Biomedical digital signal processing*.
- Ahissar, E and A Arieli (2001), “Figuring space by time.” *Neuron*, 32, 185–201.
- Ahl, AS (1986), “The role of vibrissae in behavior: a status review.” *Veterinary Research Communications*, 10, 245–268.
- Aloimonos, J., I. Weiss, and A. Bandyopadhyay (1988), “Active vision.” *International Journal of Computer Vision*, 1, 333–356.
- Anderson, S.R., M.J. Pearson, A.G. Pipe, T.J. Prescott, P. Dean, and J. Porrill (2010), “Enhanced detection of robot whisker contacts by adaptive cancellation of self-generated signals.” *IEEE Transactions on Robotics*, 99, 1–12.
- Anjum, F., H. Turni, P.G.H. Mulder, J. van der Burg, and M. Brecht (2006), “Tactile guidance of prey capture in Etruscan shrews.” *Proc Natl Acad Sci U S A*, 103, 16544–16549.
- Arabzadeh, E., S. Panzeri, and M.E. Diamond (2006), “Deciphering the spike train of a sensory neuron: counts and temporal patterns in the rat whisker pathway.” *The Journal of neuroscience*, 26, 9216.
- Arabzadeh, E., E. Zorzin, and M.E. Diamond (2005), “Neuronal encoding of texture in the whisker sensory pathway.” *PLoS Biology*, 3, e17.

- Armstrong-James, M., K. Fox, and A. Das-Gupta (1992), “Flow of excitation within rat barrel cortex on striking a single vibrissa.” *Journal of neurophysiology*, 68, 1345.
- Bello, J. B. and M. Sandler (2000), “Techniques for automated music transcription.” *International Symposium on Music Information Retrieval*.
- Berg, Rune W and David Kleinfeld (2003), “Rhythmic whisking by rat: retraction as well as protraction of the vibrissae is under active muscular control.” *J Neurophysiol*, 89, 104–117.
- Bermejo, Roberto, Akshat Vyas, and H Philip Zeigler (2002), “Topography of rodent whisking—i. two-dimensional monitoring of whisker movements.” *Somatosens Mot Res*, 19, 341–346.
- Bernard, M., S. NGuyen, P. Pirim, A. Guillot, J.A. Meyer, and B. Gas (2010), “A supramodal vibrissa tactile and auditory model for texture recognition.” *From Animals to Animats 11*, 188–198.
- Betarbet, R., T.B. Sherer, and J.T. Greenamyre (2002), “Animal models of parkinson’s disease.” *Bioessays*, 24, 308–318.
- Birdwell, J.A., J.H. Solomon, M. Thajchayapong, M.A. Taylor, M. Cheely, R.B. Towal, J. Conradt, and M.J.Z. Hartmann (2007), “Biomechanical models for radial distance determination by the rat vibrissal system.” *J Neurophysiol*, 98, 2439–2455.
- Brecht, M, B Preilowski, and M M Merzenich (1997), “Functional architecture of the mystacial vibrissae.” *Behav Brain Res*, 84, 81–97.
- Bronnikov, S V., O S. Kuzmicheva, and V I Vettegren (1999), “Scale effect of young’s modulus of highly oriented polymers.” *Mechanics of Composite Materials (Latvia) (USA)*, 34, 595–600.
- Brooks, R. (1986), “A robust layered control system for a mobile robot.” *Robotics and Automation, IEEE Journal of*, 2, 14–23.
- Brooks, R.A. (1991), “Intelligence without representation.” *Artificial intelligence*, 47, 139–159.

Brunelli, R. (2009), *Template matching techniques in computer vision: theory and practice*. John Wiley & Sons Inc.

Carvell, G E and D J Simons (1990), “Biometric analyses of vibrissal tactile discrimination in the rat.” *J Neurosci*, 10, 2638–2648.

Chernova, O. F. and V. F. Kulikov (2011), “Structural differences between the shafts of mammalian vibrissae and hairs and their causes.” *Doklady Biological Sciences*, 438, 182–185.

Cohen, J. (1968), “Weighted kappa: Nominal scale agreement provision for scaled disagreement or partial credit.” *Psychological bulletin*, 70, 213.

Cohen, J. et al. (1960), “A coefficient of agreement for nominal scales.” *Educational and psychological measurement*, 20, 37–46.

Collewijn, H. and E. Kowler (2008), “The significance of microsaccades for vision and oculomotor control.” *Journal of Vision*, 8.

Cooley, J.W. and J.W. Tukey (1965), “An algorithm for the machine calculation of complex Fourier series.” *Math. Comput*, 19, 297–301.

Cortes, C. (1995), “Support vector machine.” *Learning*, 20, 273–297.

Crowell, B. (2000), *Vibrations and waves*, volume 3. Light and Matter.

Davison, A.J. and D.W. Murray (2002), “Simultaneous localization and map-building using active vision.” *Pattern Analysis and Machine Intelligence, IEEE Transactions on*, 24, 865–880.

Dearden, A. and Y. Demiris (2005), “Learning forward models for robots.” In *International Joint Conference on Artificial Intelligence*, volume 19, 1440, Citeseer.

Dehnhardt, G. and G. Ducker (1996), “Tactual discrimination of size and shape by a california sea lion (*zalophus californianus*).” *Animal Learning and Behavior*, 24, 366–374.

- Dehnhardt, G, B Mauck, W Hanke, and H Bleckmann (2001), “Hydrodynamic trail-following in harbor seals (*phoca vitulina*).” *Science*, 293, 102–104.
- Deschenes, M., J. Bourassa, and A. Parent (1996), “Striatal and cortical projections of single neurons from the central lateral thalamic nucleus in the rat.” *Neuroscience*, 72, 679–687.
- Deschenes, M., E. Timofeeva, P. Lavallee, and C. Dufresne (2005), “The vibrissal system as a model of thalamic operations.” *Cortical function: a view from the thalamus*, 149, 31.
- Diamond, M.E., M. von Heimendahl, P. Itskov, and E. Arabzadeh (2008 (c)), “Response to: Ritt et al.,” embodied information processing: vibrissa mechanics and texture features shape micromotions in actively sensing rats.” *Neuron* 57, 599-613.” *Neuron*, 60, 743.
- Diamond, M.E., M. von Heimendahl, P.M. Knutsen, D. Kleinfeld, and E. Ahissar (2008 (a)), “‘where’ and ‘what’ in the whisker sensorimotor system.” *Nat Rev Neurosci*, 9, 601–612.
- Dissanayake, M.W.M.G., P. Newman, S. Clark, H.F. Durrant-Whyte, and M. Csorba (2001), “A solution to the simultaneous localization and map building (SLAM) problem.” *Robotics and Automation, IEEE Transactions on*, 17, 229–241.
- Dörfl, J. (1982), “The musculature of the mystacial vibrissae of the white rat.” *Journal of anatomy*, 135, 147–154.
- Dörfl, J. (1985), “The innervation of the mystacial region of the white mouse. a topographical study.” *Journal of anatomy*, 142, 173–184.
- Doucet, A., N. De Freitas, and N. Gordon (2001), *Sequential Monte Carlo methods in practice*. Springer Verlag.
- Downie, J.S., K. West, A. Ehmann, and E. Vincent (2005), “The 2005 music information retrieval evaluation exchange: Preliminary overview.” In *Proceedings of the 2005 International Symposium on Music Information Retrieval* (J.D. Reiss and G.A. Wiggins, eds.), 320–323.
- Envisiontec (2011), “<http://www.envisiontec.de/index.php?id=60>.”

Eurich, C.W. and H. Schwegler (1997), “Coarse coding: Calculation of the resolution achieved by a population of large receptive field neurons.” *Biological Cybernetics*, 76, 357–363.

Fend, M. (2005), “Whisker-based texture discrimination on a mobile robot.” *Advances in Artificial Life*, 302–311.

Fend, M., S. Bovet, and V.V. Hafner (2005), “The artificial mouse-a robot with whiskers and vision.” *Signal [V]*, 5, 6.

Fend, M., S. Bovet, and R. Pfeifer (2006), “On the influence of morphology of tactile sensors for behavior and control.” *Robotics and Autonomous Systems*, 54, 686–695.

Fend, M., S. Bovet, H. Yokoi, and R. Pfeifer (2003), “An active artificial whisker array for texture discrimination.” In *Proc. IEEE/RSJ Int. Conf. Intel. Robots and Systems IROS2003*, volume 2.

FFTW (1998), “FFTW <http://www.fftw.org>.”

Foffani, G., ML Morales-Botello, and J. Aguilar (2009), “Spike timing, spike count, and temporal information for the discrimination of tactile stimuli in the rat ventrobasal complex.” *The Journal of Neuroscience*, 29, 5964.

Forbes, A.D. (1995), “Classification-algorithm evaluation: Five performance measures based on confusion matrices.” *Journal of Clinical Monitoring and Computing*, 11, 189–206.

Fox, C. W., B. Mitchinson, M. J. Pearson, A. G. Pipe, and T. J. Prescott (2009a), “Contact type dependency of texture classification in a whiskered mobile robot.” *Autonomous Robots*.

Fox, C. W. and T. J. Prescott (2011), “Mapping with sparse local sensors and strong hierarchical priors.” In *Proceedings of Towards Autonomous Robotic Systems (Springer)*. Submitted to TAROS 2011.

Fox, C. W., Evans, M. H., N. F. Lepora, M. J. Pearson, A. Ham, and T. J. Prescott (2011),

“Crunchbot: a mobile whiskered robot platform.” In *Proceedings of Towards Autonomous Robots*, Springer.

Fox, C. W., **Evans, M. H.**, M. J. Pearson, and T. J. Prescott (2008), “Towards temporal inference for shape recognition from whiskers.” In *Towards Autonomous Robotic Systems* (Subramanian Ramamoorthy and Gillian M. Hayes, eds.), 226 – 233.

Fox, C. W., **Evans, M. H.**, M. J. Pearson, and T. J. Prescott (2012), “Tactile SLAM with a whiskered robot.” Submitted to ICRA 2012.

Fox, C. W., **Evans, M. H.**, and T. J Prescott (2009b), “Template-based classification of whisker contact edge orientation and radial distance in a simulated mobile robot.” Poster. Barrels XXI.

Frigo, M. and S.G. Johnson (1998), “Fftw: An adaptive software architecture for the fft.” In *Acoustics, Speech and Signal Processing, 1998. Proceedings of the 1998 IEEE International Conference on*, volume 3, 1381–1384, IEEE.

Fundin, BT, FL Rice, K. Pfaller, and J. Arvidsson (1994), “The innervation of the mystacial pad in the adult rat studied by anterograde transport of hrp conjugates.” *Experimental brain research*, 99, 233–246.

Gibson, J M and W I Welker (1983), “Quantitative studies of stimulus coding in first-order vibrissa afferents of rats. 2. adaptation and coding of stimulus parameters.” *Somatosens Res*, 1, 95–117.

Gill, A. (1962), *Introduction to the Theory of Finite-state Machines*, volume 16. McGraw-Hill New York.

Gold, J.I. and M.N. Shadlen (2001), “Neural computations that underlie decisions about sensory stimuli.” *Trends in Cognitive Sciences*, 5, 10–16.

Gopal, V. and M.J.Z. Hartmann (2007), “Using hardware models to quantify sensory data acquisition across the rat vibrissal array.” *Bioinspir Biomim*, 2, S135–45.

Gordon, N.J., D.J. Salmond, and A.F.M. Smith (1993), “Novel approach to nonlinear/non-Gaussian Bayesian state estimation.” In *Radar and Signal Processing, IEE Proceedings F*, volume 140, 107–113, IET.

Grant, R.A., B. Hutchinson, C.W. Fox, and T.J. Prescott (2009), “Active touch sensing in the rat: Anticipatory and regulatory control of whisker movements during surface exploration.” *Journal of Neurophysiology*, 101, 862–874.

Guic-Robles, E., C. Valdivieso, and G. Guajardo (1989), “Rats can learn a roughness discrimination using only their vibrissal system.” *Behavioural Brain Research*, 31, 285–289.

Gurney, Kevin, Tony J Prescott, Jeffery R Wickens, and Peter Redgrave (2004), “Computational models of the basal ganglia: from robots to membranes.” *Trends Neurosci*, 27, 453–459.

Hafner, V.V. (2005), “Cognitive maps in rats and robots.” *Adaptive Behavior*, 13, 87.

Hafner, V.V., M. Fend, P. König, and K.P. Körding (2004), “Predicting properties of the rat somatosensory system by sparse coding.” *Neural Information Processing-Letters and Reviews*, 4, 11–18.

Hafner, V.V., M. Fend, M. Lungarella, R. Pfeifer, P. König, and K.P. Körding (2003), “Optimal coding for naturally occurring whisker deflections.” In *Proceedings of the 2003 joint international conference on Artificial neural networks and neural information processing*, 805–812, Springer-Verlag.

Haidarliu, S., E. Simony, D. Golomb, and E. Ahissar (2010), “Muscle architecture in the mystacial pad of the rat.” *The Anatomical Record: Advances in Integrative Anatomy and Evolutionary Biology*, 293, 1192–1206.

Hall, E.H. (1879), “On a new action of the magnet on electric currents.” *American Journal of Mathematics*, 2, 287–292.

Hammersley, J.M. and D.C. Handscomb (1975), *Monte carlo methods*. Taylor & Francis.

Hartmann, M.J. (2001), “Active sensing capabilities of the rat whisker system.” *Autonomous Robots*, 11, 249–254.

Hartmann, M.J.Z, N.J. Johnson, R.B. Towal, and C. Assad (2003), “Mechanical characteristics of rat vibrissae: resonant frequencies and damping in isolated whiskers and in the awake behaving animal.” *J Neurosci*, 23, 6510–6519.

Hill, D.N., R. Bermejo, H.P. Zeigler, and D. Kleinfeld (2008), “Biomechanics of the vibrissa motor plant in rat: rhythmic whisking consists of triphasic neuromuscular activity.” *The Journal of Neuroscience*, 28, 3438.

Hipp, J., E. Arabzadeh, E. Zorzin, J. Conradt, C. Kayser, M. E. Diamond, and P. Konig (2006), “Texture signals in whisker vibrations.” *J Neurophysiol*, 95, 1792–1799.

Hutson, KA and RB Masterton (1986), “The sensory contribution of a single vibrissa’s cortical barrel.” *Journal of neurophysiology*, 56, 1196.

Jadhav, S.P., J. Wolfe, and D.E. Feldman (2009), “Sparse temporal coding of elementary tactile features during active whisker sensation.” *Nat Neurosci*, 12, 792–800.

Johansson, R.S. and A.B. Vallbo (1979), “Tactile sensibility in the human hand: relative and absolute densities of four types of mechanoreceptive units in glabrous skin.” *The Journal of physiology*, 286, 283.

Juan, L. and O. Gwun (2010), “A comparison of sift, pca-sift and surf.” *International Journal of Image Processing (IJIP)*, 3.

Jung, D. and A. Zelinsky (1996), “Whisker based mobile robot navigation.” In *Intelligent Robots and Systems’ 96, IROS 96, Proceedings of the 1996 IEEE/RSJ International Conference on*, volume 2, 497–504, IEEE.

Kaneko, M., N. Kanayama, and T Tsuji (1998), “Active antenna for contact sensing.” *Robotics and Automation, IEEE Transactions on*, 14, 278–291.

- Ke, Y. and R. Sukthankar (2004), “Pca-sift: A more distinctive representation for local image descriptors.” *2004 IEEE Computer Society Conference on Computer Vision and Pattern Recognition (CVPR’04) - Volume 2*.
- Kim, D.E. and R. Moller (2004), “A biomimetic whisker for texture discrimination and distance estimation.” In *From Animals to Animats 8, Proceedings of the International Conference on the Simulation of Adaptive Behaviour* (S. Schaal et al, ed.), 140–149, MIT Press.
- Kim, D.E. and R. Moller (2007), “Biomimetic whiskers for shape recognition.” *Robotics and Autonomous Systems*, 55, 229–243.
- Kleinfeld, D., E. Ahissar, and M.E. Diamond (2006), “Active sensation: insights from the rodent vibrissa sensorimotor system.” *Curr Opin Neurobiol*, 16, 435–444.
- Kleinfeld, D., R.W. Berg, and S.M. O’Connor (1999), “Anatomical loops and their electrical dynamics in relation to whisking by rat.” *Somatosensory & motor research*, 16, 69–88.
- Knutsen, P.M. and E. Ahissar (2009), “Orthogonal coding of object location.” *Trends in Neurosciences*, 32, 101–109.
- Knutsen, P.M., A. Biess, and E. Ahissar (2008), “Vibrissal kinematics in 3D: tight coupling of azimuth, elevation, and torsion across different whisking modes.” *Neuron*, 59, 35–42.
- Knutsen, P.M., M. Pietr, and E. Ahissar (2006), “Haptic object localization in the vibrissal system: behavior and performance.” *J Neurosci*, 26, 8451–8464.
- Koss, MC and SC Wang (1972), “Brainstem loci for sympathetic activation of the nictitating membrane and pupil in the cat.” *American Journal of Physiology—Legacy Content*, 222, 900.
- Krupa, D J, M S Matell, A J Brisben, L M Oliveira, and M A Nicolelis (2001), “Behavioral properties of the trigeminal somatosensory system in rats performing whisker-dependent tactile discriminations.” *J Neurosci*, 21, 5752–5763.
- Krupa, D.J., M.C. Wiest, M.G. Shuler, M. Laubach, and M.A.L. Nicolelis (2004), “Layer-

specific somatosensory cortical activation during active tactile discrimination.” *Science*, 304, 1989–1992.

Land, MF (1969a), “Movements of the retinae of jumping spiders (salticidae: Dendryphantinae) in response to visual stimuli.” *Journal of experimental biology*, 51, 471.

Land, MF (1969b), “Structure of the retinae of the principal eyes of jumping spiders (salticidae: Dendryphantinae) in relation to visual optics.” *Journal of experimental biology*, 51, 443.

Leonard, J.J. and H.F. Durrant-Whyte (1991), “Simultaneous map building and localization for an autonomous mobile robot.” In *Intelligent Robots and Systems' 91. Intelligence for Mechanical Systems, Proceedings IROS'91. IEEE/RSJ International Workshop on*, 1442–1447, Ieee.

Lepora, N. F., C. W. Fox, **Evans, M. H.**, B. Mitchinson, A. Motiwala, J.C.W. Sullivan, M. J. Pearson, J. Welsby, A. G. Pipe, K. Gurney, and T. J. Prescott (2011), “A general classifier of whisker data using stationary naive Bayes: Application to BIOTACT robots.” In *Proceedings of Towards Autonomous Robotic Systems (Springer)*.

Lepora, N. F., M. J. Pearson, B. Mitchinson, **Evans, M. H.**, C. W. Fox, A. G. Pipe, K. Gurney, and T. J. Prescott (2010a), “Naive Bayes novelty detection for a moving robot with whiskers.” In *Proceedings of IEEE ROBIO*.

Lepora, N.F., C.W. Fox, M.H. Evans, M.E. Diamond, K. Gurney, and T.J. Prescott (2012), “Optimal decision-making in mammals: insights from a robot study of rodent texture discrimination.” *Journal of The Royal Society Interface*.

Lepora, N.F., **Evans, M. H.**, C. W. Fox, M. E. Diamond, K. Gurney, and T.J. Prescott (2010b), “Naive Bayes texture classification applied to whisker data from a moving robot.” *Proc. IEEE World Congress on Comp. Int. WCCI2010*.

Lettvin, J.Y., H.R. Maturana, W.S. McCulloch, and W.H. Pitts (1959), “What the frog’s eye tells the frog’s brain.” *Proceedings of the IRE*, 47, 1940–1951.

Lewis, D. (1998), “Naive Bayes at forty: The independence assumption in information retrieval.” *Machine Learning: ECML-98*, 4–15.

Lichtenstein, S H, G E Carvell, and D J Simons (1990), “Responses of rat trigeminal ganglion neurons to movements of vibrissae in different directions.” *Somatosens Mot Res*, 7, 47–65.

Loomis, M.S. (1942), *The Braille Reference Book: For Grades I, II/2, and II*. Harper & Bros.

Lottem., E and R Azouz. (2008), “Dynamic translation of surface coarseness into whisker vibrations.” *Journal of Neurophysiology*.

Lungarella, M., V.V. Hafner, R. Pfeifer, and H. Yokoi (2002), “An artificial whisker sensor for robotics.” In *Proceedings of the IEEE/RSJ International Conference on Intelligent Robots and Systems (IROS)*, 2931–2936.

Megson, T.H.G. and T.H.G. Megson (2005), *Structural and stress analysis*. Butterworth-Heinemann.

Mehta, S.B., D. Whitmer, R. Figueroa, B.A. Williams, and D. Kleinfeld (2007), “Active spatial perception in the vibrissa scanning sensorimotor system.” *PLoS biology*, 5, e15.

Melexis (2008), “www.melexis.com/Assets/MLX90333_Datasheet_5276.aspx.”

Meyer, J.A., A. Guillot, B. Girard, M. Khamassi, P. Pirim, and A. Berthoz (2005), “The psikharpax project: Towards building an artificial rat.” *Robotics and Autonomous Systems*, 50, 211–223.

Mitchinson, B., C.J. Martin, R.A. Grant, and T.J. Prescott (2007), “Feedback control in active sensing: rat exploratory whisking is modulated by environmental contact.” *Proc Biol Sci*, 274, 1035–1041.

- Mitchinson, B., M. Pearson, A.G. Pipe, and T.J. Prescott (2010), “Biomimetic robots as scientific models: A view from the whisker tip.” In *Neuromorphic and Brain-based Robots* (J Krichmar, ed.), MIT Press. In press.
- Mitchinson, B. et al. (2004), “Empirically inspired simulated electro-mechanical model of the rat mystacial follicle-sinus complex.” *Proceedings of the Royal Society of London. Series B: Biological Sciences*, 271, 2509.
- Montemerlo, M., S. Thrun, D. Koller, and B. Wegbreit (2002), “FastSLAM: A factored solution to the simultaneous localization and mapping problem.” In *Proceedings of the National conference on Artificial Intelligence*, 593–598, Menlo Park, CA; Cambridge, MA; London; AAAI Press; MIT Press; 1999.
- Morley, JW, AW Goodwin, and I. Darian-Smith (1983), “Tactile discrimination of gratings.” *Experimental brain research*, 49, 291–299.
- Munz, M., M. Brecht, and J. Wolfe (2010), “Active touch during shrew prey capture.” *Frontiers in Behavioral Neuroscience*, 4.
- Nanocure (2011), “<http://www.envisiontec.de/index.php?id=49>.”
- Neimark, M.A., M.L. Andermann, J.J. Hopfield, and C.I. Moore (2003), “Vibrissa resonance as a transduction mechanism for tactile encoding.” *J Neurosci*, 23, 6499–6509.
- Newman, P. and Kin Ho (2005), “SLAM loop closing with visually salient features.” In *Proceedings of the 2005 IEEE International Conference on Robotics and Automation*, 635–642.
- Nguyen, Q.T. and D. Kleinfeld (2005), “Positive feedback in a brainstem tactile sensorimotor loop.” *Neuron*, 45, 447–457.
- N’Guyen, S., P. Pirim, and JA Meyer (2009), “Elastomer-based tactile sensor array for the artificial rat psikharpx.” In *Proceedings of the International Symposium on Electromagnetic Fields in Mechatronics, Electrical and Electronic Engineering*, ISEF.

N'Guyen, S., P. Pirim, and J.A. Meyer (2010), "Tactile texture discrimination in the robot psikharpax." In *Proc. Int. Conf. Bio-Inspired Systems and Signal Processing, (Valencia, Spain)*.

Olshausen, B.A. et al. (1996), "Emergence of simple-cell receptive field properties by learning a sparse code for natural images." *Nature*, 381, 607–609.

Orvis, K.H. and H.D. Grissino-Mayer (2002), "Technical note standardizing the reporting of abrasive papers used to surface tree-ring samples." *Tree-Ring Research*, 58, 47–50.

Panzeri, S., R. Petersen, S. Schultz, M. Lebedev, and M. Diamond (2001), "The role of spike timing in the coding of stimulus location in rat somatosensory cortex." *Neuron*, 29, 769–777.

Pearson, M. J., B. Mitchinson, J. Welsby, A. G. Pipe, and T. J. Prescott (2010), "Scratchbot: Active tactile sensing in a whiskered mobile robot." *From Animals to Animats SAB2010*.

Petersen, C.C.H. (2007), "The functional organization of the barrel cortex." *Neuron*, 56, 339–355.

Petersen, R.S., M. Brambilla, M.R. Bale, A. Alenda, S. Panzeri, M.A. Montemurro, and M. Maravall (2008), "Diverse and temporally precise kinetic feature selectivity in the VPm thalamic nucleus." *Neuron*, 60, 890–903.

Popovic, RS (1989), "Hall-effect devices." *Sensors and Actuators*, 17, 39–53.

Prescott, T.J. and C. Ibbotson (1997), "A robot trace maker: modeling the fossil evidence of early invertebrate behavior." *Artificial Life*, 3, 289–306.

Prescott, T.J., B. Mitchinson, and M.R.A. Grant (2011), "Vibrissal behavior and function." *Scholarpedia* http://www.scholarpedia.org/article/Vibrissal_behavior_and_function, 6, 6642.

Prescott, T.J., M.J. Pearson, C. Fox, **Evans, M. H.**, B. Mitchinson, S. Anderson, and A.G. Pipe

- (2010), “Towards biomimetic vibrissal tactile sensing for robot exploration, navigation and object recognition in hazardous environments.” *Proc. RISE2010*.
- Prescott, Tony J, Fernando M Montes Gonzalez, Kevin Gurney, Mark D Humphries, and Peter Redgrave (2006), “A robot model of the basal ganglia: behavior and intrinsic processing.” *Neural Netw*, 19, 31–61.
- Rao, Singiresu (2004), *Mechanical Vibrations*, 4th edition. Pearson.
- Rice, F.L. and H. Van Der Loos (1977), “Development of the barrels and barrel field in the somatosensory cortex of the mouse.” *The Journal of Comparative Neurology*, 171, 545–560.
- Ritt, Jason., Mark L. Andermann, and Christopher Ir. Moore (2008), “Embodied information processing: Vibrissa mechanics and texture features shape micromotions in actively sensing rats.” *Neuron*, 57, 599–613.
- Rosenblueth, A. and N. Wiener (1945), “The role of models in science.” *Philosophy of Science*, 12, 316–321.
- Russell, R.A. (1992), “Using tactile whiskers to measure surface contours.” *Robotics and Automation. Proceedings. 1992 IEEE International Conference on*, 2, 1295–1299.
- Russell, R.A. and J.A. Wijaya (2003), “Object location and recognition using whisker sensors.” In *Australasian Conference on Robotics and Automation*, 761–768, Citeseer, URL citeseer.ist.psu.edu/dearden98bayesian.html.
- Russell, R.A. and J.A. Wijaya (2005), “Recognising and manipulating objects using data from a whisker sensor array.” *Robotica*, 23, 653–664.
- Sachdev, Robert N S, Takashi Sato, and Ford F Ebner (2002), “Divergent movement of adjacent whiskers.” *J Neurophysiol*, 87, 1440–1448.
- Salisbury, Jr., J. (1984), “Interpretation of contact geometries from force measurements.” *Robotics and Automation. Proceedings. 1984 IEEE International Conference on*, 1, 240–247.

Sarko, D.K., F.L. Rice, and R.L. Reep (2011), “Mammalian tactile hair: divergence from a limited distribution.” *Annals of the New York Academy of Sciences*, 1225, 90–100.

Schiebel, E., H. Busby, and K Waldron (1986), “Design of a mechanical proximity sensor.” *Robotics and Automation. Proceedings. 1986 IEEE International Conference on*.

Semba, K and B R Komisaruk (1984), “Neural substrates of two different rhythmical vibrissal movements in the rat.” *Neuroscience*, 12, 761–774.

Seth, A.K., J.L. McKinstry, G.M. Edelman, and J.L. Krichmar (2004), “Texture discrimination by an autonomous mobile brain-based device with whiskers.” In *Proc. IEEE Int. Conf. Robot. Autom. ICRA2004*, 4925–4930.

Shuler, M.G., D.J. Krupa, and M.A.L. Nicolelis (2002), “Integration of bilateral whisker stimuli in rats: role of the whisker barrel cortices.” *Cerebral Cortex*, 12, 86.

Simons, D.J., EG Jones, and IT Diamond (1995), “Neuronal integration in the somatosensory whisker/barrel cortex.” *Cerebral cortex: the barrel cortex of rodents*, 11, 263–298.

Sinclair, J, J.J. Kuo, and H.R. Burton (2000), “Effects on discrimination performance of selective attention to tactile features.” *Somatosensory & Motor Research*, 17, 145–157.

Solomon, J.H. and M.J. Hartmann (2006), “Biomechanics: Robotic whiskers used to sense features.” *Nature*, 443, 525.

Solomon, J.H. and M.J.Z. Hartmann (2008), “Artificial whiskers suitable for array implementation: Accounting for lateral slip and surface friction.” *IEEE Transactions on Robotics*, 24, 1157–1167.

Solomon, J.H. and M.J.Z. Hartmann (2011), “Radial distance determination in the rat vibrissal system and the effects of weber’s law.” *Philosophical Transactions of the Royal Society B: Biological Sciences*, 366, 3049–3057.

- Solomon, Joseph H. and Mitra J Hartmann (2009), “Extracting object contours with the sweep of a robotic whisker using torque information.” *The International Journal of Robotics Research*.
- Stansfield, S. (1986), “Primitives, features, and exploratory procedures: Building a robot tactile perception system.” In *Robotics and Automation. Proceedings. 1986 IEEE International Conference on*, volume 3, 1274–1279, IEEE.
- Stützgen, Maik C., Stephanie Kullmann, and Cornelius Schwarz (2008), “Responses of rat trigeminal ganglion neurons to longitudinal whisker stimulation.” *J Neurophysiol*, 100, 1879–1884.
- Stützgen, Maik C, Johannes Ruter, and Cornelius Schwarz (2006), “Two psychophysical channels of whisker deflection in rats align with two neuronal classes of primary afferents.” *J Neurosci*, 26, 7933–7941.
- Sullivan, J.C.W., B. Mitchinson, M. J. Pearson, **Evans, M. H.**, N. F. Lepora, C. W. Fox, C. Melhuish, and T. J. Prescott (2011), “Tactile discrimination using active whisker sensors.” *IEEE Sensors*, Issue:99.
- Szwed, Marcin, Knarik Bagdasarian, and Ehud Ahissar (2003), “Encoding of vibrissal active touch.” *Neuron*, 40, 621–630.
- Szwed, Marcin, Knarik Bagdasarian, Barak Blumenfeld, Omri Barak, Dori Derdikman, and Ehud Ahissar (2006), “Responses of trigeminal ganglion neurons to the radial distance of contact during active vibrissal touch.” *J Neurophysiol*, 95, 791–802.
- Takehiko, B. and T. Haruo (1991), “Cerebral cortical and brainstem areas related to the central control of lens accommodation in cat and monkey.” *Comparative Biochemistry and Physiology Part C: Comparative Pharmacology*, 98, 229–237.
- Evans, M. H.**, C. W. Fox, N.F. Lepora, M. J. Pearson, and T. J. Prescott (2010a), “Whisker-object contact speed affects radial distance estimation.” In *Proceedings IEEE ROBIO*.

Evans, M. H., C. W. Fox, M. J. Pearson, and T. J. Prescott (2008), “Radial distance to contact estimation from dynamic robot whisker information.” Poster. Barrels XXI.

Evans, M. H., C. W. Fox, M. J. Pearson, and T. J. Prescott (2010b), “Tactile discrimination using template classifiers: Towards a model of feature extraction in mammalian vibrissal systems.” In *Proceedings of the 11th International Conference on Simulation of Adaptive Behaviour. (SAB 2010) From Animals to Animats*.

Evans, M. H., C. W. Fox, and T. J. Pearson, M. J. and Prescott (2009a), “Spectral template based classification of robotic whisker sensor signals in a floor texture discrimination task.” In *Proceedings of Towards Autonomous Robotic Systems (TAROS 2009)* (T Kyriacou, U. Nehmzow, C. Melhuish, and M. Witkowski, eds.), 19–24.

Evans, M. H., C. W. Fox, M. J. Pearson, and T. J. Prescott (2009b), “Object location, orientation, and velocity extraction from artificial vibrissal signals.” In *Society for Neuroscience Abstracts. Society for Neuroscience (Program No. 174.8/Z12)*.

Thrun, Sebastian (2002), “Probabilistic robotics.” *Communications of the ACM*, 45, 52–57.

Thrun, Sebastian, Wolfram Burgard, and Dieter Fox (2006), *Probabilistic Robotics*. MIT.

Torvik, A. (1956), “Afferent connections to the sensory trigeminal nuclei, the nucleus of the solitary tract and adjacent structures. an experimental study in the rat.” *The Journal of Comparative Neurology*, 106, 51–141.

Towal, R. Blythe and Mitra J. Hartmann (2006), “Right-left asymmetries in the whisking behavior of rats anticipate head movements.” *J Neurosci*, 26, 8838–8846.

Towal, R. Blythe and Mitra J. Z. Hartmann (2008), “Variability in Velocity Profiles During Free-Air Whisking Behavior of Unrestrained Rats.” *J Neurophysiol*, 100, 740–752, URL <http://jn.physiology.org/cgi/content/abstract/100/2/740>.

- Tuan, Y.F. (1974), *Topophilia: A study of environmental perception, attitudes, and values*. Columbia Univ Pr.
- Ueno, N., M.M. Svinin, and M Kaneko (Dec 1998), “Dynamic contact sensing by flexible beam.” *Mechatronics, IEEE/ASME Transactions on*, 3, 254–264.
- Van Der Loos, H. (1976), “Barreloids in mouse somatosensory thalamus.” *Neuroscience Letters*, 2, 1–6.
- Veinante, P and M Deschenes (1999), “Single- and multi-whisker channels in the ascending projections from the principal trigeminal nucleus in the rat.” *J Neurosci*, 19, 5085–5095.
- Vincent, J.F.V., O.A. Bogatyreva, N.R. Bogatyrev, A. Bowyer, and A.K. Pahl (2006), “Biomimetics: its practice and theory.” *Journal of the Royal Society Interface*, 3, 471.
- Vincent, SB (1912), “The function of the vibrissae in the behavior of the white rat, behav.” *Monographs*, 1, 7–81.
- von Heimendahl, Moritz, Pavel M. Itskov, Ehsan Arabzadeh, and Mathew E. Diamond (2007), “Neuronal activity in rat barrel cortex underlying texture discrimination.” *PLoS Biol*, 5, 2696–2708.
- Welker, WI (1964), “Analysis of sniffing of the albino rat.” *Behaviour*, 223–244.
- Williams, C.M. and E.M. Kramer (2010), “The advantages of a tapered whisker.” *PloS one*, 5, e8806.
- Willner, P. (1984), “The validity of animal models of depression.” *Psychopharmacology*, 83, 1–16.
- Wilson, J.F. and Z. Chen (1995), “A whisker probe system for shape perception of solids.” *Journal of dynamic systems, measurement, and control*, 117, 104.
- Wolfe, J., D.N. Hill, S. Pahlavan, P.J. Drew, D. Kleinfeld, and D.E. Feldman (2008), “Texture

coding in the rat whisker system: slip-stick versus differential resonance.” *PLoS biology*, 6, e215.

Wolpert, D.M., Z. Ghahramani, and M.I. Jordan (1995), “An internal model for sensorimotor integration.” *Science*, 269, 1880.

Woolsey, T.A. (1970), “The structural organization of layer iv in the somatosensory region (si) of the mouse cerebral cortex: The description of a cortical field composed of discrete cytoarchitectonic units.” *Brain Res*, 17, 205–242.

Young, W.C., R.G. Budynas, and R.J. Roark (2003), *Roark’s formulas for stress and strain*, 7th edition. .

Yu, Chunxiu, Dori Derdikman, Sebastian Haidarliu, and Ehud Ahissar (2006), “Parallel thalamic pathways for whisking and touch signals in the rat.” *PLoS Biol*, 4, e124.

Zhang, Y., J. Liu, G. Hoffmann, M. Quilling, K. Payne, P. Bose, and A. Zimdars (2010), “Real-time indoor mapping for mobile robots with limited sensing.” In *Mobile Adhoc and Sensor Systems (MASS), 2010 IEEE 7th International Conference on*, 636–641, IEEE.